A COMPARATIVE STUDY OF ADVANCED SUSPENSION DAMPERS FOR VIBRATION AND SHOCK ISOLATION PERFORMANCE

A.S.M. Shawkatul Islam

A Thesis
in
The Department
of
Mechanical and Industrial Engineering

Presented in Partial Fulfillment of the Requirements
for the Degree of Master of Applied Science (Mechanical Engineering) at
Concordia University
Montreal, Quebec, Canada

March 2005

Your file Votre référence
ISBN: 0-494-04419-5
Our file Notre référence
ISBN: 0-494-04419-5

ABSTRACT

A COMPARATIVE STUDY OF ADVANCED SUSPENSION DAMPERS FOR VIBRATION AND SHOCK ISOLATION PERFORMANCE

A.S.M. Shawkatul Islam

Electro-Rheological (ER) and Magneto-Rheological (MR) fluid based advanced suspension dampers are emerging to be the next generation of suspension dampers. ER damper and MR damper have gained wide spread attention in academia as well in auto industries due to their attractive features and promising performance potential to overcome the limitations of existing dampers in market. This work presents a comprehensive study of four different suspension dampers, where each are modeled, validated and assigned a set of parameters to facilitate a comparison of performance. The dampers considered include linear passive damper, two-stage asymmetric non-linear damper, ER damper and MR damper. The vibration and shock isolation performance of the dampers are compared using a four degree-of-freedom pitch plane ride model. A wide range of performance measure is considered in this investigation, namely - sprung and unsprung mass responses, relative motions, drift, pavement load etc. The study reveals superior vibration and shock isolation performance of ER damper and MR damper for vehicle sprung mass compared to linear passive damper and asymmetric non-linear damper. Since the dampers are designed as symmetric in compression and rebound, they are immune from ride height drifting problem. At higher frequencies (above 10 Hz), the dampers transmit higher load to pavement

compared to other two. The study suggests that asymmetricity should be included in the design of these dampers to achieve improved performance over the entire frequency range. A properly tuned MR damper with controller to provide asymmetric characteristics has the most potential for superior performance for all responses.

ACKNOWLEDGEMENTS

The author wishes to express his sincere appreciation and thanks to his supervisor Dr. A.K.W. Ahmed for his guidance, suggestions and continued encouragement throughout the course of this investigation.

Thanks due to colleagues, faculty and staff at CONCAVE Research Center of Concordia University and the Department of Mechanical and Industrial Engineering for their suggestion and encouragement for this effort.

Finally, the author would like express his special thanks to his parents, sister and friends for their love, support and encouragement throughout the way.

TABLE OF CONTENTS

CHAPTER 3

Damper Model Validation and Performance Measure

CHAPTER 4

A Comparative Study

LIST OF FIGURES

LIST OF TABLES

NOMENCLATURE

SYMBOL	DESCRIPTION
m_s	Sprung mass
I_s	Sprung mass moment of inertia
m_{uf}	Front unsprung mass
m_{ur}	Rear unsprung mass
f_{dsf}	Front suspension damping force
f_{dsr}	Rear suspension damping force
k_{sf}	Font suspension spring stiffness coefficient
k_{sr}	Rear suspension spring stiffness coefficient
c_{uf}	Front tire damping coefficient
c_{ur}	Rear tire damping coefficient
k_{uf}	Front tire stiffness coefficient
k_{uf}	Rear tire stiffness coefficient
x_s	Sprung mass displacement
θ	Sprung mass pitch displacement
x_{uf}	Front unsprung mass displacement
x_{ur}	Rear unsprung mass displacement
x_0	Road input to wheels
x_{0f}	Road input to front wheels
x_{0r}	Road input to the rear wheels
L	Track width of the vehicle

b	Distance between front axle and C.G. of the vehicle
c	Distance between rear axle and C.G. of the vehicle
m_{sq}	Sprung mass of one quarter of the vehicle
m_{uq}	Unsprung mass associated with one quarter of the vehicle
k_s	Suspension stiffness coefficient for quarter car model
f_{ds}	Suspension damping force for quarter car model
c_u	Tire damping coefficient
k_u	Tire stiffness coefficient
c_{sf}	Front suspension damping coefficient of linear passive damper
c_{sr}	Rear suspension damping coefficient of linear passive damper
C_1	High damping coefficient at compression side (asymmetric non-linear damper)
C_3	High damping coefficient at extension side (asymmetric non-linear damper)
C_2	Low damping coefficient at compression side (asymmetric non-linear damper)
C_4	Low damping coefficient at extension side (asymmetric non-linear damper)
α_e	Preset velocity at extension side (asymmetric non-linear damper)
α_c	Preset velocity at compression side (asymmetric non-linear damper)
γ_c	Compression damping reduction factor (asymmetric non-linear damper)
γ_e	Extension damping reduction factor (asymmetric non-linear damper)
p	Asymmetry factor (asymmetric non-linear damper)
P_1	Pressure at the top chamber of ER damper
P_2	Pressure at the bottom chamber of ER damper
V	Applied voltage to ER valve

ρ	Density of ER fluid
E	Electric field strength
U	Mean flow velocity
ΔP_T	Steady pressure drop across the ER valve
ΔP_0	Total pressure drop without electric field (ER damper)
ΔP_{ER}	Pressure drop due to ER effect (ER damper)
τ_{ER}	Linear function of yield stress for ER fluid
$\beta(E)$	Empirical coefficient (ER damper)
α_r	Empirical constant (ER damper)
γ_r	Empirical constant (ER damper)
m	Mass of the ER fluid within the valve channel of ER damper
A_0	Pressure area of the piston of ER damper
d	Diameter of the shock absorber piston (ER damper)
A_v	Total flow area (ER damper)
L	Channel length of ER valve
h	Height between two electrodes (ER damper)
L_e	Length between two electrodes (ER damper)
B	Width between two electrodes (ER damper)
f_G	Feedback gain of ER damper controller
v_m	Maximum Velocity (MR damper hysteresis model)
f_m	Maximum Damping Force (MR damper hysteresis model)
v_h	Zero force velocity intercept (MR damper hysteresis model)
f_h	Zero velocity force intercept (MR damper hysteresis model)

v_t	Transition Velocity (MR damper hysteresis model)
f_t	Transition force(MR damper hysteresis model)
s_h	Hysteretic slope (MR damper hysteresis model)
s_v	Linear slope (MR damper hysteresis model)
k_v	Parameter used to adjust MR damping coefficients at high velocity
α	Parameter used to adjust MR damping coefficients at low velocity
a_m	Excitation amplitude for MR damper
ω	Excitation frequency for MR damper
a_0	Identified parameter for MR damper model
a_1	Identified parameter for MR damper model
a_2	Identified parameter for MR damper model
a_3	Identified parameter for MR damper model
a_4	Identified parameter for MR damper model
I_0	Identified parameter for MR damper model
I_1	Identified parameter for MR damper model
k_0	Identified parameter for MR damper model
k_1	Identified parameter for MR damper model
k_2	Identified parameter for MR damper model
k_3	Identified parameter for MR damper model
k_4	Identified parameter for MR damper model
f_0	Identified parameter for MR damper model
C_{sky}	Adjustable gain of the 'skyhook' controller of MR damper
x_0	Amplitude of sinusoidal excitation

v_f	Forward velocity of vehicle
λ	Wave-length of sine wave
$Xmax$	Maximum amplitude of shock input
X_s	Peak amplitude of sprung mass displacement
X_0	Peak amplitude of excitation
η	Severity of shock input
ω_n	Natural frequency of the vehicle (bounce natural frequency for 4 DOF system)

CHAPTER 1

Introduction and Literature Review

1.1 Introduction

In today's ever changing world, road vehicles are not merely designed for carrying passengers and goods but also to enhance ride comfort, to provide desired handling ability, fuel efficiency, safety etc. Since the basic design for the vehicles are similar, manufacturers are giving more emphasis on factors that will distinguish one manufacturer from the other. Vehicle suspension system is one of the crucial factors, which is in the forefront of the battle to win hearts of consumers.

In the early 1900's, cars rode on carriage springs, as earlier drivers were more concerned about keeping the cars rolling over the rocks and ruts, than about the ride comfort. Pioneering vehicle manufacturers faced the challenge of enhancing control as well as ride comfort of the vehicle. The early suspension designs consisted of front wheels attached to the axle using steering spindles and kingpins. This design allowed the wheels to pivot while the axle of the vehicle remained stationary. Over the years, suspension systems have evolved into more sophisticated designs to meet the demand of time (Monroe, 2003).

A vehicle suspension system encompasses springs, dampers, torsion bars, joints, arms etc. The spring and damper are interposed between the sprung mass (mass of the vehicle body) and unsprung mass (mass of the wheels and wheel structures), and are generally mounted in parallel. The spring and shock absorber work in conjunction, as an inseparable unit to control the movements of these two distinct masses. In spite of its

name, which suggests the opposite, it is not the damper rather the spring that absorbs shock. When subjected to external road excitation, the spring does not manifest just one compression– rebound cycle, but relaxes and re-compresses a few times in an oscillatory motion before recovering its initial position. In the meantime, new shocks that could reinforce or renew movement, must be absorbed. The damper performs the critical task of slowing down and controlling these spring movements. Absence of good damper results in poor performance of vehicle. For example, wheels would dance in an uncontrolled manner on the road, causing loss of adequate contact with the road. This would ultimately make it impossible to provide tractive effort at tire-ground contact. For the same reason, braking efficiency of the vehicle is affected, and maintaining a desired trajectory becomes difficult (Sassi *et al.*, 2003). Driving safety is attained by harmonious suspension design in terms of wheel suspension, spring, steering and braking, and is reflected in an optimal dynamic behavior of the vehicle, whereas driving comfort results from keeping the physiological stress that the vehicle occupants are subjected to by vibrations, noise, and climatic conditions down to as low a level as possible (Ficher and Isermaan, 2004).

The design task of road vehicle suspension system is quite complex owing to the fact that vehicles are subjected to wide variety of operating conditions involving varying surface roughness and discontinuity (like potholes), load and speeds. The task is further complicated as performance objectives associated with vehicle ride comfort, road holding and control impose conflicting requirements for suspension design. A heavy suspension with firm springs and dampers with high damping characteristics will yield good vehicle handling and stability, keeping the tires in contact with the road and preventing frame oscillations and other problems. But such suspension system will

transfer most of the road oscillations to the passenger, causing an uncomfortable ride. One the other hand, a light suspension with soft springs and dampers with low damping characteristics will yield a more comfortable ride, but at the same time, can reduce the stability of the vehicle. Hence it is evident that there exists a conflict between ride quality and drive stability. Figure 1.1 illustrates this conflict, showing the variation of drive safety (handling and control) and ride comfort with the vehicle body mass, stiffness of suspension spring, tire stiffness and damping coefficient of the damper in so called 'Conflict Diagram' (Ficher and Isermaan, 2004).

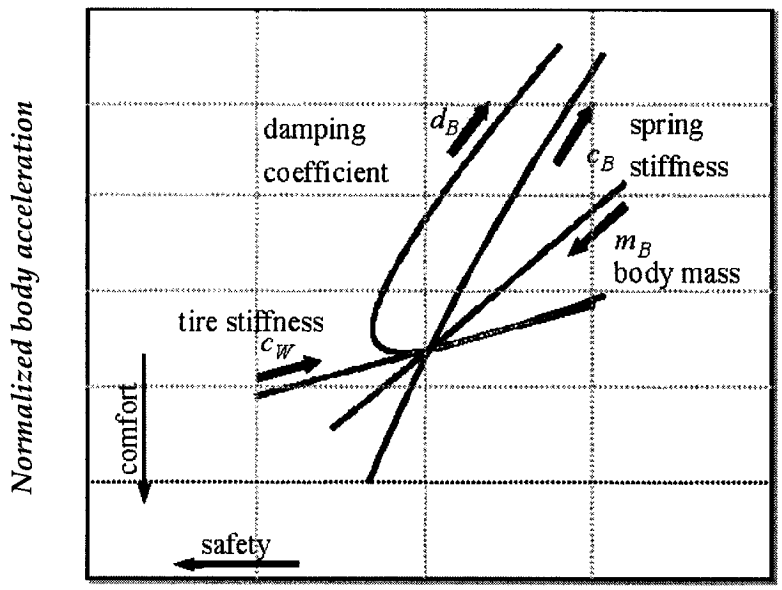

Figure 1.1: Conflict diagram representing influence of vehicle parameters (Ficher and Isermaan, 2004).

The conflict diagram represents the vehicle properties – driving comfort and safety- for a defined maneuver as a point in the Normalized Body Acceleration-Normalized Tire Load (ratio of dynamic load on tire to static load on tire) variation

diagram. It is evident that good suspension design should make compromise between safety and comfort. Respecting comfort considerations, the human body is more sensitive to vibrations generated within the frequency range of 4–8 Hz in the vertical direction and within the range of 1–2 Hz in other directions (Thomas, 1999).

Taking into considerations the conflicting performance requirements, vehicle suspensions are designed to achieve an acceptable compromise between the ride, handling and control performances. Majority of the modern vehicles use passive suspensions system consisting of a spring and a hydraulic device as damper. Traditional passive suspensions show linear symmetry properties in both compression and rebound cycle. The damping forces generated by such damper remains constant over the entire operating cycle. Passive suspension system used in today's vehicles shows highly nonlinear and asymmetric properties of suspension spring and damper (Ahmed, 2001; Warner, 1996; Rakheja and Ahmed, 1993; Rengarajan, 1991; Oueslati, 1990; Harrison and Harmond, 1986). The spring in such suspension is non-linear in nature and yields relatively low stiffness in the ride zone and progressively hardening characteristics under higher deflections. Furthermore, commercial vehicles use air springs to yield soft ride in the vicinity of the desired ride height, and asymmetric hardening and softening properties in compression and rebound, respectively. Modern passive suspensions utilize hydraulic dampers with either dual or multi-stage force-velocity characteristics. The dampers yield high viscous damping coefficient corresponding to low velocity and considerably lower damping coefficients at medium and high velocities to achieve better ride performance over a wide frequency range (Warner, 1996). The task of switching the damping coefficient from high to low is performed by pressure-sensitive valves tuned to operate at preset velocities across the suspension. Moreover, modern hydraulic dampers

yield asymmetric force-velocity characteristics in compression and rebound in order to achieve better compromise between ride and handling performance.

Efforts have been made over the years to make suspension system work in an optimal condition by optimizing suspension parameters. But because of the intrinsic limitation of passive suspension system, the improvement is effective only in a certain frequency range. An alternative to passive suspension system can be active suspension system. Active suspension system shows improved performance over a wide range of operating conditions. But due to the complexities associated with design, costs and energy demand of active suspension systems, it didn't gain popularity, and only few systems actually got to the market. The compromise between active and passive suspension can be semi-active suspension system, which was proposed in the early 1970's (Karnopp, 1974). A semi-active suspension utilizes a controller to moderate the damping properties of the damper over the operating cycle. In the event of control system failure, the semi-active suspension can still work in a passive manner, making it safe to use in vehicles. The semi-active suspension system combines the advantages of both active and passive suspensions; it provides good performance compared to passive suspensions and is economical, safe and does not require either higher-power actuators or a large power supply as required by active system (Yi and Song, 1999).

The damping force of conventional semi-active suspension dampers are regulated by adjusting the orifice area of the oil-filled damper, thus changing the resistance to fluid flow. But typically the speed of this change is very slow as mechanical motion involved in this operation. To overcome the performance limitation of the orifice type semi-active dampers, a new class of 'Smart fluid' based advanced semi-active damper has gained wide spread attention in academia as well in auto industries for their

attractive features and promising performance potential to overcome the limitations of existing dampers in market. There exist two different types of smart fluid - Electro-Rheological fluid commonly known as ER fluid, and Magneto-Rheological fluid commonly known as MR fluid. The operations of smart fluid dampers are based on alteration of fluid viscosity depending on an applied electric or magnetic field. These fluids consist of Electro-Rheological (ER) or Magneto-Rheological (MR) particles dispersed in ER or MR medium. The particles form chain-like fibrous structures in the presence of a high electric field or a magnetic field. When the electric field strength or the magnetic field strength reaches a certain value, the fluid suspension will be solidified and has high yield stress. Conversely, the suspension can be liquefied by removal of the electric field or the magnetic field. The process of change is very quick, and takes less than few milliseconds, and can be easily controlled. The energy consumption is also very small, only several watts. In general, the electric or magnetic fields is applied in the duct connecting the upper and lower chambers of a damper. Initially, ER fluid received most of the attention. But, eventually found to be not well suited due to their high voltage requirements to most applications as the MR fluid. Moreover, MR fluid based dampers have many attractive features such as high yield strength and stable hysteresis behavior over a broad temperature range (Yokoyama *et al.*, 2001).

Although there are several studies that investigates the vibration isolation performance of ER or MR based suspension damper concept with a set of parameter, there is a lack of comprehensive parametric study and investigation of isolation performance under shock excitations. The objective of this study is to compare vibration and shock isolation performance of four different suspension dampers with special emphasis on ER and MR damper. The dampers chosen for this investigation are - (a)

linear passive damper, which is used as base model to compare the performance of the candidate dampers, (b) two-stage asymmetric non-linear damper, commonly used in modern vehicles, which is a modified form of linear passive damper, (c) ER fluid based semi-active damper and (d) MR fluid based semi-active damper.

1.2 Literature Review

Earlier studies on passive suspension dampers encompass a diversity of subjects related to analytical model development, construction, role of various operating parameters, performance evaluations etc. Studies on ER and MR based damper include issues like behavior of ER and MR fluid, composition of the fluids, modeling of ER and MR fluid behavior, mode of operation, role of various operating parameters, various damper model based on ER and MR fluid, various control concept and their design to control the damping force of ER and MR damper, performance evaluation etc. The reported studies relevant to these topics are reviewed to gain understanding and background, and to formulate the scope of the investigation. The reported studies on linear passive, asymmetric non-linear, ER and MR damper are grouped in sequence and are presented in following subsections.

1.2.1 Passive Suspension Damper

Various kinds of passive suspension designs are being used in light vehicles as well as heavy vehicles. Light vehicles generally use McPherson strut suspension, coil spring suspension, wishbone or double-wishbone, multilink suspension in the front axle of the vehicle. Figure 1.2 illustrates the schematics of some of these suspensions. Heavy

vehicles employ coupled or beam axle suspension comprising springs (leaf, coil, air or rubber) in conjunction with hydraulic dampers, as shown in figure 1.3. As can be seen from these figures, regardless of configuration, the suspension system essentially comprises of a spring and a damper to act in parallel. In a passive suspension, the spring and damper can be linear or non-linear with fixed characteristics.

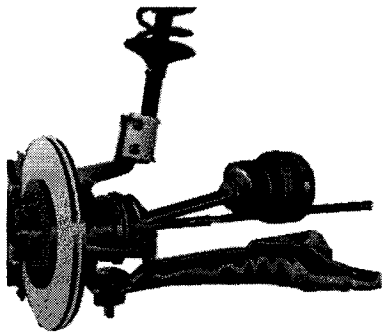

a) McPherson strut

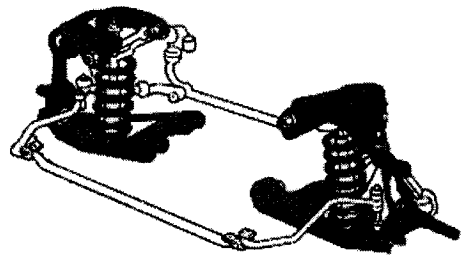

b) Coil spring type

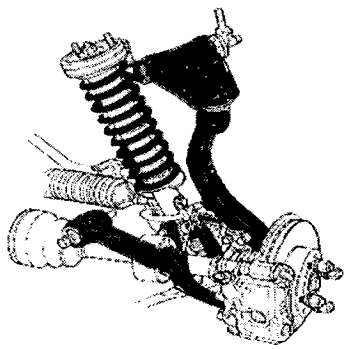

c) Double wishbone suspension

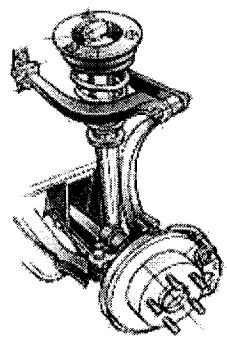

d) Multi link suspension

Figure 1.2: Schematics of some front wheel suspension system used in light vehicles (Parkin, 1999).

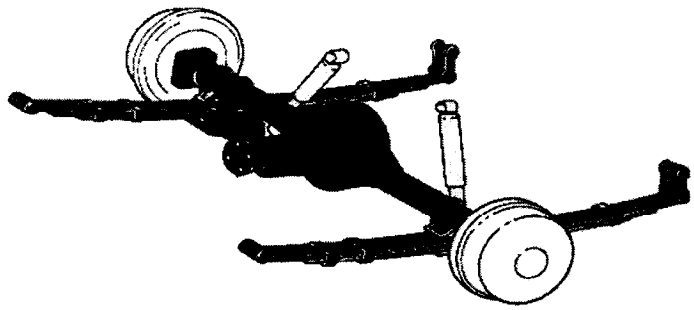

a) Solid axle, leaf spring system

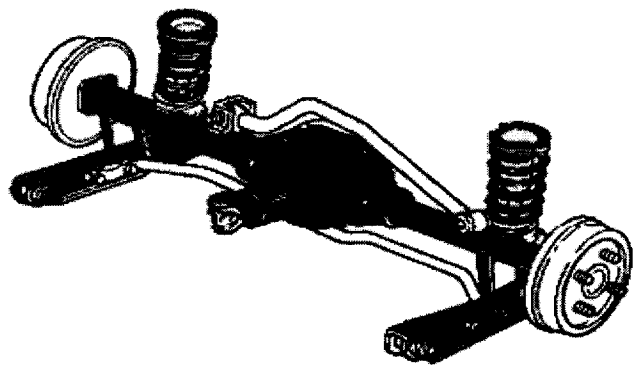

b) Solid axle, coil spring system

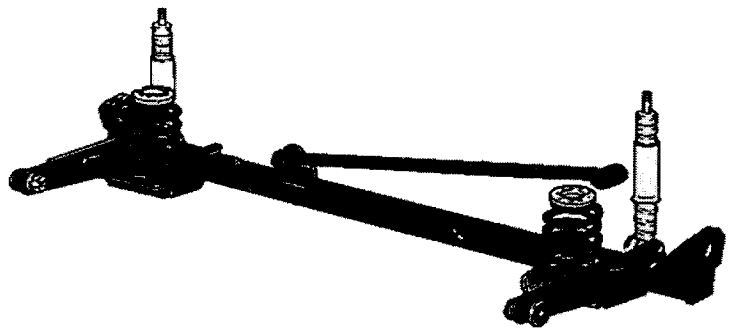

c) Beam axle system

Figure 1.3: Schematic of some rear wheel suspension system used in heavy vehicles (Parkin, 1999).

Suspension design plays an important role in the performance of vehicles like ride, handling and road holding capability. Most commonly used suspension system is passive suspension system. A passive system stores energy in a spring and dissipates it via a damper (Youn and Hac, 1995; Bastow, 1993). Figure 1.4 shows schematic of a simple vehicle model with passive suspension system. Soft suspension springs are desirable to achieve body vertical vibration attenuation at frequencies above 4 Hz, where the human body exhibit most sensitivity to vibration. The suspension systems are hence designed with soft springs to yield the vertical mode resonance of the sprung mass in 1.5 to 2 Hz range.

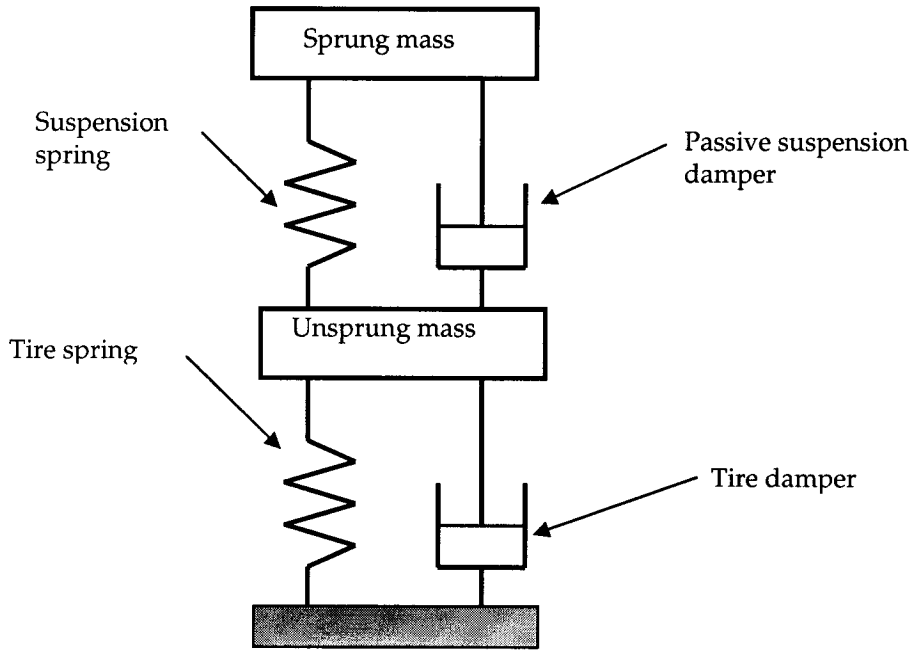

Figure 1.4: Schematic of a passive suspension concept.

Despite the fact that a softer suspension is desirable to enhance the ride vibration environment and dynamic pavement loading performance, the need of excessive rattle space (space required to accommodate the suspension spring motion) requirement is prohibitive in lowering the spring rates further. Moreover, soft springs causes excessive

body roll due to reduced effective roll stiffness of the suspension. To rectify the problem anti-roll bars are used in conjunction with soft suspension to limit the roll deflection of the body. A higher damping force is crucial to suppress the resonant motions of the vehicle body, while a lightly damped suspension might provide effective isolation from the road induced vibration (Wong 2001; Cebon 1999) at higher frequencies. Furthermore, a higher damping would lead to less variation in the dynamic forces and thus reduce the road damage potential. In general passive suspensions employ leaf, rubber, coil or air springs and hydraulic dampers. Hydraulic dampers dissipate energy through pressure drops across the orifices or valves. On the basis of construction, two basic design of hydraulic damper are in use today: (a) twin-tube design and (b) mono-tube design. Figure 1.5 (a) illustrates the schematic of a twin-tube hydraulic damper. The inner tube is known as the pressure or working cylinder, while the outer tube is known as the reserve tube. The upper mount of the damper connects to the vehicle frame, and the lower mount is connected to the unsprung mass, either directly or indirectly. The piston rod passes through a bushing and seal at the upper end of the pressure tube. The bushing keeps the rod in line with the pressure tube and facilitates the free movement of the piston. The outer or reserve tube is partly filled with hydraulic fluid and partly with an inert gas. The gas charge compensates for the flows due to area differential between the two sides of the piston and volume changes due to variations in the temperature. The flow from the pressure tube to the outer tube is controlled by a base valve located at the foot of the pressure tube. The damper piston consists of a series of bleed orifices and valves to permit the flows during compression and rebound.

The mono-tube damper has been studied extensively and described in the literatures (Causemann, 2000; Warner, 1996; Gillespie, 1992). This type of damper

usually consists of a high pressure gas tube. The pressure tube houses two pistons- a dividing piston and a working piston, as shown in figure 1.5 (b). The working piston and rod are similar to the double tube design. This piston also comprises a number of orifices and valves. The mono-tube design, consisting of the floating piston within the pressure tube, tends to yield considerably longer damper body for a specified rattle space. Some researchers have suggested an alternative design with an external accumulator containing a floating piston to reduce the damper body length, as shown in figure 1.5 (c) (Chaudhary, 1998; Joo, 1991; Sharp and Crolla, 1987).

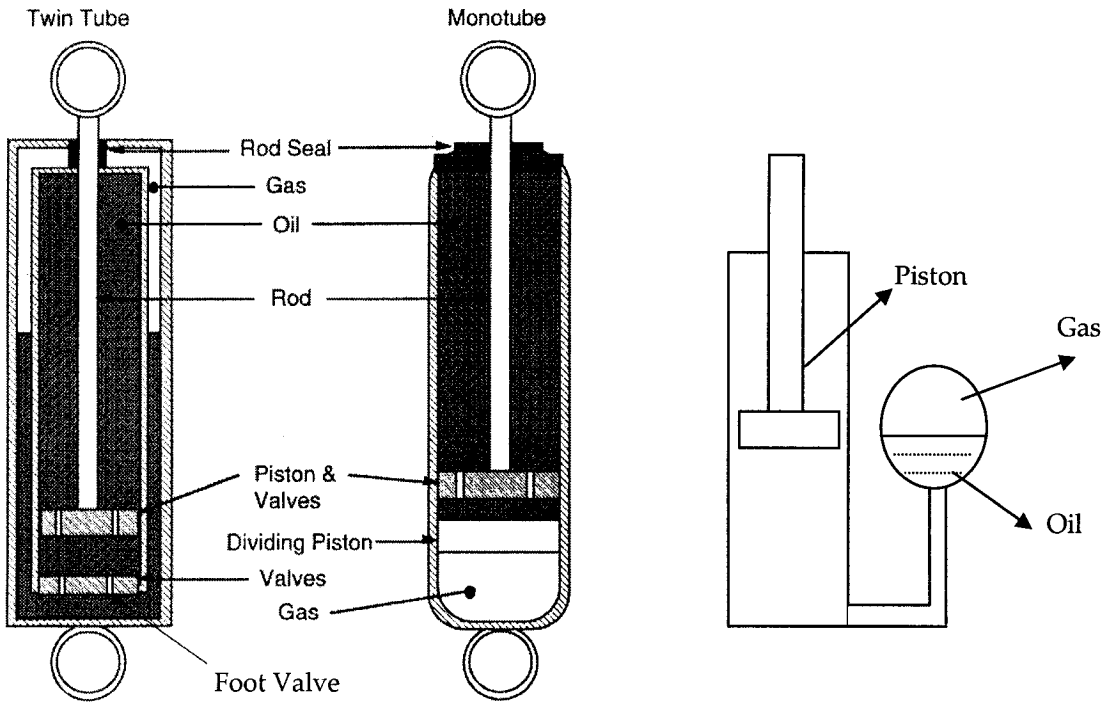

(a) (b) (c)

Figure 1.5: Different types of hydraulic damper: (a) Twin-tube , (b) Mono-tube (Gillespie, 1992) and (c) Mono-tube with an external accumulator (Joarder, 2003).

A twin-tube design has longer stroke capability and greater oil volume compared to a similar sized mono-tube unit. Thus, a twin-tube damper would provide

smoother ride characteristics. The twin tube dampers, however, often cause foaming of oil due to entrapped gas under extreme velocities or body temperature condition (Causemann, 2000). The damping characteristics of such dampers may thus deteriorate considerably under extreme operating condition. On the other hand the mono-tube design eliminates the potential for gas oil mixture and yields superior heat dissipation ability. However, the manufacturing cost of mono-tube damper is relatively higher due to precision requirements associated with high-pressure gas (Williams, 2000). Other shortcomings of the mono-tube designs include the susceptibility to side loads and dents. The variation of gas pressure caused by the increase in damper temperature tends to affect the ride height, and thus the aerodynamic losses, which could be a critical factor for racing vehicles (Warner, 1996).

Linear passive suspension system comprises of linear spring yielding linear force-deflection characteristics and hydraulic damper yielding linear force-velocity (f-v) characteristics over the operating range. However, this type of linear characteristics provides poor ride and handling performance. In order to overcome the performance limitation associated with linear passive suspension, modern passive suspension springs are designed to yield progressively hardening force-deflection characteristics, meanwhile the hydraulic dampers yield non-linear force-velocity (f-v) characteristics that are mostly asymmetric in compression and rebound. Various concepts of non-linear damping force, asymmetric in compression and rebound have been investigated using piece-wise linear formulations for the f-v characteristics. The studies have suggested that, higher damping in the rebound yields improved road holding and ride, while

lower damping coefficient at higher velocities could provide better ride (Rakheja and Woodrooffle, 1996).

The dynamic force generated by hydraulic dampers used in latest vehicles comprises of components like seal friction, gas spring effect and hydraulic flows. The contribution by hydraulic flows in the damping force is typically determined by the flows through the valves and orifices and pressure drop across the valves. The dampers invariably yield variable hydraulic resistance as a function of magnitude and direction of the piston velocity (Bert, 1973; Snowdon, 1968). Warner (1996) has described the effect of piston speed on the damper characteristics through extensive laboratory measurements and simulations. In his work, hydraulic resistance of the damper is controlled using various combinations of valving mechanisms, which are effective over different speed ranges. Based on measured force-velocity characteristics the author has suggested that the velocity ranges of a typical hydraulic damper can be termed as 'low', 'mid' and 'high'. Figure 1.6 illustrates the typical force-velocity (*f-v*) characteristics over the three speed ranges. Figure 1.7 illustrates the design of a hydraulic damper piston comprising deflection disc valves and bleed orifices. The pressure differential developed across the piston strongly dependent on the piston velocity relative to the cylinder. As shown in figure 1.7, the fluid flow at low speeds occurs through two paths: *(i)* through the bleed orifice(s); and *(ii)* leakage flow through the piston/wall clearance. Owing to relatively low-pressure differential developed at low velocity, the deflection discs remain closed. Although the leakage flow can affect the damping characteristics considerably, the low speed damping characteristics are mostly tuned through selection of number and size of the bleed orifices.

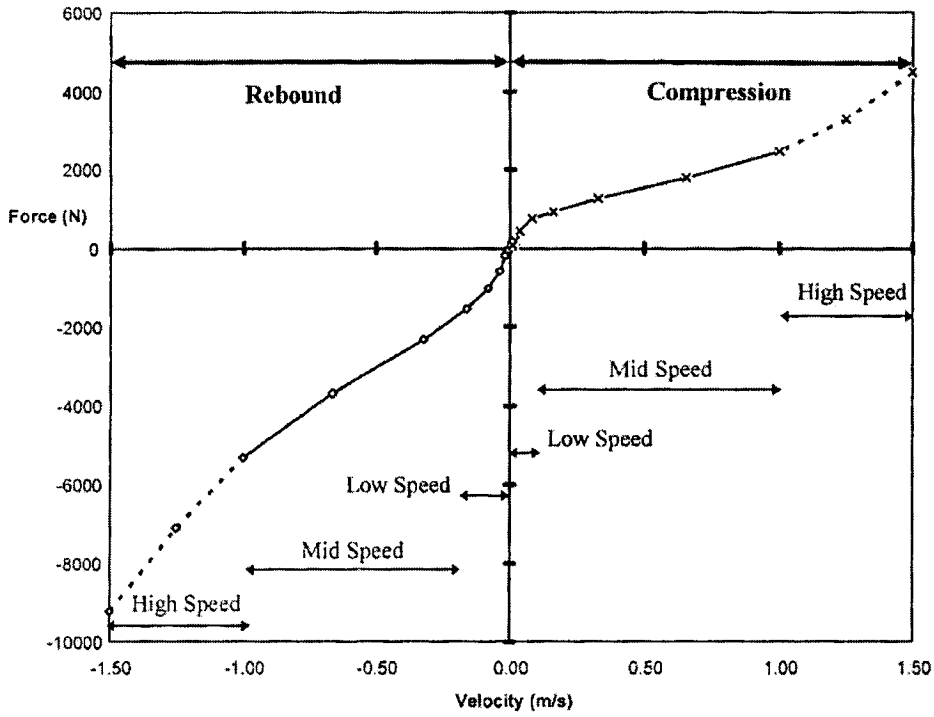

Figure 1.6: Force-velocity characteristics of a hydraulic damper (Warner, 1996).

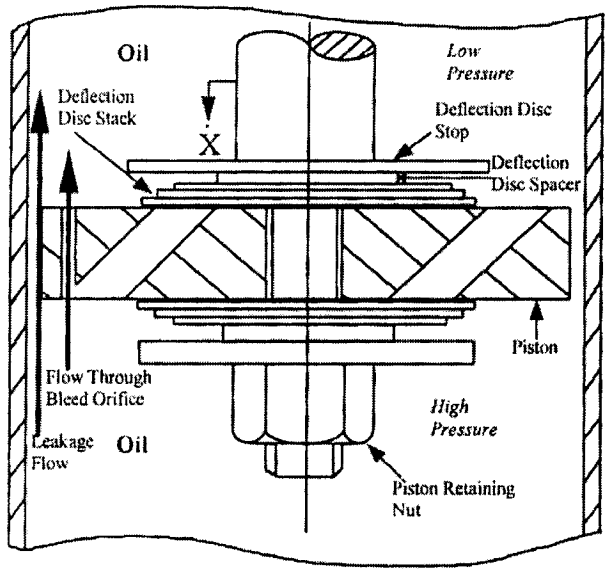

Figure 1.7: Schematic of a damper in compression mechanism for low speed (Warner, 1996).

An increase in the piston speed to the mid-speed range causes flows through three paths: (i) leakage flows, (ii) bleed orifice, and (iii) the deflection disc valves. The flows through the first two are similar to those described for the low speed, while the flows through the valve occur due to deflections of the discs caused by high pressure differential. The valve openings in compression and rebound differ due to different force-deflection characteristics of the deflection disc stack. Hence the mid-speed damping coefficients corresponding to compression and rebound are considerably different, as evident from figure 1.6. The flow areas for leakage and bleed flows are relatively small compared to deflection disc stack. As a result the flows through the deflection disc stack dominate the mid speed damping characteristics. A further increase in the piston velocity to the 'high speed' range yields higher deflection of the discs leading to higher flow path and thus considerably lower damping coefficient.

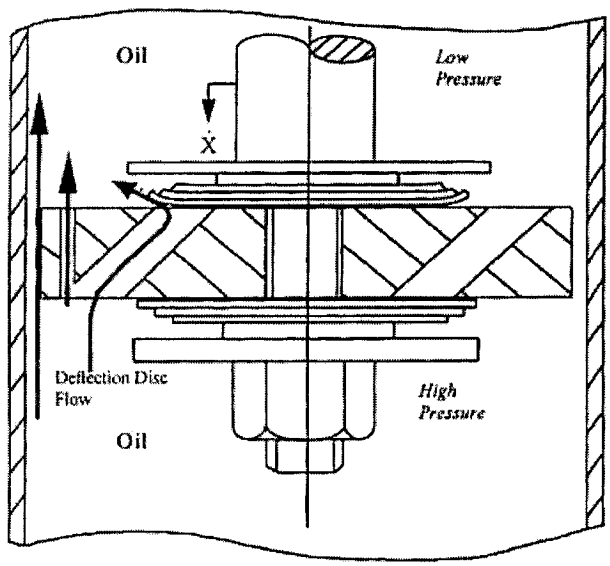

Figure 1.8: Schematic of damper compression mechanism for mid speed (Warner, 1996).

A different resistance combinations attribute to bleed orifices and valving, it is possible to achieve characteristics with digressive, linear and progressive segments, as evident in figure 1.9 (Causemann, 2000). The damping characteristics such dampers are generally determined using mechanical or servo-hydraulic test machine. At constant speed (rpm) a test machine produces various strokes in rebound and compression direction, and subsequently different compression and rebound speeds.

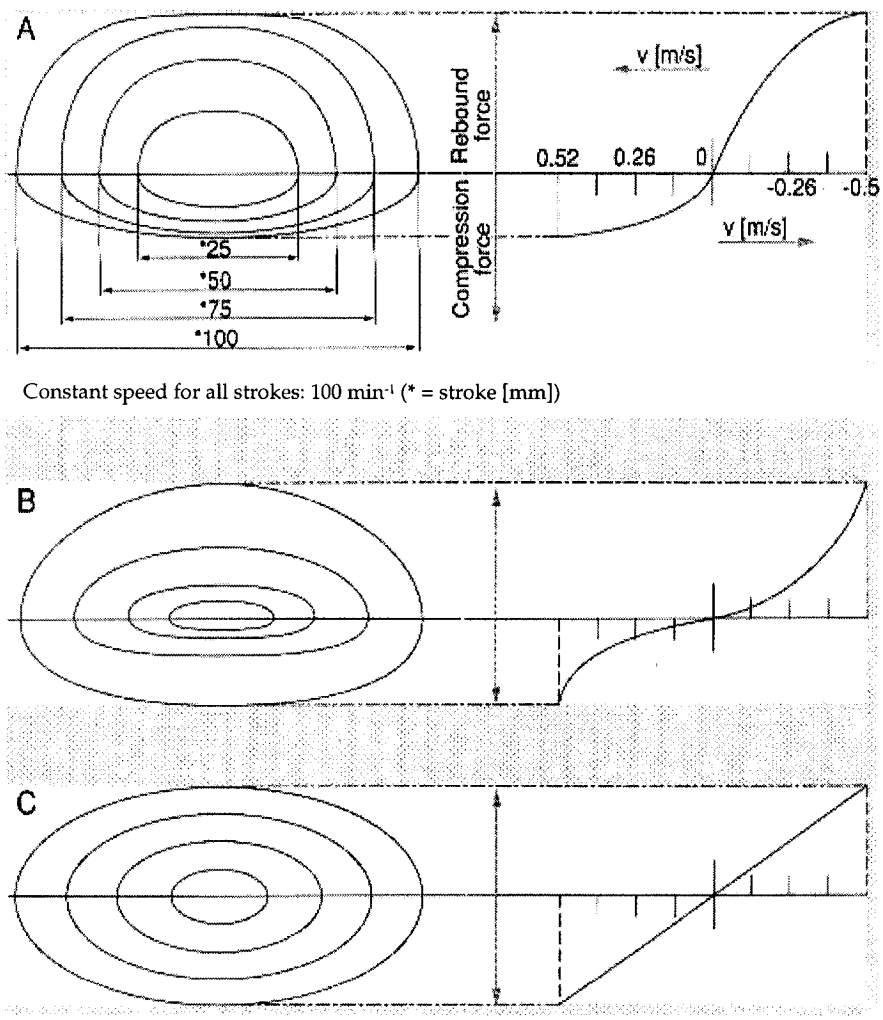

Figure 1.9: Typical force-displacement and force-velocity characteristics of non-linear asymmetric damper: A. Digressive, B. Progressive, C. Linear (Causemann, 2000).

In light of the intricacies associated with characterization and modeling of such damping phenomena and valving, the force-velocity (f-v) characteristics are widely used to study the role of damping design on the vehicle responses. The f-v characterization of the dampers establishes convenient relationship between damping force, and compression and rebound velocity. Such formulations, however, yield only maximum values of the damping forces in rebound and compression direction at various strokes or compression and rebound rates.

The ride dynamics models of various passive suspension systems reported in the literature have considered different forms of damping models ranging from simple linear viscous model to piece-wise linear models. Rajalingham and Rakheja (2003) investigated the influence of damping asymmetry on the displacement response of the sprung mass associated with orifice type hydraulic damper using a quarter-car model. Initially, the asymmetric damping mass is considered as a combination of linear viscous dampers with different damping coefficients in compression and rebound, as shown in figure 1.10. Subsequently, generalized piecewise linear models of suspension dampers have been proposed on the basis of measured force-velocity data acquired from a large number of suspension dampers. These models can be used to characterize both the symmetric and asymmetric force-velocity characteristics, as shown in figure 1.11 and 1.12. Despite the fact that, such models consider negligible contributions due to damping hysteresis, fluid compressibility and operating temperature, these models can provide an effective damping model to analyze the vehicle responses under variable damping. The symmetric force-velocity model is derived based on mean damping coefficients neglecting the contribution due to asymmetry (Rakheja and Ahmed, 1993). Earlier studies on passive dampers focus merely on the issues involving sprung mass

acceleration and were based on simple vehicle models. The discontinuities associated with switching of valves, responsible for deteriorating the performance of dampers, were not considered. Besides, the limited bandwidth of the valves allows damping variation at low frequencies only. A comprehensive study considering various passive models namely - linear, nonlinear symmetric, single stage asymmetric, and the two-stage asymmetric suspension properties was conducted by Joarder (2003) using a quarter car model. The study suggests that an asymmetric damping characteristic is responsible for ride height drifting. The drift increases with the increase of asymmetry and the excitation amplitude. However, the effect of pitch motion is neglected in this study.

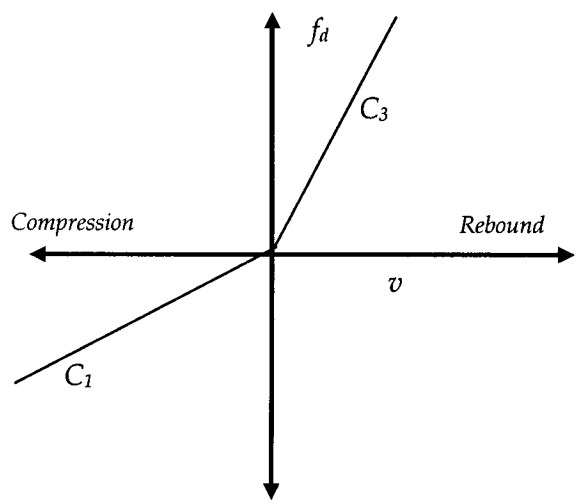

Figure 1.10: *f-v* characteristics of single-stage asymmetric non-linear damper (Joarder, 2003).

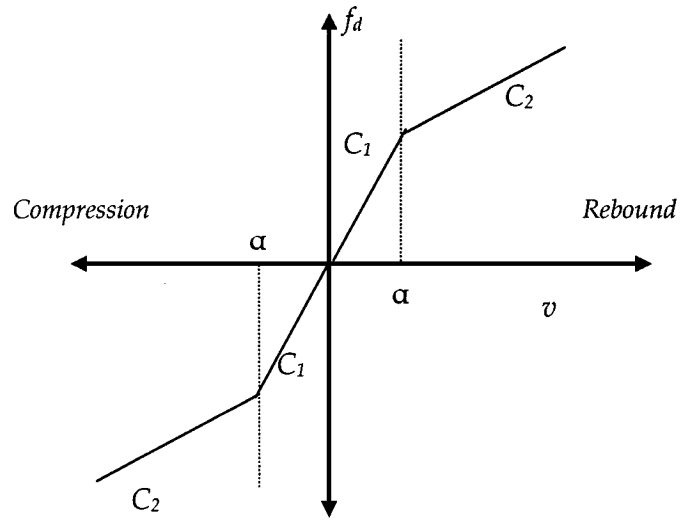

Figure 1.11: *f-v* characteristics of two-stage symmetric non-linear damper (Joarder, 2003).

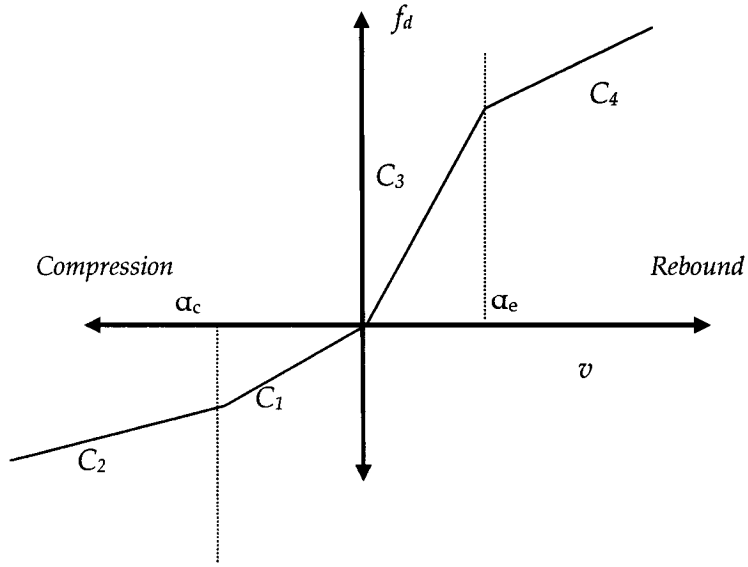

Figure 1.12: *f-v* characteristics of two-stage asymmetric non-linear damper (Joarder, 2003).

1.2.2 Electro-Rheological (ER) Fluid Based Semi-Active Suspension Damper

In the past decade, a new concept on 'Smart Fluid' based semi-active suspension damper has gained widespread attention for its attractive features and performance potential to overcome the performance limitation of existing dampers. A smart fluid is defined as one in which the resistance to flow can be controlled through the application of an electric or magnetic field. There are two main classes of smart fluid, one exploiting the Electro-Rheological (ER) effect, the other exploiting the Magneto-Rheological (MR) effect (Sims *et al.*, 1999). The pioneering efforts to discover and develop each class of smart fluid took place almost concurrently: Winslow (in 1947) described the ER phenomenon, while independent work by Rainbow (in 1948) introduced MR fluid (Jolly *et al.*, 1998). Table 1.1 shows basic comparison between ER fluid and MR fluid.

Table 1.1: Comparison between ER fluid and MR fluid (Lord Corporation, USA).

Property	*ER Fluid*	*MR Fluid*
Maximum Yield Stress	2-5 kPa	50- 100 kPa
Maximum Field	Approximately 4kV/mm (Limited by breakdown)	Approximately 250 kA/m (Limited by saturation)
Viscosity	0.1 – 1.0 Pa-s	0.1 – 1.0 Pa-s
Operable Temperature Range	10° to 90 ° C (Ionic, DC) - 25 to 125° C (Non- ionic, DC)	- 40° to 150° C (Limited by carrier fluid)
Stability	Cannot tolerate impurities	Unaffected by most impurities
Response Time	Less than 1 millisecond	Less than 1 millisecond
Density	1-2 g/cm^3	3-4 g/cm^3
Maximum Energy Density	0.001 Joule/ cm^3	0.1 Joule/ cm^3
Power Supply (Typical)	2-25 kV at 1-10 mA (2-50 Watts)	2-25 V at 1-2 A (2-50 Watts)

This type of fluids can be used for constructing controllable damping devices that can generally outperform traditional passive dampers and can provide satisfactory performance without involving cost, weight, and complexities associated with fully active system.

ER fluids typically consist of dispersion of solid particles within insulating oil. Winslow (1949), in his pioneering experiments used a variety of solid particles (e.g. starch, stone, lime, gypsum, carbon, and silica) dispersed in various type of insulating oil. Using these materials, he showed that the resistance to flow of such fluid could be significantly enhanced through the application of an electric field. Unfortunately, early reports of the performance of such fluids showed the fluids as abrasive, chemically unstable, and likely to suffer rapid deterioration (Sims *et al.*, 1999). Although US Military conducted some interesting application studies, the early promise of commercial exploitation did not materialize (Stanway *et al.*, 1996). About 30 years after Winslow's pioneering efforts, interest in engineering applications of ER fluids was revived by researchers like Stangroom (1983). He described the composition of ER fluids containing non-abrasive, micron-based polymer particles dispersed in a silicon oil carrier fluid. Brooks (1982) has described engineering devices based on this new generation ER fluid. This renaissance of ER fluid and ER based applications sparked renewed worldwide interest in exploring possibilities for commercial exploitation of fluids and devices (Sims *et al.*, 1999).

The operation of ER fluid based damper is based on the alteration of fluid viscosity triggered by an electrical stimulus. This is done by subjecting the ER fluid to an electric field of up to 6 kV/mm intensity. Under the application of electric field, the fluid particles form chain-like crystallized body-centered-tetragonal (b.c.t) lattice. When the

electric field strength reaches a certain value, the fluid suspension will solidify and has high yield stress, and requires higher force to break the chain. Conversely, the fluid suspension can be liquefied by removal of the electric field (Sims *et al.*, 1999). This phenomenon is presented in figure 1.13 (Hao, 2002). The parallel dark lines in the figure stands for two electrodes and black circles represent ER particles.

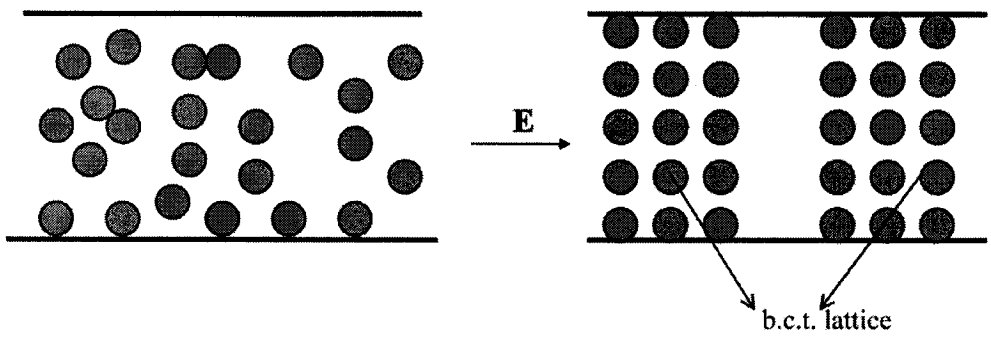

Figure 1.13: Schematic Illustration of the structure change of an ER Fluid: (a) before, and (b) after, an external electric field is applied (Hao, 2002).

After the breakthrough of 1980's, many attempts have been made by researchers to develop ER fluid for commercial production. Most of ER fluids are made of solid particulate material dispersed into an insulating non-polar liquid. The solid particulate material used in ER fluid includes inorganic non-metallic, organic and polymeric semi-conductive materials. The inorganic materials are essentially ionic crystalline material, while organic and polymeric semi-conductive materials usually have a pi (π) bond conjugated structure, and are conductive materials. The continuous liquid phase is usually silicone oil, vegetable oil, mineral oil, paraffin and chlorinated hydrocarbon oil. A good ER fluid should have: (a) a high yield stress preferably equal to or larger than 5 kPa under an electric field of 2 kV/mm, (b) a low current density passing through the

ER fluid preferably less than 20 $\mu A/cm^2$, (c) a wide working temperature range (-30 to 120°C), (d) a short response time, (e) high stability (Hao, 2002). Typically, ER fluids develop stress up to 10kPa (Bayer AG, 1994), and the response time is in the range of 10^{-3} s. For some specific purposes, an even faster response accompanied by high stability is required. In general, particle size is between 0.1 and 100 μm, and the particle volume fraction is between 0.05 and 0.50 for ER fluid (Hao, 2002).

Among various promising materials for ER fluids, semi-conducting polymers, including poly (acene quinone) radicals, polyaniline, copolyaniline, poly (p-pheneylene) and polymer-clay nanocomposite have been adopted as anhydrous ER fluids because of their ease in handling and superior physical properties and mesoporous molecular sieve (Kim *et al.*, 2001). Despite numerous design, construction and testing of prototype devices based on ER fluids conducted by academic researchers and by industries, mass production of ER fluids are still awaited. However, limited scale commercial ER fluids are now available from various manufactures like Bayer AG (1994).

One of the challenges of using ER fluid based damper is to model the ER fluid behavior. ER fluids behave like simple viscous fluids in the absence of an electric field, and the behavior can be described by the Newtonian shear model. Under the application of electric field, the fluid exhibits a yield phenomenon and the material does not flow until the critical yield stress value is exceeded. This yield stress value nominally increases as a quadratic function of the applied electric field. Bingham model is an idealized model to describe this yield phenomenon. The model is a good approximation for the post yield behavior, and can be used as a starting point for damper design (Kamath *et al.*, 1996, Gavin *et al.*, 1996). The Bingham plastic is used for quasi-steady loading (Kamath *et al.*, 1996). But, under dynamic loading conditions, the pre-yield

behavior, which is ignored by Bingham model, plays an important role in determining the overall dynamic characteristics of the damper. Furthermore, Bingham plastic model does not account for frequency and amplitude of excitation under dynamic loading conditions, which must also be considered (Kamath and Wereley, 1997). Hong *et al.* (2003) have proposed five different models to predict the field-dependent damping force of an ER damper. The models are Bingham plastic model, hysteresis bi-viscous model, Bouc-Wen model and hydro-mechanical model. The parameters of the models are identified using a set of experimental data that are obtained by changing electric field and excitation frequency. The study shows that pre-yield hysteresis behavior of ER damper can be analyzed in a number of ways. Chen *et al.* (2001) have shown that response of systems with ER damper can be analyzed by using viscous and bilinear hysteresis model. Wereley *et al.* (2004) have designed and fabricated an ER mono-tube damper fitted with an ER valve in the piston head as well as a leakage valve. The apparent viscosity of ER fluid based on Bingham plastic analysis with leakage showed accuracy for experimental force-displacement and force-velocity behavior. The analysis using apparent bi-viscous constitutive behavior improved the correlation with damping measurements which demonstrates that ER damper exhibits apparent bi-viscous behavior when it is augmented with a leakage or piston bleed valve.

In general, there are three main modes of operation for ER damper devices: flow, shear, and squeeze. In flow mode, the fluid is forced between a pair of stationary electrodes, and the resistance to flow is controlled by adjusting the applied electric field. In shear mode, the electrodes can move in relation to each other. This occurs if they are placed on the piston and cylinder walls, and the fluid is forced between them. Finally, in squeeze mode, the fluid between the electrodes is squeezed as the electrode gap

changes. This occurs when the electrodes are placed on the piston head and cylinder end (Sims *et al.*, 2000). Study of ER dampers by Kamath *et al.* (1996) suggest that, mixed mode dampers have higher passive damping than flow mode dampers, and the active damping characteristics of both the fixed and moving electrode dampers are very similar.

Earlier researchers like Petek (1992) designed suspension system using ER fluid to validate the use of ER technology in damper applications. In this design, the ER fluid is placed directly inside the annular duct of the damper. Under the application of voltage, electric field is created perpendicular to the fluid flow, which increases pressure drop requiring higher force to move the piston and causes slow displacement of the piston. As a result improved vibration isolation is achieved.

Construction of ER damper has significant influence on its performance. Researchers have developed different types of configurations to maximize the benefit of using ER based system. Shaohua and Meiyan (2001) have developed an ER damper consisting of three concentric cylinders (inner, middle and outer). The damper piston is laid in the inner cylinder which is separated into two cavities. Experimental results concluded that, increase in electric field strength increases apparent viscosity of ER fluid, and temperature rise reduces the viscosity of ER fluid. Furthermore, with the increase of frequency and amplitude, velocity of ER fluid flowing through electric field increases and makes the shear rate of ER fluid to increase. As a result, the apparent viscosity of the fluid and the damping force decreases.

Damping force generated by ER damper is composed of two parts: background damping and electric induced damping. The background damping is determined mainly by the construction of damper, and the electric induced damping is determined by the

applied electric field. The rate of electric to background damping shows that the adjustability of ER damper is dictated by electric field strength and the apparent viscosity of ER fluids. The to-and-fro flow of ER fluid between two cavities of the damper is also the function of electric field strength.

Typically, semi-active control is used to control the damping force generated by ER damper. With the use of semi-active control, ER damper works as semi-active suspension system. A schematic of semi-active suspension is shown in figure 1.14.

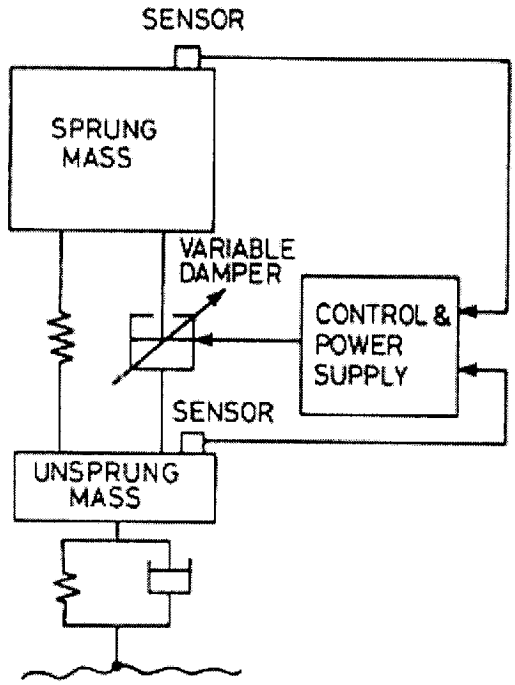

Figure 1.14: Concept of a semi-active suspension (Wong, 2001).

Yeo *et al.* (2001) have compared four different ER fluid dampers to determine the Bingham characteristics and response time using a quarter car model. Of them one was fabricated with Arabian glue and rests were produced by Loctite (Henkel, Germany),

Bayer AG, Germany, and Shokubai, Japan. Results of the study suggested that, at sprung mass natural frequency, vibration isolation can be improved up to 50% by using sky-hook controller, indicating the feasibility of ER fluid damper for use in suspension system. But, the absence of a controller increases the transmissibility by an amount of 25% compared to a passive damper. This is due to the fact that the damping force generated without proper controller is merely the result of viscous damping without ER effect, and it is not enough for vibration isolation. Thus, it is better to use linear passive damper than to use ER damper without controller. At the unsprung mass natural frequency, the gains are almost the same without drastic difference. The unsprung mass transmissibility shows that vibration characteristics using sky-hook control scheme is worse than system with no-controller or passive damper. It is observed that, vibration isolation decreases rapidly with increase of time delay. The authors have suggested that the response time should be within 70 ms to achieve vibration isolation up to 50% of passive suspension system. For isolation up to 30% the response time less than 236 ms is required.

Other researchers have also used sky-hook controller in their damper design and have seen improvement in terms of vibration. Suh and Yeo (1999) developed and manufactured an ER damper based on Bingham-plastic model and employed Sky-hook control algorithm to control the damping force. The model is incorporated in a quarter car model and subsequently to a real car. Results showed better vibration isolation than passive damper. Yeo *et al.* (2001) have also used sky-hook control algorithm and saw improvement in performance.

Sims *et al.* (1997) have suggested that it is possible to apply a linear control strategy in non-linear ER damper. The authors have derived a quasi-steady model of ER

damper under proportional feedback. It was observed that linear input-output characteristics can be obtained over a range defined by the open loop force-velocity characteristics of the ER damper. Furthermore, the force velocity characteristics (i.e. effective damping coefficient) can be pre-specified by defining the value of gain term in the feedback model. Nakano (1995) presented an ER fluid based damper. The damper model in conjunction with a quarter car model and a feedback controller provides improved vibration isolation. Choi and Kim (2000) have developed an orifice type ER damper controlled by the intensity of electric field as well as piston motion. The damper is incorporated with a full-car model to evaluate performance under bump and random road profiles employing an optimal controller and observed to improve ride quality.

Various dampers based on industry developed ER fluids have also been studied by researchers in combination with different type of damper configurations. Sassi *et al.* (2003) have retrofitted a classic passive damper with commercial ER fluid Rheobay VP AI 3565, developed by Bayer AG, Germany. The model is tested for different speeds and electric fields. Results showed that, the generated damping characteristics could be drastically changed when an electrical field is induced inside the damper and when the size of the movable electrode is increased. The numerical results showed that an optimal damping value should be obtained to provide a compromise between vehicle stability and ride comfort. The authors have suggested that on-off type controller is not suitable for this type of damper. Instead, the controller should vary the applied high voltage based on input excitations. The damper has shown significant improvement compared to a passive suspension damper.

Same fluid (Bayer Rhobay 3565 ER fluid) is used by Lindler and Wereley (1999) to develop a double adjustable type ER fluid based shock absorber. Results indicates

that an applied electric field in the gap between the cylinder electrodes increases the yield stress of the fluid between the cylinders, which alters the velocity profile of the fluid and raises pressure required for a given flow rate. The experimental results also demonstrated that an eccentricity between the two cylinder electrodes allows electric control of post-yield damping coefficient.

Kamath and Wereley (1997) have designed and fabricated a mixed mode moving electrode type damper for aerospace application, using the VersaFlo ER-100 type fluid manufactured by Lord Corporation, USA. The damper consists of two electrodes, moving relative to each other. The resisting force of the damper is then the sum of the viscous drag due to relative motion between the electrodes and the pressure drag force created through the electrode gap. The model was subjected to a sinusoidal excitation frequency of 10Hz, electric field between 0 and 3 kV/mm and displacement amplitude of 0.5, 1.0, and 3.0mm. The results indicated improved vibration isolation. The authors have suggested possible use of that this type of dampers for automotive applications to achieve improved vibration isolation performance.

Although numerous works have been done on ER based damper design, field test of the damper has not gained that much attention. Only a few researchers like Choi *et al.* (2001) undertook field test to evaluate performance characteristics of a semi-active ER suspension system associated with a skyhook controller. For the study, four individual ER dampers are manufactured and are experimentally evaluated to determine field dependent damping characteristics of the candidate dampers. Subsequently, the dampers are assembled in a road vehicle and various tests are performed. It has been demonstrated through bump and sinusoidal road tests that ride comfort of vehicles can be significantly improved by controlling the semi-active ER

suspension system. Improvement of the steering stability is also observed as a result of reduction of the pitch and roll motion. The result proved that ER fluid based system can be effectively employed to the passenger vehicle and can improve both ride comfort and handling performance.

To overcome the performance limitation of existing ER fluids, polyurethane based fluid is proposed by Bloodworth and Wendth (1995). This fluid can be used in a standard automotive damper modified with ER valve, and can generate variable damping forces in the range of 2-6kN, thus demonstrates the practical utility of this type of ER fluid. The fluids exhibit a stable ER effect which remains virtually unchanged even after prolonged use at elevated temperatures and high shear stress.

One of the major drawbacks of ER damper is its high voltage requirement, which in someway made it less favorable for automotive application. To address this issue, Kim *et al.* (1999) have presented an ER suspension system with an energy regenerative mechanism which can generate electric field required to achieve satisfactory damping force without external power source. In this system, the reciprocal motion the ER damper is converted to rotary motion, which in subsequently amplified by gears and makes a generator to produce electricity. The system was tested using an on-off controller and was found to provide favorable vibration isolation performance. The power produced was enough to operate the ER suspension system for a passenger car.

1.2.3 Magneto-Rheological (MR) Fluid Based Semi-Active Suspension Damper

Over fifty years ago both Rabinow and Winslow described basic MR fluid formulations that were as strong as the MR fluids of today. The MR fluid used by Rabinow consisted of nine parts by weight of carbonyl iron to one part of silicone oil,

petroleum oil or kerosene. Optionally he would add grease or other thixotropic additive to this suspension to improve settling stability (Carlson, 2001). A typical MR fluid described by Winslow consisted of 10 parts by weight of carbonyl iron suspended in mineral oil. To this suspension Winslow would add ferrous naphthenate or ferrous oleate as a dispersant and a metal soap such as lithium stearate or sodium stearate as a thixotropic additive (Carlson, 2001).

In general, MR fluids are dispersions composed of meso-scale (1–10 μm) ferromagnetic or ferrimagnetic particulates dispersed in organic or aqueous carrier liquid (Genç and Phulé, 2002). A typical MR fluid consists of 20-40% by volume of relatively pure soft iron particle, suspended in carried liquid like mineral oil, synthesis oil, water or a glycol (Carlson, 2000). Similar to ER fluid, MR fluid did not receive much attention till mid 1990's. In past few years, many different ceramic, metal, and alloy based compositions have emerged, which can be used to prepare MR fluid. The most common magnetic material used for MR fluids preparation is high purity iron powder derived from decomposition of iron penta-carbonyl (Genç and Phulé, 2002).

In the 'off' state, in terms of their consistency, MR fluids appear similar to liquid paints and exhibit comparable levels of apparent viscosity (0.1–1 Pa/s, at low shear rates) (Carlson and Weiss, 1994). Under the application of magnetic field generated by series of magnetic coil under the application of the command current, considerable increase of the static yield stress of MR fluid occurs. As a result MR particles become magnetized and behave like tiny magnets. Magnetic interaction energy between these particles is minimized when they line up along the direction of the magnetic field. A high shear stress or pressure difference is required to break this structure formed in MR

fluids. The field causes the iron particles in the MR fluid to form a chain in the direction perpendicular to the flow of fluid through the orifice, increasing the fluid's apparent viscosity. This effect is illustrated in figure 1.15. The fluid is capable of changing from a free-flowing liquid to a near solid state in less than 10ms, enabling real-time control of damping force (McManus *et al.*, 2002).

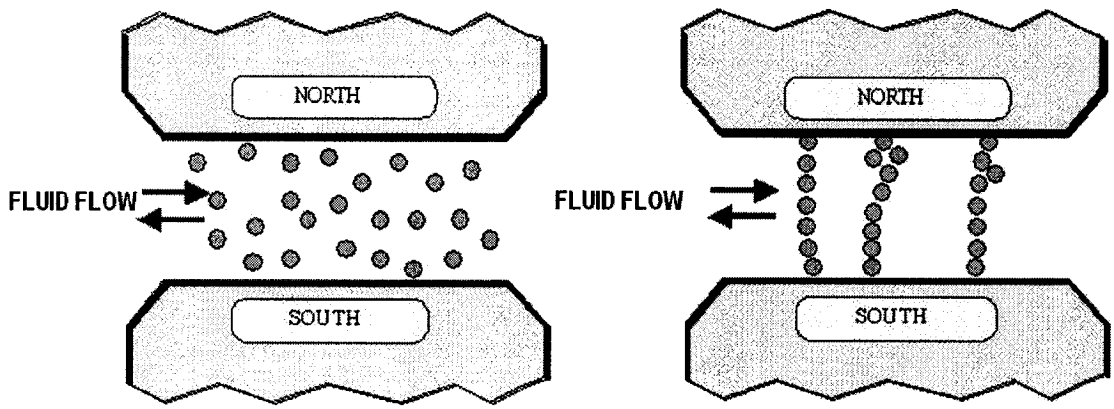

Figure 1.15: Response of MR fluid to applied magnetic field (McManus *et al.*, 2002).

The strength of the fluid (i.e. the value of static yield stress) increases as the applied magnetic field increases. The increase, however, is nonlinear since the particles are ferromagnetic or ferrimagnetic, and the magnetization in different parts of the particles occurs non-uniformly (Ginder and Davis, 1994). Depending upon the composition of MR fluid and the flux density generated by the applied magnetic field, the fluid can develop a dynamic yield stress up to about 100 kPa (Phulé and Ginder, 1997). Higher saturation magnetization materials can increase the maximum dynamic yield stress of the fluid. But the cost and availability of such materials are the limiting factors here. The yield stress development in MR fluids can occur within few milliseconds if the electrical circuit responsible for generating the magnetic field is

optimized (Phulé, 2001). Depending on the magnetic circuit design, this response time is about 10–20 ms. Thus MR fluids represent one of the fastest electromechanical interfaces for mechanical applications (Genç and Phulé, 2002).

A large number of studies attempted to characterize the behavior of the MR fluids. Studies on magnetic properties of MR fluid suggested that, the fluid is rapid, reversible, reliable, and can have smooth transition from a free flowing state to a semi-solid state upon the application of external magnetic field (McManus *et al.*, 2002; Simon *et al.*, 2001). These studies have also demonstrated that MR fluid possess many attractive features such as high yield strength, low viscosity and stable hysteretic behavior over a broad temperature range.

The quality of a good MR fluid depends on the type of application in which the MR fluid is used, operating conditions and length of exposure. MR fluid suitable for one application may not work for another type of device. In considering the quality of an MR fluid it is important to consider the actual operating conditions rather than just the rheological behavior measured under normal laboratory conditions. MR fluid durability and life are considered to be significant barriers to commercial success than yield strength or stability (Carlson, 2001).

Choi and Wereley (2001) have compared the performance of ER and MR based damper by introducing a non-dimensional input called Bingham number, which is a measure of relative importance of field-dependent yield stress and the viscous stress. The results of the analysis showed that ER valve has higher dynamic pressure range and faster response time than MR valve for the same Bingham number. But practical value of Bingham number is limited by factors like dielectric breakdown, saturation etc. Based on practical values of Bingham number, ER valve shows faster response time, but does not

have higher pressure range than MR valve. This indicates that, ER fluid-based system is suitable for practical applications demanding relatively low controllable performance and fast response time while MR fluid-based system is suitable for applications with relatively high controllable performance and slow response time.

A wide range of MR fluid based dampers are currently being explored for the potential implementation in vehicle suspension. Several analytical and experimental studies have clearly established superior potential performance benefits of MR dampers in vehicle applications in relation to conventional hydraulic dampers (McManus *et al.*, 2002). MR dampers offer high viscous damping corresponding to high velocities in the pre-yield condition, while the post-yield saturation corresponding to high velocities can be characterized by a considerably lower viscous damping coefficient.

The conflicting requirements of adequate ride, road-holding, handling and directional control stability performance of the road vehicles entails variable damping (Milliken and Douglas, 1995), which could be achieved using MR damper with minimal power consumption. The semi-actively controlled MR fluid damper offer rapid variation in damping properties in a consistent fail-safe manner, since they continue to provide adequate damping, in a passive manner, in the event of a control hardware malfunction (Carlson and Sproston, 2000).

The instantaneous damping force developed by MR damper is directly related to the command current generated by controller. The typical force-velocity (f-v) characteristics of MR damper is illustrated in figure 1.16. The curves presents the damping force generated under different values of control current, ranging from 0 to 1.5 A. The curves presented in the figure reveal nearly symmetric f-v characteristics in the compression and rebound.

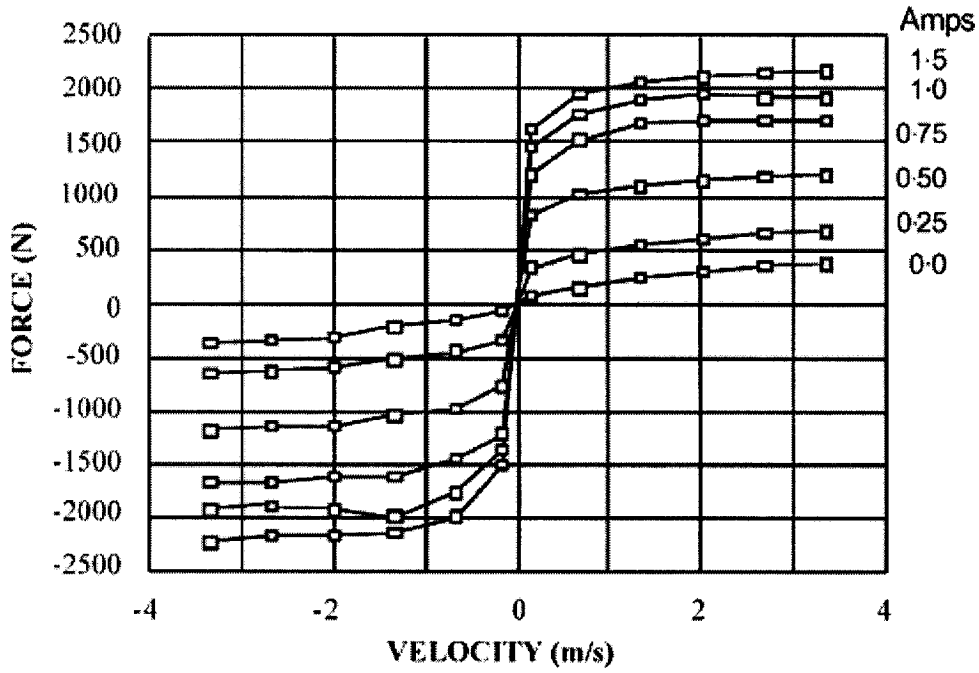

Figure 1.16: *f-v* characteristics of a MR fluid damper as function of coil current (McManus *et al.*, 2002).

Under low-to-medium levels of control current the *f-v* curve may be considered to provide two-stage damping: a high damping coefficient at low velocities and a lower coefficient at higher velocity. The transition from high-to-low damping coefficient occurs at a preset velocity. Under higher level of control current, the *f-v* curve can be considered to provide three sequential stages defining a maximum damping coefficient at velocities less than 0.02 m/s, an intermediate value at velocities from 0.02 to 0.06 m/s and a low coefficient at high velocities (McManus *et al.*, 2002).

The results presented in figure 1.16 shows the mean *f*-v characteristics corresponding to piston velocities, assuming negligible hysteresis. In reality, MR dampers invariably exhibit strong hysteresis and force-limiting nonlinearities, resulting from pre-yield behavior at low velocity and post-yield saturation at high velocity. The hysteretic *f-v* characteristics of such dampers are strongly dependent on the applied

control current, frequency and magnitudes of excitations, magnitudes of position and velocity of the piston in a nonlinear manner (Choi *et al.*, 1997; Spencer *et al.*, 1997; Wereley *et al.*, 1999; Muriuki *et al.*, 2003). The presence of hysteresis could cause a number of undesirable effects, including loss of control, poor robustness, limit life cycle and steady-state error etc. (Khalil, 2002). The hysteresis behavior could also yield considerable error in the tracking control (Wen, 1976).

Only few studies have attempted to characterize the hysteretic *f-v* properties of such dampers (Muriuki *et al.*, 2003; Wereley *et al.*, 1999, Choi *et al.*, 1997; Spencer *et al.*, 1997), while the theoretical characterization over a wide range of excitation frequency condition has not yet been reported. Considerable efforts have been made to characterize the hysteretic properties of such a damper using regression based models in order to facilitate the development and implementation of an effective controller for realizing desirable controlled variations in the damping force. Ma *et al.* (2002) have tested a cylindrical type MR damper model RD-1005-3 manufactured by Lord Corporation. The authors have used Equivalent Characterize Method (ECM) on the basis of the experimental data to formulate a hysteresis model synthesis to characterize the hysteric and non-linearity function of the MR damper. The analytical model can approximately present the hysteretic characteristic of the MR damper. Choi *et al.* (1997) formulated the hysteretic steady state dynamic characteristics of the MR-fluid damper using an algebraic formulation derived from the experimental data. The formulation comprised of two polynomial functions to match both the positive and negative acceleration curves of the hysteretic *f-v* cycle. The model could describe the steady state dynamic properties of the MR-fluid damper under specific excitation condition.

Wereley *et al.* (1999) have reviewed various models to characterize the damping behavior of MR damper under sinusoidal loading. The models include linear and viscous damping model, nonlinear Bingham plastic model, nonlinear bi-viscous model and non -linear hysteretic bi-viscous model. The study did not consider the control property and the effect of excitation. Among the models, the nonlinear hysteresis bi-viscous model considers the hysteresis behavior using the piecewise linearization technique and the model results are correlated with the experimental data under fixed excitation condition and control current. Bitman *et al.* (2001) have suggested that the Bingham plastic model has a zero shear stress discontinuity, which leads to inaccuracies in modeling and simulation. Instead of Bingham model, they have suggested Eyring model, which has a smooth transition through the zero shear rate condition, and also has two rheological constants for a constant field. Spencer *et al.* (1997) proposed a model combining the Bouc-Wen hysteron and a linear viscous damper and a spring in parallel, which can be formulated by a set of differential equations. The Bouc-Wen model accounts for the hysteresis effects that are commonly observed by MR dampers. The results revealed that the damping force varies with control signal in a linear manner.

The other flaw with MR fluid based system is the viscosity of MR fluid, which is highly sensitive to temperature. As a result, the damping force is a function of temperature (Gordaninejad and Breese, 1999). The test on a prototype MR damper conducted by Gordaninejad and Breese (1999) shows that, with the rise of temperature viscosity decreases and consequently the damping force decreases. The increase of current input further decreases the damping force. This is due to the increase in the input electric power to the system. The amount of force decrease is significant and can have major impact on the control system design of MR fluid dampers.

Most devices that use MR fluid can be classified as having either fixed poles (pressure driven flow mode) or relatively moveable poles (direct-shear mode). Figure 1.17 shows schematic of operational model of MR damper. Examples of pressure driven flow (PDF) mode devices include servo-valves, dampers and shock absorbers. Examples of direct-shear mode devices include clutches, brakes, chucking and locking devices. A third mode of operation known as squeeze-film mode has also been used in low motion, high force applications Jolly *et al.* (1998).

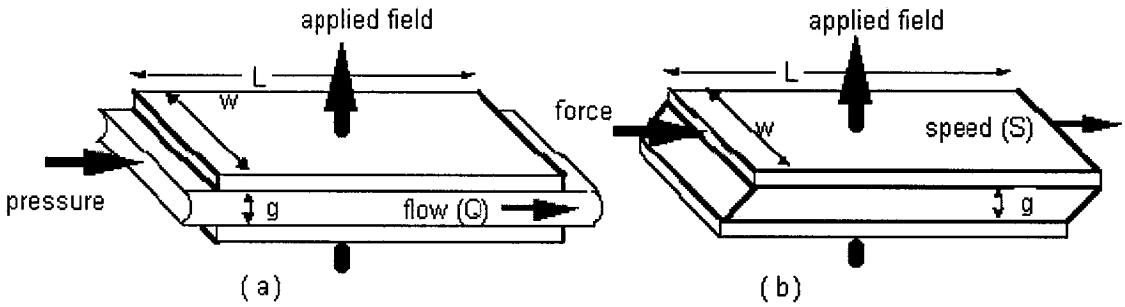

Figure 1.17: Basic operational models for controllable MR fluid devices: (a) pressure driven flow mode, (b) direct shear mode (Jolly *et al.*, 1998).

In contrast to ER fluid, mass production of MR fluids have been seen in past few years. Especially, Lord Corporation, USA took the pioneer role in producing MR fluid and MR fluid based devices. They have developed a variety of MR fluid based damper since mid-1990. Carlson and his team at Lord Corporation first presented their ideas in 1995 (Carlson *et al.*, 1995). Figure 1.18 illustrates a MR fluid based damper developed by Lord Corporation. The damper consists of a nitrogen-charged accumulator and two MR fluid chambers separated by a piston. The piston with annular orifice comprises coils to generate magnetic field for the fluid. The applied magnetic field causes variation in viscous and shear properties of the fluid, which eventually yields variations in the

damping force developed by the damper. For the particular damper illustrated in the figure, a DC current, limited to 2 A at 12 V, serves as the command signal for the coils.

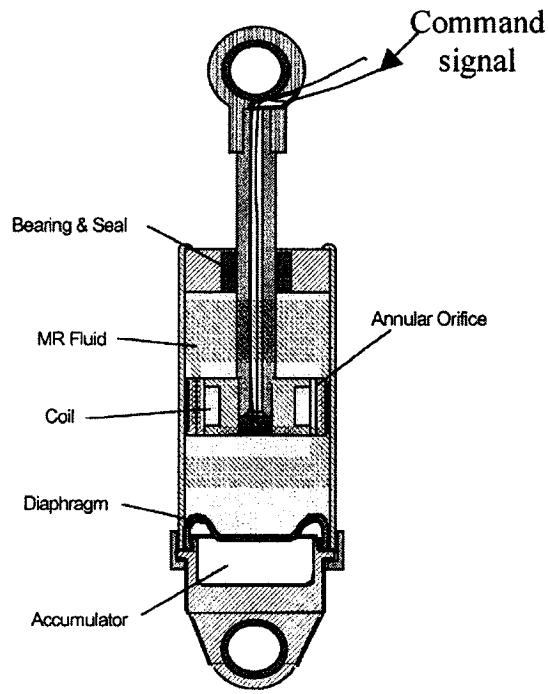

Figure 1.18: Schematic configuration of a MR fluid damper (McManus *et al.*, 2002).

In the past few years various studies have focused on MR fluid based damper technology. Kim *et al.* (1999) have suggested that improved ride comfort can be achieved in the frequency range of 4 and 8 Hz using a Linear Quadratic (LQ) control in MR damper. However ride stability at higher frequencies cannot be achieved because of time delay associated with such MR damper. Vibration control responses of a commercial vehicle equipped with the passive primary damper and the semi-active MR seat damper has been evaluated under both bump and random road conditions. It has been demonstrated via HILS method that both vertical displacement and acceleration at the driver's seat have been remarkably attenuated under bump road conditions by using

MR seat damper associated with semi-active skyhook controller. The Power Spectral Density (PSD) under the random road excitation was significantly reduced by MR seat damper (Choi and Han, 2003).

Yao *et al.* (2002) have proposed suspension system with MR 132-LD type MR damper from Lord Corporation. The Bouc–Wen model is adopted to characterize the performance of the damper. Experimental results indicated that the acceleration response of sprung mass, suspension travel, and tire deflection are effectively controlled around the body resonance. The semi-active control strategy used for the investigation is found to provide superior control compared to passive and constant control strategies. Lee and Jeon (2001) have designed a seat suspension using the same damper (MRF-132LD) to improve the ride quality and prevent the health risk of drivers compared to conventional seats. The damper is capable of providing wide range of damping force according to applied currents. The time delay of the damper is found to be about 20ms. Several control algorithms are used to control the damper such as sky-hook, continuous sky-hook and relative displacement. Among them, the continuous sky-hook controller is found to be the best for random road condition and bump input.

McManus *et al.* (2002) have developed a MR fluid based semi-active suspension system, integrated within a suspension seat. The damper improved vibration isolation by providing high damping force when the seat displacement approached the end limits of the free travel of the suspension, and lower damping closer to mid-ride. The MR fluid damper thus has potential to achieve a better compromise between shock and vibration attenuation performance of suspension seats than linear passive damper. Nam *et al.* (2001) have proposed a model to control seat vibration of a commercial vehicle, where ER dampers are used as primary suspensions and MR damper is used as seat damper.

Semi-active skyhook control is implemented via HILS for both primary and seat suspension. Both vertical displacement and acceleration of the seat reduced considerably under bump test employing the proposed MR seat damper. Furthermore, Power Spectral Density (PSD) of acceleration at the driver's seat has been significantly reduced under random test by using the MR seat damper.

In order to extend the use of MR based system and to make it portable, Kelso (2001) has developed a MR damper which is portable for wide variety research and development applications, at the same time being inexpensive to construct, service and rebuild. It is evident that this MR technology, comprising of simple, commercial-off-the-shelf (COTS) components where possible, presents an attractive, practical and cost effective solution.

Gordaninejad and Kelso (2000) have developed and evaluated a controllable MR damper for High Mobility Multi-purpose Wheeled Vehicle (HMMWV) which emulates the original equipment manufacturer (OEM) shock absorber behavior in passive mode, and provides a wide controllable damping force range. The design also allows integration of current hydraulic automotive shock absorber technology, such as by-pass valves and over-travel protection. In conjunction with a semi-active control system, this technology has shown promise for implementation into ground vehicles. MR based system can also be used in motor-cycle suspension system. Ericksen and Gordaninejad (2003) have designed, constructed and tested one such MR fluid based damper for an off-road motorcycle. The damper showed similar performance to that of an OEM damper at its passive-off mode while maintaining the OEM stroke length performance.

Yokoyama *et al.* (2001) synthesized a sliding mode controller, in which a skyhook control model is used as the reference model for tracking control. The study concluded

that the skyhook model could yield superior vibration isolation performance of the MR-damper when considered in conjunction with a quarter-vehicle model. Lee and Choi (2000) employed the same skyhook control law for a full–vehicle model and concluded that it could effectively attenuate the sprung mass resonant vibration.

Lam and Liao (2001) have designed a semi-active control scheme using the sliding mode control law to generate the desired damping force. In this scheme, the control signal derived from a feedback loop rather than the skyhook control. Choi *et al.* (2002) applied the PID control law to track the desired damping force for a full-vehicle model and also proposed a H_∞ controller to realize robustness against sprung mass uncertainties. Yao *et al.* (2002) analyzed a MR based damper utilizing Bouc-wen model, and applied in the traditional feedback scheme for synthesizing the semi-active control. However, no attempt is made to account for contribution due to hysteresis. Liao and Wang (2003) utilized the LQG control law in conjunction with acceleration feedback to realize damper force tracking with reference to an optimal damping force. Guo *et al.* (2004) employed the neural network control strategy including an error back propagation algorithm with quadratic momentum of the multi-layer forward neural network.

Despite few unfavorable conditions for automotive applications, MR fluid based damper system was produced for 2002 Cadillac Seville STS (Gilbert and Jackson, 2002). The fluid used in the damper can respond within 1ms resulting in a 5 time faster reaction than previous passive systems.

Kelso (2001) has suggested that a competitive 'whole approach' for a semi-active MR system can be viewed as a system of separate components: parameter sensing, intelligent control, power delivery, and MR hardware technology. The development of

any one single component will not successfully evolve without addressing the cost efficiency and commercialization concerns of other three.

1.3 Scope and Objective of the Investigation

From the literature review it is evident that linear passive suspension damper has poor ride and handling performance. To overcome the performance limitations of linear passive damper, asymmetric non-linear dampers have been designed and are widely used in modern vehicles. Still, the vibration and shock isolation performance of asymmetric dampers are not satisfactory. However, hydraulic semi-active concepts to control the damping force based on response have been extensively investigated to improve the performance, these concepts are known to have limitations due to slow response time. Electro-Rheological (ER) and Magneto-Rheological (MR) fluid based advanced suspension dampers are emerging to be the next generation of suspension dampers with their attractive features and promising performance potential to overcome the limitations of existing passive as well as hydraulic semi-active damper. Although there are several studies that investigate the vibration isolation performance of a specific damper concept (either ER or MR damper) with a set of parameter, there is a lack of comprehensive parametric study and investigation of isolation performance under shock excitations. Majority of the studies only compared either ER or MR damper with linear passive damper, despite the fact that asymmetric dampers are widely used in modern vehicles. Moreover, most of the studies used simple quarter car model for investigation of performance of the dampers, neglecting the pitch motion and bounce-pitch coupling of the vehicle motions. The pitch motion of the vehicle affects the stability as well as adversely effect the ride quality of the vehicle. Thus, it is important to include

the pitch motion in the study of damper performance. The performance measures used for most of the studies are limited to sprung mass vibration isolation performance of the damper, neglecting the performances like unsprung mass vibration isolation , relative motion, pavement load, ride height drift and shock isolation performance.

Hence, there is a need of a comprehensive comparative study of vibration and shock isolation performance of passive, asymmetric non-linear, ER and MR damper using a four degree-of-freedom pitch plane model. Also it is important to select a set of comparable performance measures (e.g. sprung and unsprung mass responses, relative motions, drift, pavement load etc.) to have wider understanding of damper performance. Such study will provide broad understanding of comparative performance of ER and MR fluid based advanced suspension system with passive and asymmetric system, as well as show comparison between performance of ER and MR damper. Any such comparison however will not be meaningful unless vehicle parameters are same, while the suspension parameters are tuned to produce comparable results by all the system considered. A significant effort thus must be devoted in selecting damper parameters and controller for its effectiveness in performing for the selected vehicle.

The overall objective of this work is to present a comprehensive study of linear passive, two-stage asymmetric non-linear, ER and MR damper to analyze their vibration and shock isolation performance using a four degree-of-freedom pitch plane model and a set of performance measures. The specific objectives of the dissertation research are as follows-

a. To develop analytical models of linear passive, two-stage asymmetric non-linear, ER and MR damper.

b. Modify the damper models and design appropriate controllers to ensure the best performance from the dampers.

c. To develop a 4 DOF pitch-plane model to facilitate the comparative study.

d. Validate the performance of the dampers by comparing with published results.

e. To select a set of realistic performance measures for comprehensive comparative performance study of the dampers.

f. Develop appropriate simulation models using MATLAB® SIMULINK to study the comparative performance of the dampers.

g. Analyze the performance of the dampers using quarter car model to observe their behavior and tune parameters to obtain comparable performance by all the dampers considered.

h. Compare the performance of the dampers using a 4 DOF pitch plane model under pure bounce and pitch excitations.

i. Compare the performance of the dampers using a 4 DOF pitch plane model under the influence of shock input.

j. To study the effect of higher excitation amplitude in the performance of the dampers.

1.4 Organization of the Thesis

In chapter 2, analytical models of linear passive, two-stage asymmetric non-linear, ER and MR damper are developed using published works. Modifications of the dampers and controllers are made to ensure best performance from each candidate dampers. A 4 DOF pitch plane model is developed which incorporates the dampers

individually to study their behavior. Damper parameters for candidate dampers are also proposed.

In chapter 3, the individual performances of the dampers are validated against published results. A set of performance measures is selected to compare the performances of the candidate dampers

In chapter 4, a comprehensive study is performed using the 4 DOF pitch-plane model to compare the performance of the candidate dampers under pure bounce, pure pitch, and shock excitations. The effects of higher amplitude excitations in the performances of the dampers are also investigated.

The major conclusions and recommendations for the future works are summarized in chapter 5.

CHAPTER 2

Vehicle Ride and Suspension Damper Models

2.1 General

Vehicle system represents complex vibration characteristics which can be modeled using a simple one degrees-of-freedom (DOF) to a complex three-dimensional model with multiple DOF. In this chapter, some of the vehicle ride models used for vibration and shock isolation analysis are discussed. Among the vehicle models, 2 DOF based quarter car model is commonly used by researchers to study vibration isolation performance of ground vehicles. Simplicity in design and good ability to predict vibration isolation performance of vehicles are the reasons behind the popularity of quarter car model. Although quarter car model provides good understanding of vibration isolation, it fails to predict effect of pitch motion (angular motion of vehicle), which sometimes adversely affects the ride quality of the vehicle. Thus, it is important to include the pitch motion in the analytical vehicle model to understand effect of pitch in vehicles. This can be done by considering a 4 DOF pitch-plane model, commonly known as half car model. Very few studies have considered 4 DOF pitch plane to analyze performance of different kinds of dampers. For this comparative performance study, 4 DOF pitch plane model is selected to have in-depth understanding of the vibration isolation performance of ground vehicles.

In the later part of this chapter, four different suspension damper models, used for this comparative study, are discussed. Analytical models for all the dampers along with values of various parameters are presented.

2.2 Vehicle Models for Vibration and Shock Performance Analysis

The vibration and shock response of most ground vehicles can be represented by seven-degree-of-freedom (DOF) system, namely - sprung mass bounce, roll and pitch, and bounce motion of four wheels, when independent wheel suspensions are considered. Figure 2.1 shows a 7 DOF ride model for a ground vehicle.

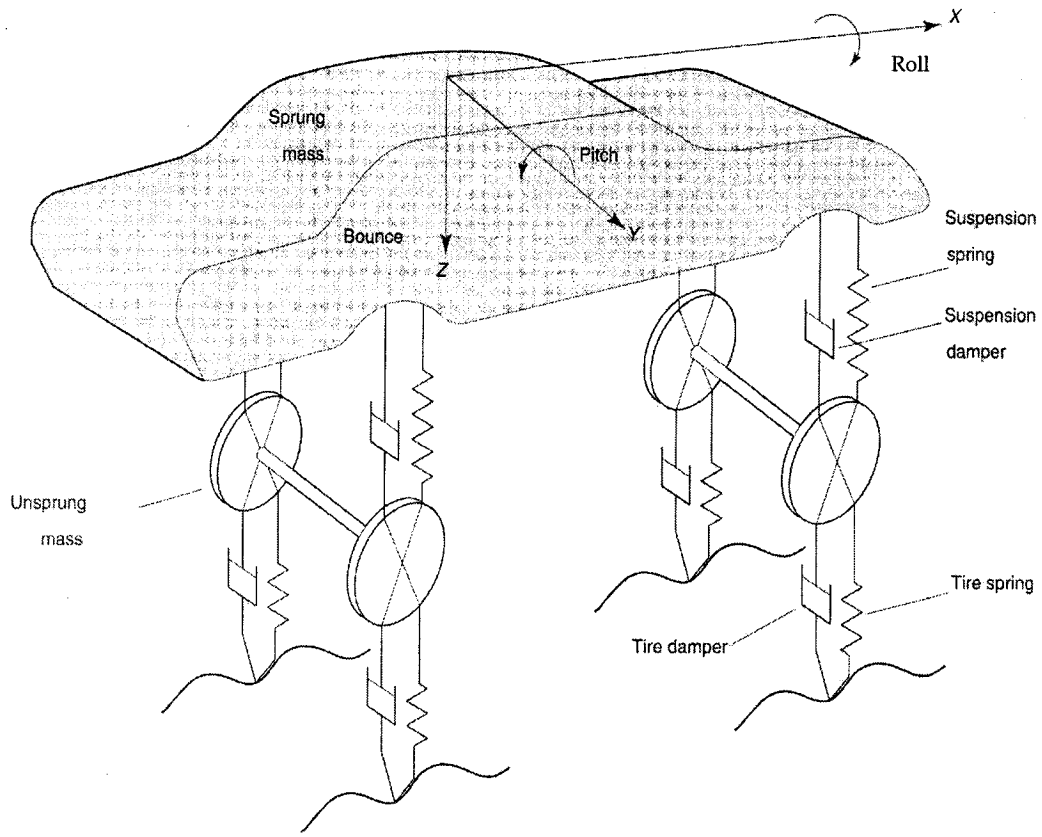

Figure 2.1: 7 DOF ride model for a ground vehicle (Ahmed, 2001).

The roll motions of road vehicles with low Center of Gravity (C.G.) are known to be considerably small in magnitude. Furthermore, the wheelbase (the longitudinal distance between centers of the front and rear axles) of majority of the vehicles is significantly

larger than track width (lateral distance between wheels). Thus the vehicular roll motion can be neglected compared to magnitude of vertical and pitch motions and the 7 DOF model can be reduced to a simplified 4 DOF pitch plane model for vibration analysis. The model is presented in figure 2.2. This 4 DOF model can be effectively used to establish the bounce and pitch motions of the sprung mass, and bounce motion of the axles or wheels. In this model, m_s and I_s represent the mass and pitch mass moment of inertia of the half the vehicle sprung mass. Hence, the model is also known as half-car model (Ahmed, 2001).

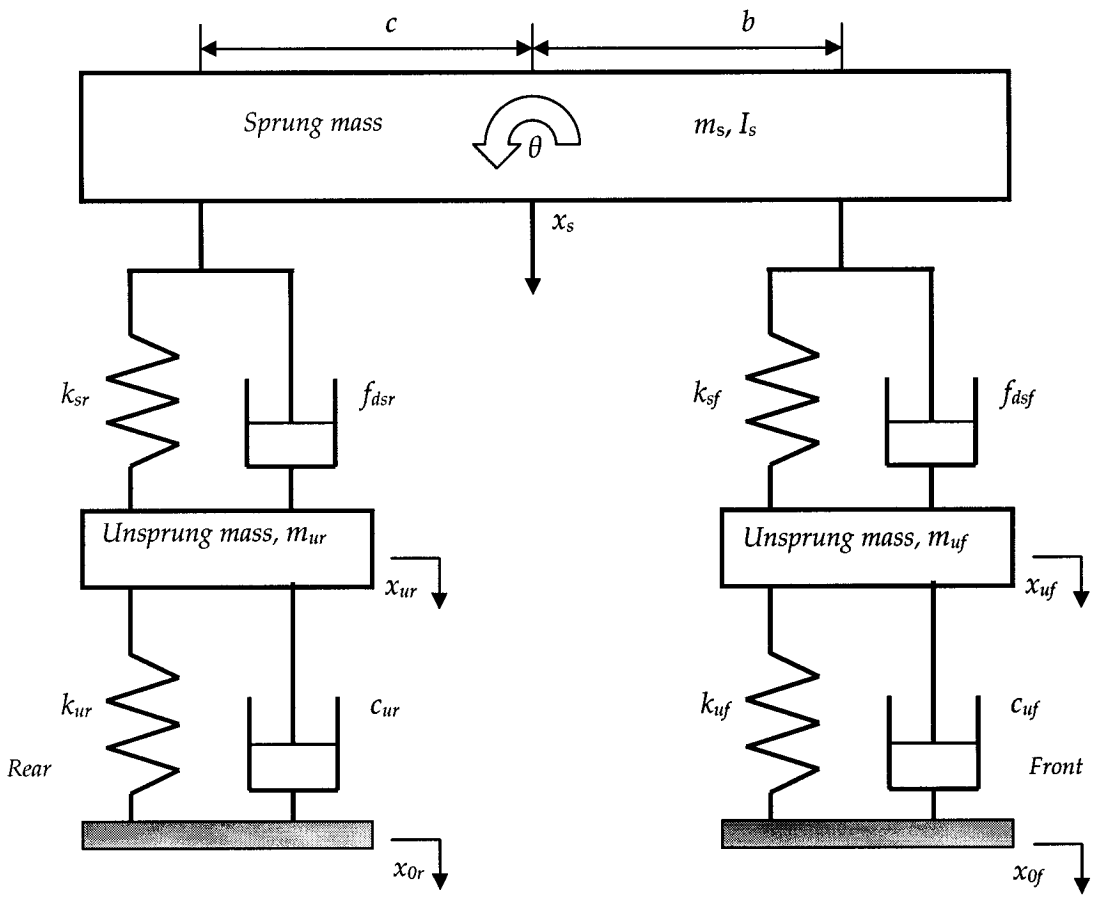

Figure 2.2: Schematic diagram of a 4 DOF pitch plane ride model.

However this half-car model can be used for analysis of full vehicle by utilizing 'Lumped Mass' method. In this method, m_s and I_s for the whole vehicle is considered, instead for half of the vehicle, and the suspension systems and tire on the front axle and the suspension systems and tire on the rear axle are lumped together, and considered as a single unit in the front and in the rear respectively. In this way the analysis provides better insight to the performance of the full vehicle, instead of just predicting the performance of half of the vehicle. The same principle is adopted for current study. The 4 DOF vehicle model can provide qualitative insight into the functions of the suspension, particularly the effects of the sprung and unsprung masses, spring stiffness, rattle space, and the tire and suspension forces. Furthermore, the effect of pitch motion can also be analyzed by using this model.

The model can be further simplified to a 2 DOF pitch plane model (figure 2.3), which can predict qualitative bounce and pitch motions of the sprung mass, assuming negligible contributions due to axle and tire assembly.

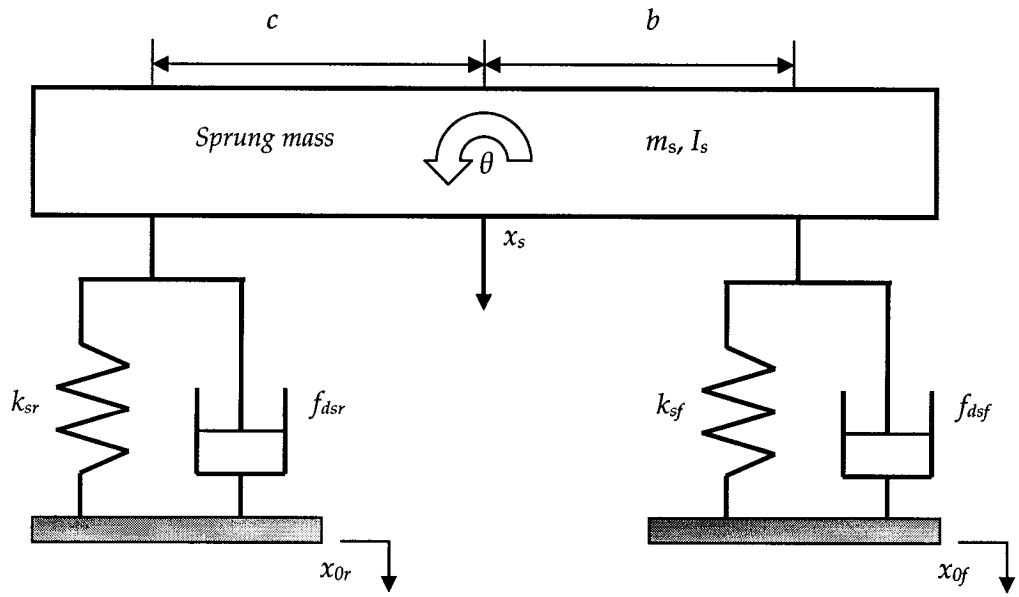

Figure 2.3: Schematic diagram of a 2 DOF pitch plane ride model

In this model, the road input (x_{0f}, x_{0r}) is taken to be same as for the wheels, and is suitable for estimation of the bounce and pitch natural frequencies, and associated mode shapes. This model is also suitable for study of off-road vehicles without sprung suspension, where the stiffness and damping elements relate to the properties of tires alone (Ahmed, 2001).

Similarly, a 2 DOF quarter-car model, shown in figure 2.4, is commonly utilized to evaluate sprung and unsprung mass bounce characteristics and dynamic rattle space. In this model, the effect of pitch motion is neglected and only the bounce motion caused by road irregularities is considered. The mass of the vehicle supported by the suspension is represented by the sprung mass, m_{sq} while the masses due to wheel and tire assembly, and the brakes are lumped together with portions of the steering and suspension masses, and represented as the equivalent unsprung mass, m_{uq}. In this case, m_{sq} is one-quarter of the sprung mass with one set of suspension and wheels.

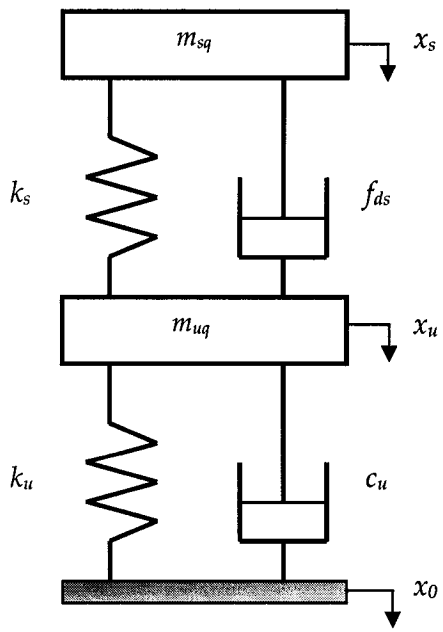

Figure 2.4: Schematic diagram of a 2 DOF quarter car ride model.

2.3 Equations of Motion

The vibration and shock isolation performance of ground vehicles to different excitations can be investigated though the analysis of models previously presented in figure 2.2, 2.3, and 2.4. For this study, the 4 DOF pitch plane model and quarter car model presented in figure 2.2 and 2.4 are chosen to compare the performance of the dampers. As discussed earlier, the 4 DOF half-car model is used to study the performance of the whole vehicle by considering sprung mass, m_s and mass moment of inertia, I_s for the whole vehicle, and the suspension systems and tire on the front axle and the suspension systems and tire on the rear axle are lumped together, and considered as a single unit in the front and in the rear respectively. For the 4 DOF pitch plane model (figure 2.2), the coupled differential equations of motion for the masses are derived about their respective static equilibrium using the D'Alembert's principle. The resulting equations of motion can be expressed as follows –

$$m_s \ddot{x}_s + f_{dsf} + f_{dsr} + k_{sf}(x_s - b\theta - x_{uf}) + k_{sr}(x_s + c\theta - x_{ur}) = 0 \quad \text{..... (2.1)}$$

$$I_s \ddot{\theta} - bf_{dsf} + cf_{dsr} - bk_{sf}(x_s - b\theta - x_{uf}) + ck_{sr}(x_s + c\theta - x_{ur}) = 0 \quad \text{..... (2.2)}$$

$$m_{uf} \ddot{x}_{uf} - f_{dsf} + c_{uf}(\dot{x}_{uf} - \dot{x}_{0f}) + k_{sf}(x_{uf} - x_s + b\theta) + k_{uf}(x_{uf} - x_{0f}) = 0 \quad \text{..... (2.3)}$$

$$m_{ur} \ddot{x}_{ur} - f_{dsr} + c_{ur}(\dot{x}_{ur} - \dot{x}_{0r}) + k_{sr}(x_{ur} - x_s - c\theta) + k_{ur}(x_{ur} - x_{0r}) = 0 \quad \text{..... (2.4)}$$

where, m_s, I_s, m_{uf} and m_{ur} represents the sprung mass, mass moment of inertia of sprung mass, front unsprung mass and rear unsprung mass of the vehicle, respectively. f_{dsf}, f_{dsr}, k_{sf} and k_{sr} represents front suspension damping force, rear suspension damping force, front suspension spring stiffness coefficient, rear suspension spring stiffness coefficient respectively. c_{uf}, c_{ur}, k_{uf} and k_{ur} represents front tire damping coefficient, rear tire damping coefficient, front tire stiffness coefficient, rear tire stiffness coefficient respectively. x_s, x_{uf},

x_{ur},x_{0f} and x_{0r} represents the sprung mass displacement, displacement of front unsprung mass, displacement of rear unsprung mass, road input to front wheels, road input to the rear wheels respectively. θ is the pitch motion of the sprung mass. b and c represents the distance between front axle and C.G., and the distance between rear axle and C.G. of the vehicle respectively. The quantity $c_{uf}(\dot{x}_{uf} - \dot{x}_{0f})$ and $c_{ur}(\dot{x}_{ur} - \dot{x}_{0r})$ represents damping force generated by front tire and rear tire respectively.

Similarly, the equations of motion for the 2 DOF quarter car model, presented in figure 2.4 can be written as –

$$m_{sq}\ddot{x} + f_{ds} + k_s(x_s - x_u) = 0 \qquad \text{..... (2.5)}$$

$$m_{uq}\ddot{x}_u - f_{ds} + c_u(\dot{x}_u - \dot{x}_0) - k_s(x_s - x_u) + k_u(x_u - x_0) = 0 \qquad \text{..... (2.6)}$$

where, m_{sq}, m_{uq}, k_s, f_{ds}, k_u and c_u represents one quarter sprung mass of the vehicle, unsprung mass associated with one tire of the vehicle, suspension spring stiffness for one suspension, damping force of one damper, tire stiffness coefficient (one tire), tire damping coefficient (one tire), respectively. x_s, x_u ,x_0 represents the sprung mass displacement, unsprung mass displacement, road input to one tire of the vehicle, respectively. The quantity $c_u(\dot{x}_u - \dot{x}_0)$ represents damping force generated by one tire of the vehicle.

In the above expressions, the term f_{ds} used to represent the suspension damping force is not defined. f_{ds} depends on the type of suspension damper used and is discussed in details in the following subsection.

2.4 Suspension Damper Models

The vehicle suspensions are required to provide better vibration and shock isolation to vehicles at wide variety of operating conditions involving varying surface roughness and discontinuity (like potholes), load and speeds. The task is furthermore complicated as performance objectives associated with vehicle ride comfort, road holding and control impose conflicting requirements for suspension design. Taking into considerations the conflicting performance requirements, vehicle suspensions are designed to achieve an acceptable compromise between the ride, handling and control performance. Majority of the modern vehicles use passive suspensions dampers consisting of hydraulic system. Traditional passive suspensions have linear symmetry properties in both compression and rebound cycle. Thus, the damping force generated by such dampers remains constant over the whole operating cycle of the vehicle. Passive dampers used in today's vehicles shows highly non-linear and asymmetric properties of suspension springs and dampers (Ahmed, 2001; Warner, 1996; Rakheja and Ahmed, 1993; Rengarajan, 1991; Oueslati, 1990; Harrison and Harmond, 1986). The non-linear asymmetric suspensions are mainly hydraulic dampers with either dual or multi-stage force-velocity characteristics. The damping forces of such dampers are varied as a function of preset velocity of the vehicle. The dampers yield high viscous damping coefficient corresponding to low velocity and considerably lower damping coefficients at medium and high velocities to achieve a better compromise between vehicle ride and handling performance (Warner, 1996). The task of switching the damping coefficient from high to low is performed by pressure-sensitive valves tuned to operate at preset velocities across the suspension. The hydraulic dampers yield asymmetric force-velocity

characteristics in compression and rebound in order to achieve improved road-handling performance and adequate control of wheel-hop motions.

To overcome the performance limitation associated with passive dampers, and cost associated with active dampers, semi-active dampers are introduced. In the conventional semi-active dampers, the damping forces are regulated by adjusting the orifice area of the oil-filled damper, thus changing the resistance to fluid flow. But the changing of speed is very slow as mechanical motion involved in this operation. To overcome the performance limitations, a new class of semi-active dampers based on Electro-Rheological(ER) fluid and Magneto-Rheological (MR) fluid have gained enormous attention among researchers and in industry. The operations of this type of dampers are based on the alteration of the viscosity of the fluids depending on an applied electric or magnetic field. ER or MR fluids consist of Electro-Rheological (ER) or Magneto-Rheological (MR) particles dispersed in an ER or MR medium. In the presence of a high electric field or a magnetic field the particles form chain-like fibrous structures. When the electric field strength or the magnetic field strength reaches a certain value, the suspension will be solidified and has high yield stress. Conversely, the suspension can be liquefied by removal of the electric field or the magnetic field. The process of change is very quick, and takes less than few milliseconds, and can be easily controlled.

In this study, the performances of four different damper models are compared. The dampers are - (i) linear passive damper, (ii) two-stage asymmetric non-linear damper, (iii) Electro-Rheological (ER) damper and (iv) Magneto-Rheological (MR) damper. These damper models are discussed in the following subsections.

2.4.1 Linear Passive Damper

Linear passive suspension systems are based on simple spring-damper concept. The system stores energy in a spring and dissipates it via a damper (Youn and Hac, 1995; Bastow, 1993). These types of dampers are generally fixed orifice based hydraulic system and have fixed damping properties throughout the operating range. Since, the damping properties of this type of dampers are fixed, the goal of such damper design is to improve the ride performance by making compromise between ride and handling properties of the vehicle. A higher damping force is crucial to suppress the resonant motions of the vehicle body, while a lightly damped suspension might provide effective isolation from the road induced vibration (Wong, 2001; Cebon, 1999). Furthermore, a higher damping would lead to less vibration in the dynamic forces and thus reduce the road damage potential. A suspension system with higher damping would also improve the handling performance by minimizing the wheel-hop and thus potential loss of tire-road contact.

The total damping force generated by a passive damper can be represented by the product of velocity and damping coefficient of the suspension damper. For a linear passive damper, equations 2.1 to 2.4 presented for the vehicle system shown in figure 2.2 can be rewritten as-

$$m_s \ddot{x} + c_{sf}(\dot{x}_s - b\dot{\theta} - \dot{x}_{uf}) + c_{sr}(\dot{x}_s + c\dot{\theta} - \dot{x}_{ur}) + k_{sf}(x_s - b\theta - x_{uf}) + k_{sr}(x_s + c\theta - x_{ur}) = 0 \quad \text{..... (2.7)}$$

$$I_s\ddot{\theta} - bc_{sf}(\dot{x}_s - b\dot{\theta} - \dot{x}_{uf}) + cc_{sr}(\dot{x}_s + c\dot{\theta} - \dot{x}_{ur}) - bk_{sf}(x_s - b\theta - x_{uf}) + ck_{sr}(x_s + c\theta - x_{ur}) = 0 \quad \text{..... (2.8)}$$

$$m_{uf}\ddot{x}_{uf} + c_{sf}(\dot{x}_{uf} + b\dot{\theta} - \dot{x}_s) + c_{uf}(\dot{x}_{uf} - \dot{x}_{0f}) + k_{sf}(x_{uf} - x_s + b\theta) + k_{uf}(x_{uf} - x_{0f}) = 0 \quad \text{..... (2.9)}$$

$$m_{ur}\ddot{x}_{ur} + c_{sr}(\dot{x}_{ur} - c\dot{\theta} - \dot{x}_s) + c_{ur}(\dot{x}_{ur} - \dot{x}_{0r}) + k_{sr}(x_{ur} - x_s - c\theta) + k_{ur}(x_{ur} - x_{0r}) = 0 \quad \text{..... (2.10)}$$

where, m_s, I_s, m_{uf}, m_{ur}, k_{sf}, k_{sr}, c_{uf}, c_{ur}, k_{uf}, k_{uf}, x_s, x_{uf}, x_{ur}, x_{0f}, x_{0r}, θ, b and c have same meaning as used in equation 2.1 to 2.4 and c_{sf}, c_{sr} represents front suspension damping coefficient, rear suspension damping coefficient respectively.

Similarly, equations 2.5-2.6 can be represented by the following equations for a linear passive suspension system-

$$m_{sq}\ddot{x} + c_s(\dot{x}_s - \dot{x}_u) + k_s(x_s - x_u) = 0 \qquad \text{..... (2.11)}$$

$$m_{uq}\ddot{x}_u - c_s(\dot{x}_s - \dot{x}_u) + c_u(\dot{x}_u - \dot{x}_0) - k_s(x_s - x_u) + k_u(x_u - x_0) = 0 \qquad \text{..... (2.12)}$$

where, the quantities m_{sq}, m_{uq}, k_s, f_{ds}, k_u, c_u, x_s, x_u and x_0 have same meaning as used in equation 2.5 and 2.6 and c_s represents the damping coefficient of one suspension damper.

For this study, the suspension damping coefficients for the passive dampers are based on a damping ratio of 15%. The values are typical of those used for a small size passenger car (Ahmed, 2001), and are presented in table 2.1.

Table 2.1: Damping properties of linear passive damper.

Parameter	***Value***	***Unit***
Front suspension damping coefficient (front axle), c_{sf}	1,000	Ns/m
Rear suspension damping coefficient (rear axle), c_{sr}	1,000	Ns/m

2.4.2 Asymmetric Non-Linear Damper

The suspension dampers used in modern vehicles are more advanced than the linear passive dampers. The dampers used in today's vehicles are designed to yield variable and asymmetric damping characteristics to achieve improved ride and road

holding performance (Rakheja and Ahmed, 1993). The dynamic force developed by modern hydraulic dampers comprises the following major components: (i) hydraulic force attributed to pressure drop across the flow paths, such as orifices and valves; (ii) restoring force due to gas spring; and (iii) seal friction force. The magnitudes of the two latter components are considerably small compared to that of the hydraulic force. Thus the dampers are mainly characterized by their hydraulic force components (Oueslati, 1990; Sharp and Crolla, 1987), which are strongly non-linear function of the velocity. Figure 2.5 illustrates a typical peak force-velocity behavior of a hydraulic damper measured under sinusoidal piston velocity (Warner, 1996). The force-velocity curve presented in figure 2.5 exhibits hysteretic behavior attributed to fluid compressibility and inertial effects. The contributions due to such factors are often considered to be small (Warner, 1996; Segel and Lang, 1981; Thompson, 1970). Furthermore, the dampers with variable orifice characteristics are adaptable to road conditions compared to earlier linear passive dampers.

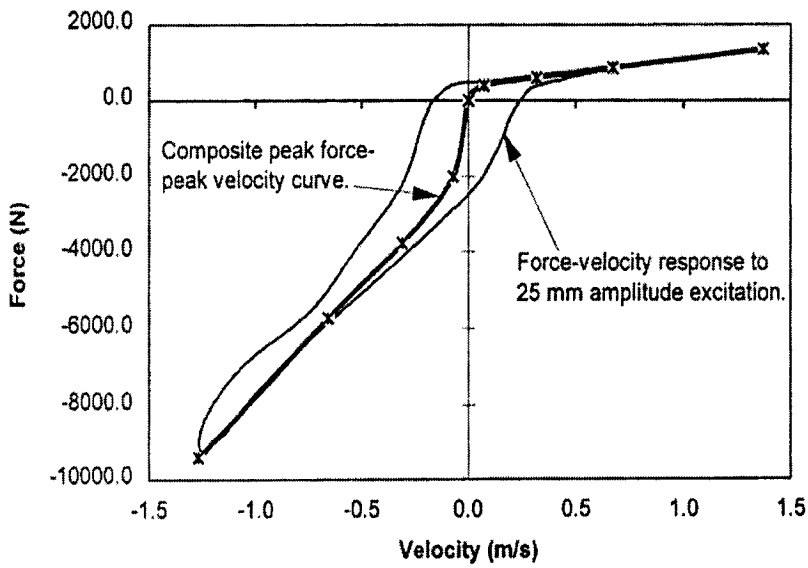

Figure 2.5: Peak force-velocity characteristics of a hydraulic damper (Warner, 1996).

However, complex nature of the damping characteristics poses considerable challenges associated with analytical modeling and analyses of modern suspension dampers. Owing to these complexities, the majority of the studies on vehicle ride analysis consider either linear or linear equivalent damping characteristics (Walker, 1996; Joo, 1991; Rengarajan, 1991; Su, 1990). Although these analyses facilitate preliminary design analysis and exploration of different damping concepts, but neglects the effects of damping asymmetry and non-linear variations with the relative velocity. Fortunately, a few studies have characterized asymmetric damping properties of modern passive dampers by a piece-wise linear function, as illustrated in figure 2.6 (Rajalingham and Rakheja, 2003; Rakheja and Ahmed, 1993, 1994). In this formulation, the low and high speed damping coefficients in compression (C_1, C_2) and rebound (C_3, C_4) for a specific damper are identified from the mean of the laboratory-measured data, while neglecting hysteresis.

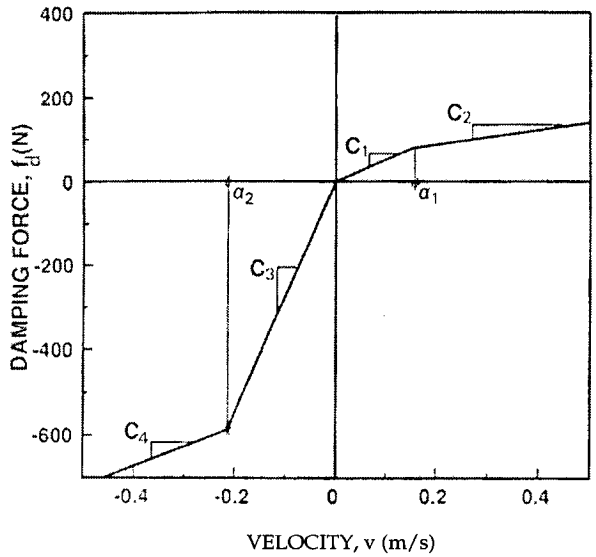

Figure 2.6: Piece-wise linear damper characterization of asymmetric force-velocity characteristics (Rakheja and Ahmed, 1993).

The velocities (α_1, α_2), where the transitions from low speed damping coefficients (C_1 and C_3) to the high speed coefficients (C_3 and C_4) occur, are also identified from the measured data. The piece-wise linear describing function models of symmetric and asymmetric suspension dampers have been effectively employed in ride dynamic models of different vehicles (Rakheja and Ahmed, 1993). The piece-wise linear representation is considered adequate to study the effects of damping asymmetry and non-linearity. As shown in figure 2.5, the composite force-velocity curve of typical hydraulic damper exhibits multi-stage and asymmetric damping characteristics. This type of composite curve can be obtained from the hysteresis loop of the force-velocity diagram by computing mean values of the peak forces for given velocities. The resulting composite curve consists of variable damping properties at different velocities. Such composite force-velocity (f-v) characteristics can adequately describe the mean f-v characteristics and the damping asymmetry, although they neglect the contributions due to fluid compressibility and thermal effects. Based on laboratory characterization of 14 different bus suspension dampers, it was shown that the damping characteristics for the purpose of vehicle ride dynamic analysis can be effectively represented by the composite curve presented in figure 2.7. The force-velocity curve illustrated in figure 2.7 can effectively describe the low speed and high speed asymmetric damping characteristics of non-linear dampers. The damping curve reveals high damping constants (C_1 and C_3) corresponding to bleed-control at low piston velocity in compression and rebound and low damping constants (C_2 and C_4) due to blow-off flows at high piston velocity. The transitions from high to low damping in compression and extension occur at certain preset velocities, α_c and α_e, respectively, in compression and rebound.

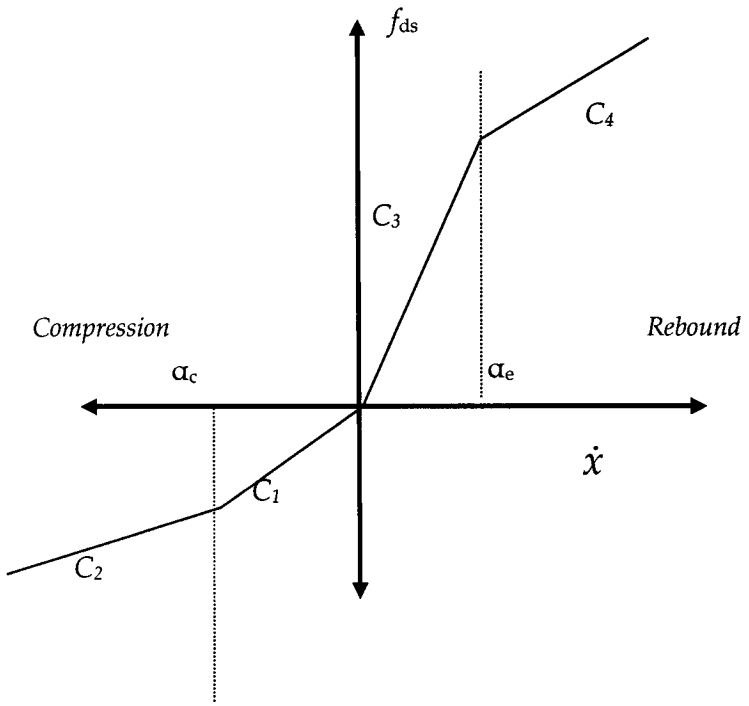

Figure 2.7: Piece-wise-wise linear representation of a two-stage asymmetric non-linear damper (Joarder, 2003).

The damping force generated by a two-stage asymmetric damper can then be expressed as:

$$f_{ds} = \begin{cases} C_1\dot{x}; & for\ \alpha_c \le \dot{x} \le 0 \\ C_1\alpha_c + C_2(\dot{x} - \alpha_c); & for\ \dot{x} \le \alpha_c \\ C_3\dot{x}; & for\ 0 \le \dot{x} \le \alpha_e \\ C_3\alpha_e + C_4(\dot{x} - \alpha_e); & for\ \dot{x} \ge \alpha_e \end{cases} \quad \text{..... (2.13)}$$

Denoting $p=C_3/C_1$ as the asymmetry factor corresponding to low piston velocity, and compression and rebound damping reduction factors as $\gamma_c=C_2/C_1$ and $\gamma_e=C_4/C_3$, the damping force can be expressed in terms of low speed damping coefficient, C_1:

$$f_{ds} = \begin{cases} C_1\dot{x}; & for\ \alpha_c \le \dot{x} \le 0 \\ (1-\gamma_c)C_1\alpha_c + \gamma_c C_1\dot{x}; & for\ \dot{x} \le \alpha_c \\ pC_1\dot{x}; & for\ 0 \le \dot{x} \le \alpha_e \\ (1-\gamma_e)pC_1\alpha_e + p\gamma_e C_1\dot{x}; & for\ \dot{x} \ge \alpha_e \end{cases} \quad \text{..... (2.14)}$$

The two-stage asymmetric non-linear damper model presented in equation 2.14 provides effective estimation of the damping force presented by a variable orifice type non-linear damper. Earlier researchers have used the mathematical model to analyze performance of asymmetric non-linear dampers and reported good correlation between the real damper performance and the performance presented by the analytical model. If the damping properties of such dampers are tuned properly, they can provide better performance compared to linear passive suspension dampers. Thus, this damper is considered as one of the candidate damper for the comparative study.

The values of the parameters C_1, C_2, C_3, C_4, α_e and α_c of the model are adopted from the literature of Rakheja and Ahmed (1993) and are presented in table 2.2.

Table 2.2: Parameters for two-stage asymmetric non-linear damper.

Parameter	*Value*	*Unit*
High damping coefficient at compression side, C_1	514.5	Ns/m
High damping coefficient at extension side, C_3	2747.5	Ns/m
Low damping coefficient at compression side, C_2	177	Ns/m
Low damping coefficient at extension side, C_4	462	Ns/m
Preset velocity at extension side, α_e	0.1524	m/s
Preset velocity at compression side, α_c	-0.2163	m/s

The two-stage asymmetric non-linear damper can be incorporated in the 4 DOF model by replacing damping forces f_{dsf} and f_{dsr} in equation 2.1 to 2.4 by the damping force f_{ds} of two-stage asymmetric non-linear damper represented in equation 2.14.

2.4.3 Electro-Rheological(ER) Damper

The ER damper utilized for this study is adopted from the work presented by Nakano (1995). The work includes an analytical model and a test model of the ER damper. Moreover, the author has suggested different control schemes for the damper. Figure 2.8 shows schematic representation of the ER damper. It consists of an ER suspension made of strong acid ion exchange resin particles of about 5μm in diameter dispersed in 20 cSt silicon oil. The two cylinder chambers divided by a piston are connected to each other by an ER valve with several pairs of electrodes placed in parallel, and are filled with ER fluid. Figure 2.9 shows arrangement of electrodes in the ER valve of the damper. The properties of the ER fluid of the damper are controlled by applied electric field, which is a function of the input voltage. The ER valves works to change the damping force f_{ds} by controlling the pressure difference P_1-P_2 between both chambers with an electric signal.

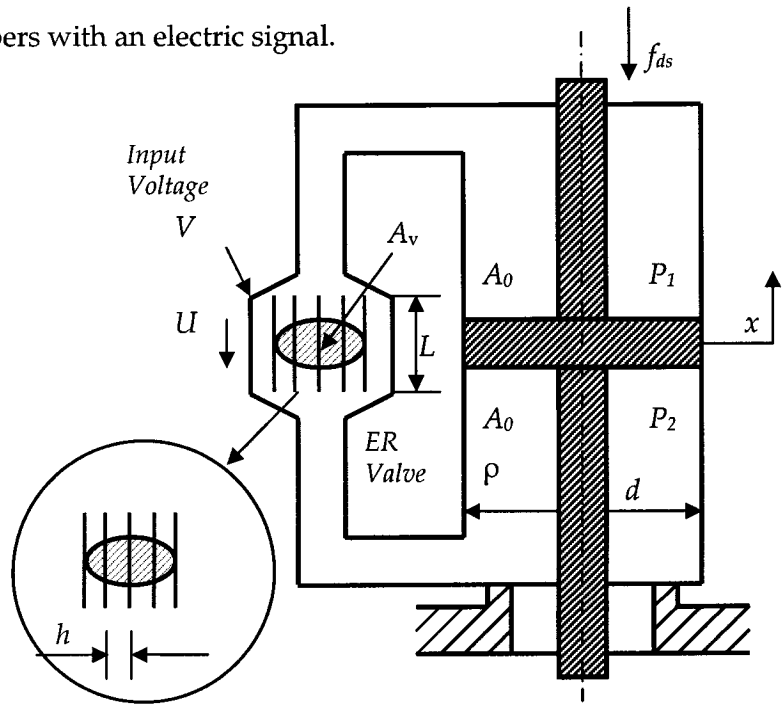

Figure 2.8: Schematic representation of analytical model of ER damper (reproduced from Nakano, 1995).

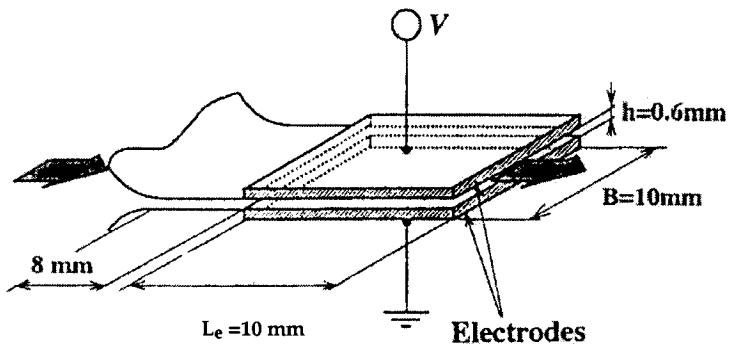

Figure 2.9: Arrangement of electrodes in the ER valve (Nakano, 1995).

The analytical model of electronically variable damping force produced in the ER damper is derived assuming that the ER fluid is incompressible and the ER valve response to applied electric signals is quasi-steady. The pressure difference $P_1 - P_2$ between both cylinder chambers of the ER damper is controlled by the ER valve, and can be estimated from the pressure drops ΔP_T across the ER valve as a function of applied electric field strength E and the mean flow velocity U. Consequently, considering the inertia of ER fluid between the electrodes of the ER valve and the pressure drop ΔP_T, the damping force f_{ds} is given as follows:

$$f_{ds} = A_0 (P_1 - P_2) = A_0 \{ \frac{m}{A_v} \frac{dU}{dt} + \Delta P_T(E,U) \} \quad \text{..... (2.15)}$$

where, A_0 is the pressure area of the piston, m $(= \rho L A_v)$ is the total mass of ER fluid within the ER valve channel, A_v is the total flow area, L is the channel length of ER valve, and ρ is the density of ER fluid.

Considering the mass conservation of ER fluid in the ER damper the following relationship between the mean flow velocity U and the displacement of the piston relative to cylinder (i.e. relative displacement of sprung mass and unsprung mass, $x_s - x_u$) can be established as shown in equation 2.16.

$$U = \frac{A_0}{A_v}\frac{dx}{dt} \quad \frac{dU}{dt} = \frac{A_0}{A_v}\frac{d^2x}{dt^2} \qquad \text{..... (2.16)}$$

The steady pressure drop ΔP_T across ER valve damper is measured in terms of mean flow velocity U and the electric field strength $E = V/h$ [kV/mm] (V: the applied voltage to ER valve), using a piston cylinder–ER valve experimental apparatus.

The ΔP_T is divided into two components represented by equation 2.17. ΔP_0 corresponds to the total pressure drop without electric field and an ER component ΔP_{ER} due to ER effects. The viscous component of ΔP_0 [kPa] can be related to the mean flow velocity U [cm/s] by the linear function of $\Delta P_0 = 0.67\ U$, obtained experimentally. The component ΔP_{ER} tends to decrease with increasing U, and is a linear function of yield stress τ_{ER} [kPa] represented by an approximate function (equation 2.19) obtained through a curve fitting of experimental data.

$$\Delta P_T = \Delta P_0 + \Delta P_{ER} \cdot sgn\,(U) \qquad \text{..... (2.17)}$$

$$\Delta P_{ER} = (3L_e/h)\,\tau_{ER} \qquad \text{..... (2.18)}$$

$$\tau_{ER} = \alpha_r E^2 - (\alpha_r E^2 - \gamma_r E^2)\,(1 - e^{-\beta(E)|U|}) \qquad \text{.....(2.19)}$$

$$\beta(E) = 0.0265/\ E^2\ \text{[s/cm]} \qquad \text{..... (2.20)}$$

The values of different parameters of the ER damper, as proposed by Nakano (1995) and the estimated mass of ER fluid are presented in table 2.3.

Table 2.3: Parameters of ER damper.

Parameter	*Value*	*Unit*
Pressure area of the piston of ER damper, A_0	2827	mm^2
Diameter of the damper piston, d	60	mm
Total flow area, A_v	1800	mm^2
Channel length of ER valve, L	30	mm
Height between two electrodes, h	0.6	mm
Length between two electrodes, L_e	10	mm
Width between two electrodes, B	10	mm
Empirical constant, α_r	0.28	$kPa.mm^2/kV^2$
Empirical constant, γ_r	0.07	$kPa.\ mm^2/kV^2$

The ER damper can be incorporated in the 4 DOF model by replacing damping forces f_{dsf} and f_{dsr} in equation 2.1 to 2.4 by the damping force f_{ds} of ER damper represented in equation 2.15.

The damping force, f_{ds}, however depends on the electric field (E), which must be controlled based on a control methodology.

2.4.3.1 Control Methodology

To illustrate the control methodology, a simple quarter car representation of vehicle suspension with ER damper is shown in figure 2.10. Here the damping force produced by the ER damper can be changed during any part a vibration cycle by supplying a voltage V depending on response variable. Common strategy to vary damping with such semi-active device is to utilize damping to minimize response, while avoid damping during the part of the cycle when damping contributes to increase in the

sprung mass response. This can be achieved by monitoring sprung mass and unsprung mass velocity and displacement and identifying the sign of the responses.

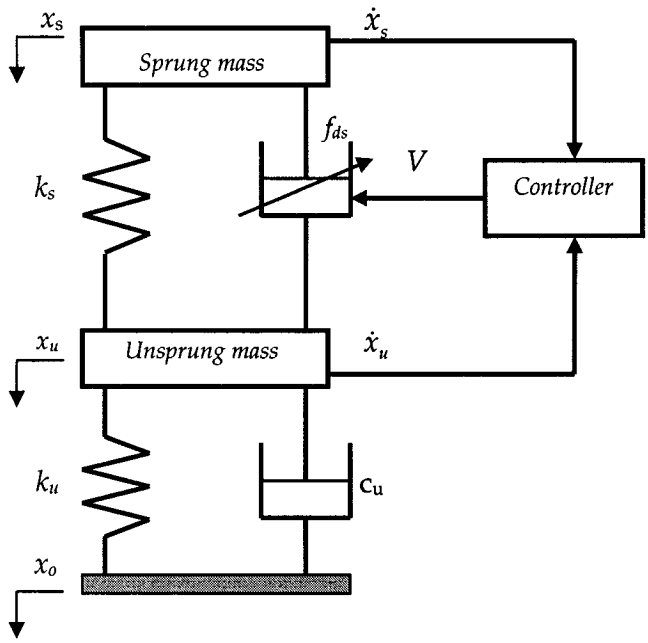

Figure 2.10: Control methodology for ER damper.

The control strategy used in this investigation is proposed by Nakano (1995), and performs best among several scheme investigated by the author. In this scheme the voltage supply to electrodes are modulated to control the damping force in the following manner:

$$V = \sqrt{(f_G \mid \dot{x}_s \mid)}; \qquad \dot{x}_s \cdot (\dot{x}_s - \dot{x}_u) > 0$$

$$V = 0; \qquad \dot{x}_s \cdot (\dot{x}_s - \dot{x}_u) \leq 0 \qquad \text{..... (2.21)}$$

In the above expressions, V is the applied voltage to the controller, f_G is the feedback gain, $\dot{x}_s$ and $\dot{x}_u$ are the velocity of the sprung mass and unsprung mass, respectively. For this study, the controller gain, f_G, is chosen to be $6kV^2s/m$ by trail and error method, to achieve improved ride performance for the vehicle parameters used.

2.4.4 Magneto-Rheological (MR) Damper

As discussed in chapter 1, Lord Corporation is the leading manufacturer of MR dampers. For this study, a cylindrical type MR damper model RD-1005-3, manufactured by Lord Corporation, is selected for the analysis of the characteristics of MR type damper. The schematic diagram of the damper is shown in figure 2.11.

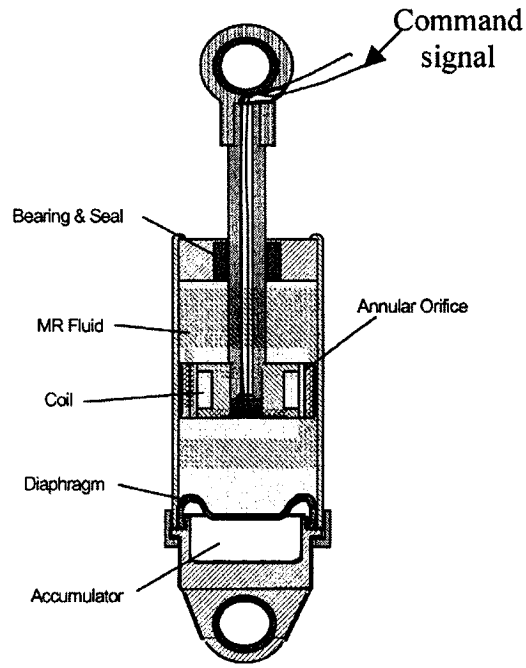

Figure 2.11: Schematic representation of MR damper (Ma *et al.*, 2002).

The damper consists of a nitrogen-charged accumulator, which is located at the bottom of the damper. The two MR fluid chambers are separated by virtue of a piston. A number of coils are located within the piston and annular orifice area, which generates magnetic field for the fluid. Under the application of magnetic field, variations in viscous and shear properties of the fluid occurs, which eventually yields variations in the damping force developed by the damper. Ma *et al.* (2002) have tested this damper at CONCAVE research center of Concordia University. The properties of the MR fluid of the damper are controlled by the applied magnetic field, which is a function of the

excitation current. A DC current of maximum 2A is used as the command signal as well as the input for the coils. The force-velocity (*f-v*) and force-displacement characteristics of the damper are measured in the laboratory over a wide range of excitation variables. The hysteresis phenomenon in the MR damper was evaluated under harmonic excitations in the frequency range of 0.1–15 Hz. A total of 245 experiments for different combinations of current excitations (0.00, 0.25, 0.50, 0.75, 1.00, 1.25 and 1.50 A) and strokes (2.5, 6.35, 12.7 and 19.05 mm) have been performed. The amplitudes for displacement excitations at higher frequencies were limited to lower values to ensure that the damper was operating within safe velocity limits.

The test results indicate that MR damper invariably exhibits hysteresis behavior, especially when the response becomes inelastic. Ma *et al.* (2002) have applied Equivalent Characterize Method (ECM) on the basis of the experimental data to formulate a hysteresis model synthesis to characterize the hysteric and non-linearity function of the MR damper.

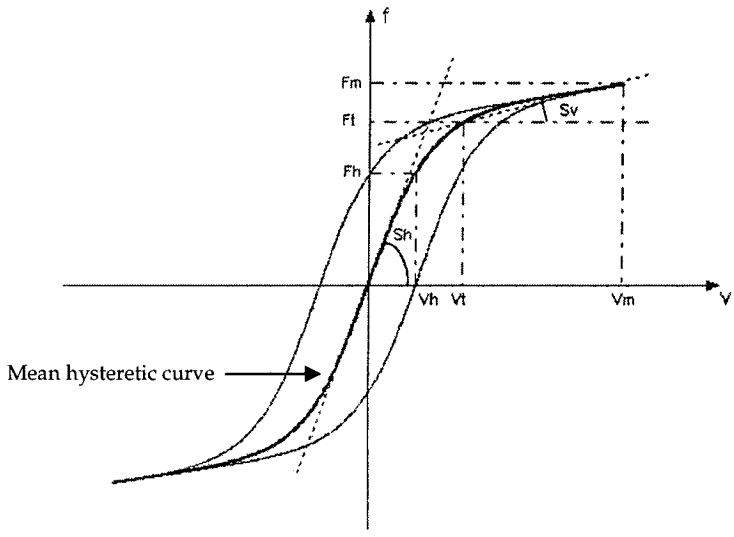

Figure 2.12: Hysteretic *f-v* characteristics of MR damper (Ma *et al.*, 2002).

The characterization is based upon consideration of the observed physical features such as pre-yield behavior, post-yield force saturation, transition velocity and force and control current dependence. The measured *f-v* characteristics of the MR damper corresponding to a certain control current and excitation condition can be represented by a generalized hysteresis loop shown in figure 2.12.

In order to effectively depict and synthesis the model of hysteretic *f-v* characteristics, eight different parameters are proposed (figure 2.12). The parameters are described below-

(i) v_m, *Maximum Velocity*: Maximum instantaneous velocity of the damper piston motion in a certain frequency and stroke, the dimension is m/s.

(ii) f_m, *Maximum Damping Force*: Maximum instantaneous damping force of the damper with respect to certain v_m and control current i (amps), the dimension is kN.

(iii) v_h, *Zero Force Velocity Intercept*: Instantaneous velocity yielding zero damping force in a certain operating condition, the dimension is m/s.

(iv) f_h, *Zero Velocity Force Intercept* : Instantaneous damping force due to zero velocity in a certain operating condition, the dimension is kN.

(v) v_t, *Transition Velocity* : Instantaneous velocity transiting the damping from mean hysteresis saturation to linear amplification, the dimension is m/s.

(vi) f_t, *Transition Force*: Instantaneous mean hysteresis damping force with respect to a certain v_t, the dimension is kN.

(vii) s_h, *Hysteretic Slope:* Slope of the mean hysteric loop at the origin, the dimension is $kN/(m/s)^{-1}$.

(viii) s_v, *Linear Slope* : Slope of the mean hysteresis linear amplification in higher velocity, the dimension is $kN/(m/s)^{-1}$.

Based on the generalized parameters the damping force generated by the MR damper can be expressed in the following manner (Ma *et al.*, 2002) -

$$f_{ds} = f_t(i).[\ \{1 - e^{-\alpha(v \pm v_h)}\} / \{1 + e^{-\alpha(v \pm v_h)}\}\ ] .\ (1 + k_v .\ |v|) \qquad \ldots\ldots (2.22)$$

where, f_{ds} denotes the damping force as a function of the control current i and piston velocity v, and v_h is the piston velocity corresponding to zero damping force, given by-

$$v_h = \text{sign}\ (\ddot{x}).\ k_4.\ v_m.\ [1 + \{k_3/1 + e^{-a_3.(i + I_1)}\} - (k_3/1 + e^{-a_3.I_1})] \qquad \ldots\ldots\ldots (2.23)$$

f_t is transition force, which depends upon i and the peak velocity v_m, given by-

$$f_t(i) = f_0.(1 + e^{\ a_1.v_m})\ [\ 1 + \{\ k_2/1 + e^{-a_2.(i + I_0)}\} - (\ k_2/1 + e^{-a_2.I_0})\ ] \qquad \ldots\ldots\ldots (2.24)$$

The parameters k_v and α, used to adjust the damping coefficients at high and low velocities respectively, are expressed as functions of the peak velocity v_m, and are given by -

$$k_v = k_1.\ e^{-a_4.v_m} \qquad \ldots\ldots (2.25)$$

$$\alpha = a_0 / (1 + k_0.\ v_m) \qquad \ldots\ldots\ldots (2.26)$$

The model presented in equation 2.22 requires identification of 13 parameters from the measured data, namely f_0, I_0, I_1, a_0, a_1, a_2, a_3, a_4, k_0, k_1, k_2, k_3, k_4. The values are presented in table 2.4. The peak velocity parameter v_m can be estimated from the instantaneous displacement x, velocity $\dot{x}$ ($v = \dot{x}$), and acceleration $\ddot{x}$ responses across the piston of the damper.

For harmonic excitations parameter v_m is obtained from the following equation-

$$v_m = a_m .\ \omega\ = \sqrt{\{(\ \dot{x}\ )^2 - \ddot{x}.\ x\}} \qquad \ldots\ldots (2.27)$$

where, a_m and ω are excitation amplitude and frequency respectively.

Table 2.4: Identified parameters for MR damper model (Ma *et al.*, 2002).

Parameter	*Value*	*Unit*
a_0	990	None
a_1	1.75	$(m/s)^{-1}$
a_2	2.85	$(amps)^{-1}$
a_3	1.55	$(amps)^{-1}$
a_4	4.60	$(m/s)^{-1}$
I_0	0.05	$(amps)^{-1}$
I_1	-0.08	$(amps)^{-1}$
k_0	112.5	None
k_1	5.55	None
k_2	19.4	None
k_3	2.90	None
k_4	0.095	None
f_0	13.9	N

The MR damper can be incorporated in the 4 DOF model by replacing damping forces f_{dsf} and f_{dsr} in equation 2.1 to 2.4 by the damping force f_{ds} of MR damper presented in equation 2.22.

2.4.4.1 Control Methodology

The controller synthesis for MR damper is quite a challenging job owing to the hysteresis and force-limiting characteristics of the damper. The semi-active control strategies employed in vibration control suggests that the magnitude of mass acceleration increases when the suspension spring force takes the same direction as the

damping force (Jolly *et al.*, 1989). The most commonly used semi-active control strategy is 'skyhook' control, which is based on the 'skyhook' control law proposed by Karnopp *et al.* (1974). The control law suggests that the damper should be switched to high damping mode, when the absolute mass velocity is in phase with the damper relative velocity. Otherwise, the damper should be switched off. For the current study, skyhook control law based controller is used to control the damping force of MR damper. Using a quarter car model, the control scheme is presented in figure 2.13.

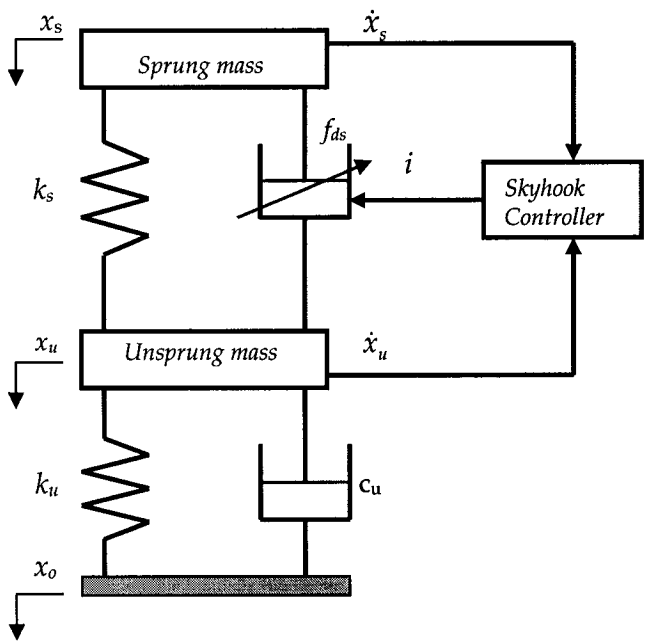

Figure 2.13: Schematic representation of the control scheme for MR damper.

The 'skyhook' control synthesis is formulated to modulate the control current (i) supply to the MR damper to control the damping force, f_d, in the following manner-

$$i = C_{sky} | \dot{x}_s | ; \qquad \dot{x}_s \cdot (\dot{x}_s - \dot{x}_u) \geq 0 \qquad 0 < i \leq i_{max} ; \qquad \text{..... (2.28)}$$

$$i = 0; \qquad \dot{x}_s \cdot (\dot{x}_s - \dot{x}_u) < 0$$

where, C_{sky} is the adjustable gain of the 'skyhook' controller, $\dot{x}_s$ and $\dot{x}_u$ are the velocity of the sprung mass and unsprung mass respectively. The control current (*i*) should be limited to a peak value depending on the coil design of the electro-magnet.

For this study, the controller gain C_{sky} is chosen to be 10 A $(m/s)^{-1}$ by trail and error method, to achieve improved ride performance, and the control current is limited to i_{max} =1.5A for the damper used in this study.

2.5 Summary

In this chapter, different vehicle models for vibration and shock isolation performance analysis are discussed, and equations of motion for 4 DOF pitch plane and quarter car model are developed. The analytical models for the candidate dampers namely- linear passive, two-stage asymmetric non-linear, ER and MR damper are developed using published works. A skyhook controller is proposed for MR damper in this investigation. Proper gain for ER damper controller and MR damper controller have been determined to ensure improved vibration isolation performance for the candidate vehicle parameters. Design values for damper parameters for all the dampers are also proposed, such that the vibration and shock isolation performance of all the systems studied are comparable.

CHAPTER 3

Damper Model Validation and Performance Measure

3.1 General

The shock and vibration attenuation performance of vehicle suspension systems are evaluated based on the responses to known dynamic excitations. These responses are basically the measured performance of the vehicle under different road conditions. The performance evaluation may be performed either in laboratory or via computer simulation. Generally, it is more practical, versatile and economical to perform the analysis via computer simulation rather than laboratory or field-testing. A mathematical model validated against known characteristics provides a powerful tool for detailed analysis, evaluation of performances and functional limits. As discussed earlier, four different damper models are compared in this study. The mathematical models of the dampers are presented in chapter 2. First kind of damper is linear passive damper. The damping force generated by this type damper is constant, and is represented by a fixed damping coefficient. Since the damping force is linear in nature, and the responses of such a system is well known, individual validation of this kind of damper is not presented separately. Rather, the performance of this type of damper will be analyzed in chapter 4 for comparison. On the other hand, damping force generated by the rest of the dampers, namely - two-stage asymmetric non-linear damper, Electro-Rheological damper and Magneto-Rheological damper are compared with the published results to validate the characteristics of the damper models utilized for this study. The validations are presented in this chapter.

In the following chapter, these damper models are incorporated in a 4 DOF pitch plane model to investigate their comparative performance. The vibration isolation performance analysis is based on sinusoidal road excitations, and shock performance is based on round step input. These inputs are discussed in section 3.3. Finally, the performance measures used to study the comparative performance of the dampers are discussed in section 3.4.

3.2 Validation of Suspension Damper Models

Using the analytical models of the dampers presented in chapter 2, simulation model for the dampers are developed using MATLAB® SIMULINK. Data of damper parameters presented in table 2.2, 2.3 and 2.4 are used to evaluate the performance of two-stage asymmetric non-linear damper, Electro-Rheological (ER) damper and Magneto-Rheological (MR) damper respectively. It is necessary to compare the results generated by simulation model with the published results to ensure that the simulation models are capable of delivering designed damping characteristics. In the following subsections, the damping characteristics of the damper obtained from simulation are validated against the published results.

3.2.1 Two-Stage Asymmetric Non-Linear Damper

The damping force generated by a two stage asymmetric non-linear damper can be expressed by equation 2.14. To simulate the damping characteristics of the damper, damper parameters are adopted from the literature of Rakheja and Ahmed (1993). The parameters are presented in table 2.2. The force-velocity (f-v) characteristics of the damper obtained by the authors are presented in figure 3.1.

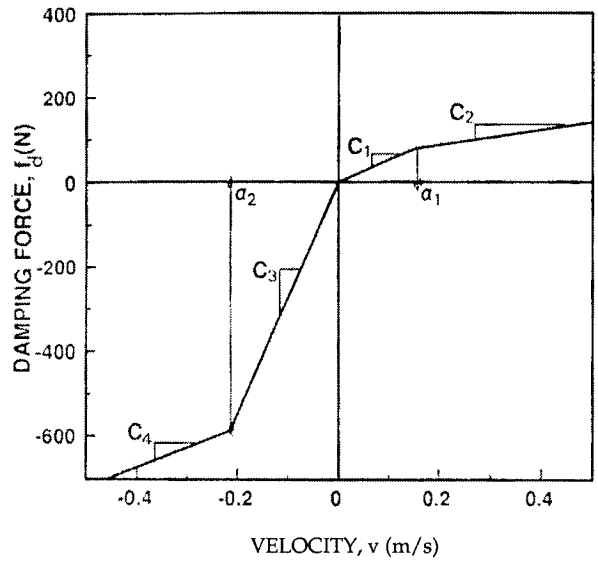

Figure 3.1: *f-v* characteristics of two-stage asymmetric non-linear damper (Rakheja and Ahmed, 1993).

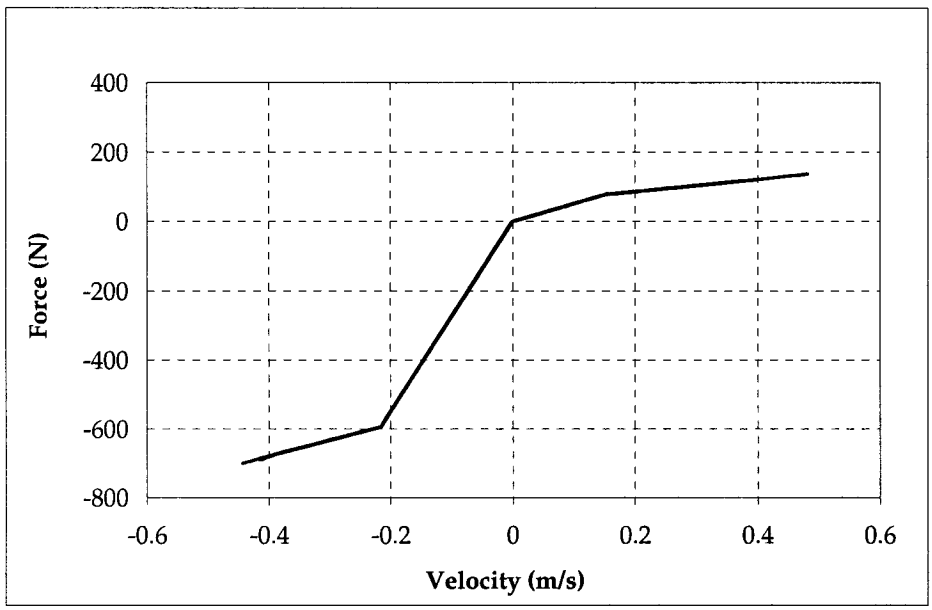

Figure 3.2: Simulated *f-v* characteristics of two-stage asymmetric non-linear damper.

Using the same data provided in their literature, the *f-v* characteristics of the damper is generated using MATLAB® SIMULINK. Figure 3.2 shows the *f-v* characteristics obtained from simulation. As seen from figure 3.1, the slopes of the *f-v* curves are C_1, C_2, C_3, C_4. The values of the slopes of figure 3.1 are C_1=514.5 N-s/m, C_2 = 177 N-s/m, C_3 = 2747.5 N-s/m, C_4= 462 N-s/m. Also, the preset velocities at extension side (right side of the plot), α_1 and at compression side (left side of the plot), α_2 are found from the figure as 0.1524 m/s and -0.2163 m/s respectively.

The slopes are found to be C_1=514.76 N-s/m, C_2 = 176.88 N-s/m, C_3 = 2747.48 N-s/m, C_4= 462.01 N-s/m for the simulated model presented in figure 3.2. Also, the preset velocities at extension side and at compression side of the simulated model are found to be 0.1524 m/s and - 0.2163 m/s respectively.

Thus, the damping force generated by the simulation model is the same as the published results.

3.2.2 Electro-Rheological (ER) Damper

As described earlier in chapter 2, the ER damper used for this study is adopted from the work presented by Nakano (1995). The damping force generated by ER damper can be expressed by equation 2.15.The damping force generated by the damper depends on the feedback gain, f_G, applied to the controller. The author has presented the force-displacement characteristics of the damper as a function of f_G. Figure 3.3 presents the force-displacement characteristics of the damper as obtained by author. Under sinusoidal excitation at a frequency of 1 Hz and amplitude of 50mm, the damping forces generated by the damper for f_G = 5kV²s/m is 500 N, for f_G = 10kV²s/m is 1000 N and

for f_G = 15kV²s/m is 1500 N. It can be seen that the damping force generated by the damper increases with the increase of feedback gain, f_G.

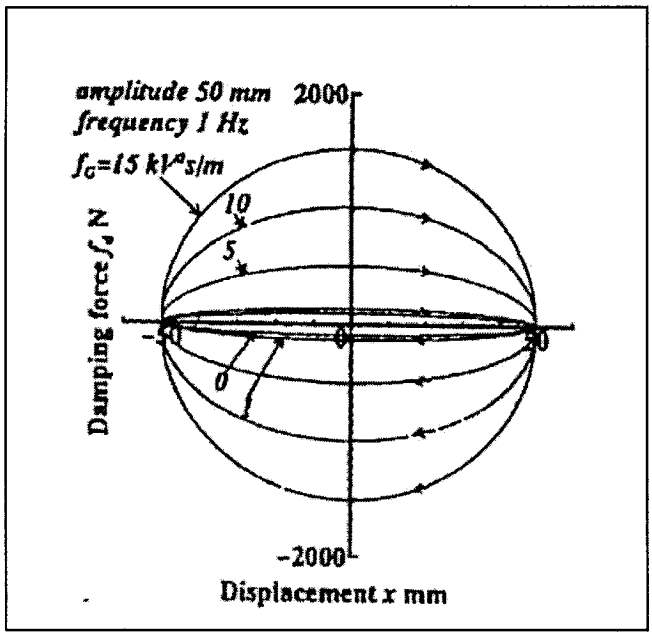

Figure 3.3: Force-displacement characteristics of ER damper (Nakano, 1995).

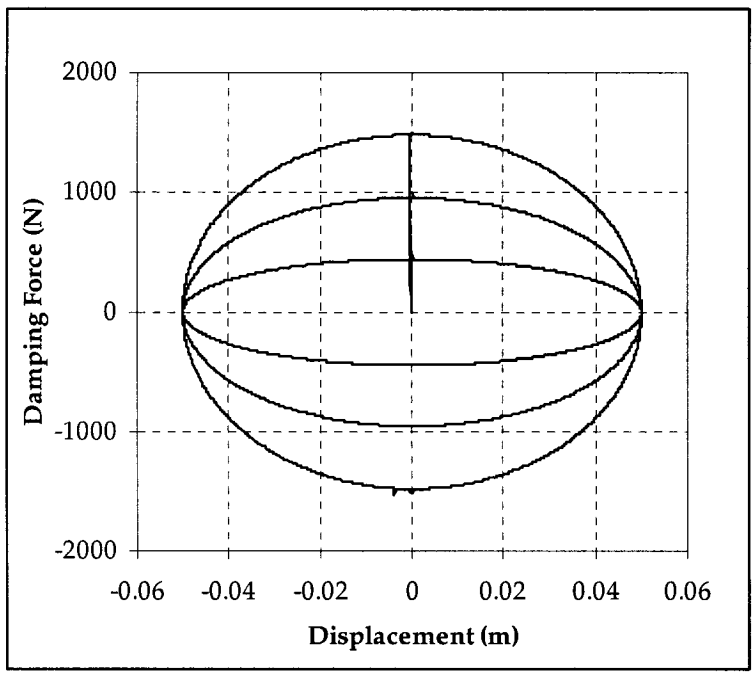

Figure 3.4: Simulated force-displacement characteristics of ER damper.

Using the same data (presented in table 2.3), the force-displacement characteristics of the damper is generated using MATLAB® SIMULINK. Figure 3.4 shows the force-displacement characteristics obtained from simulation. The simulations are carried out for the same excitation frequency (i.e. 1 Hz) and amplitude (i.e. 50 mm). Figure 3.4 shows that, the damping forces generated by the simulation model are: 490.22 N for f_G = 5kV²s/m, 999.17 N for f_G = 10kV²s/m and at 1497.1 N for f_G = 15kV²s/m. There is a little difference between the values obtained by Nakano and obtained in this study. This is due to fact that, for this study, the density of the ER fluid is assumed, since it is not available in Nakano's literature. The maximum error occurs at f_G = 5kV²s/m, which is 1.95%, which can be neglected as it will have little influence in the performance of the simulation model.

3.2.3 Magneto-Rheological (MR) Damper

As described earlier in section 2.4.4, the MR damper used for this study is adopted from the work presented by Ma *et al.* (2002). The damping force generated by MR damper can be expressed by equation 2.22. The damping force generated by the damper depends on control current applied to the damper. The force-displacement and *f-v* characteristics of the MR damper at an excitation frequency of 7.5 Hz as obtained by Ma *et al.*(2002) are presented in 3.5 and 3.7. The control currents applied to the damper are 0.25, 0.50, 0.75, 1.0, 1.25, 1.5 A.

Using the same excitation conditions and control current in conjunction with the data used by the authors (presented in table 2.4), the force-displacement and *f-v* characteristics of the damper are obtained from simulation model. Figure 3.6 and 3.8 shows the force-displacement and *f-v* characteristics obtained from simulation.

The maximum damping force generated by the damper, as shown by figure 3.5 and 3.7 are: 0.224, 0. 353, 0.435, 0.482, 0.51 and 0.518 kN for control current of 0.25, 0.50, 0.75, 1.0, 1.25, and 1.5 A respectively. Exactly same damping forces are generated by the simulation model, as evident from figure 3.6 and 3.8.

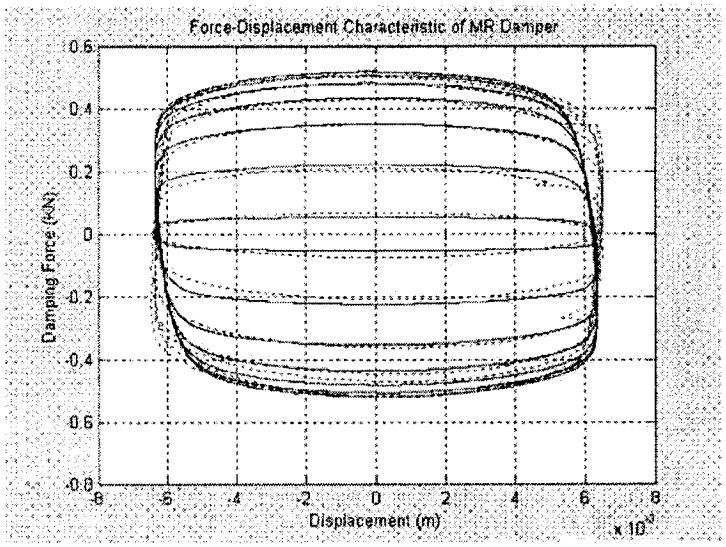

Figure 3.5: Force-displacement characteristics of MR damper (Ma *et al.*, 2002).

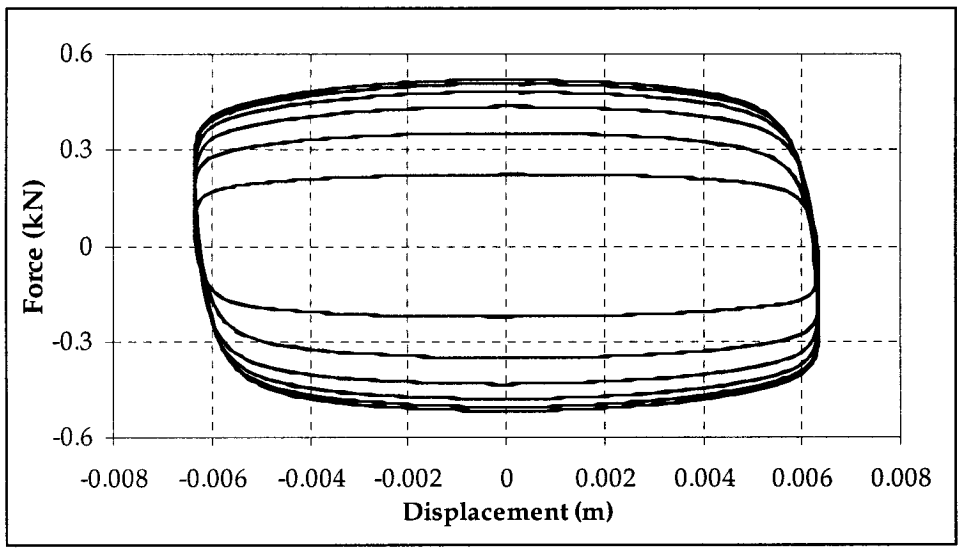

Figure 3.6: Simulated force-displacement characteristics of MR damper.

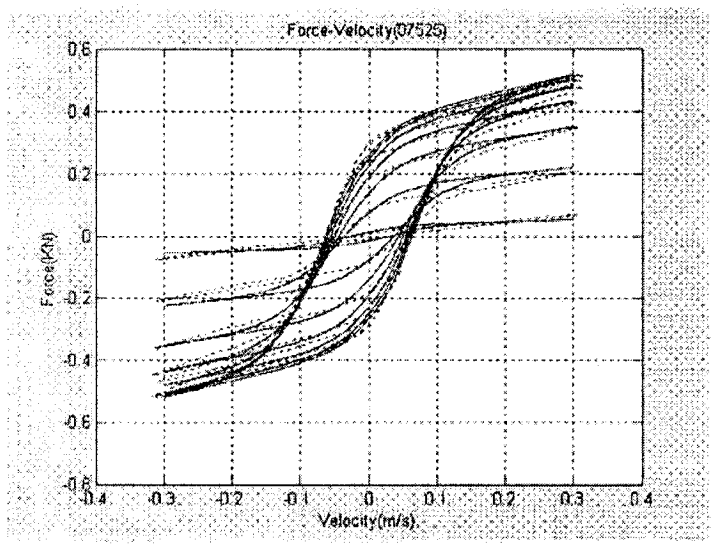

Figure 3.7: *f-v* characteristics of MR damper (Ma *et al.*, 20002).

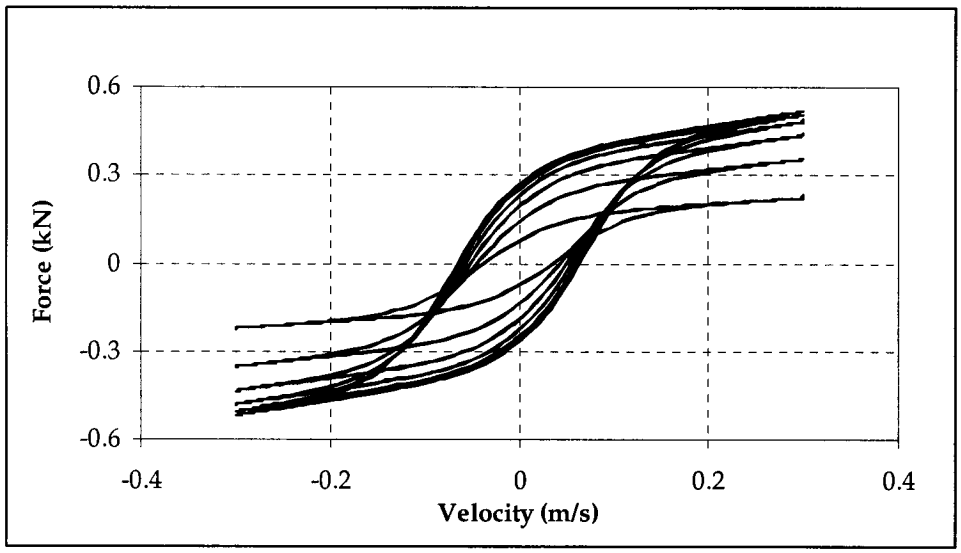

Figure 3.8: Simulated *f-v* characteristics of MR damper.

3.3 Road Excitation

Vehicle vibrations are induced mainly by road roughness, wheel non-uniformity, and the power-train. Road roughness is the main input of the interest when designing suspension system for ride performance, and is also the input over which vehicle designer has least control. Ride performance is usually studied under conditions of constant speed and straight line travel (Cole, 2001). Although, in real life road profiles are random in nature and may include abrupt motions arising from occasional potholes and discontinuities, the assumption of sinusoidal input provides highly useful results in terms of qualitative performance and comparison of designs (Ahmed, 2001). To take advantage of the pitch plane model, the study considers sinusoidal input to simulate pure bounce as well as pure pitch excitations.

Other than random road unevenness, vehicles operating in road commonly encounter bumps, which sometimes can be harmful to vehicle and its occupants. Bump input, also known as shock input, can be represented by rounded step input. A well defined rounded step input serves well for comparison of dampers under shock excitations. The following sections present detailed discussions on sinusoidal and shock input.

3.3.1 Sinusoidal Input

Roughness of a road surface is described by its elevation profile along the path, over which the wheels travel. For harmonic road motion, the road profile is assumed to be of the sinusoidal form and is given by -

$$x_0(t) = x_0 \sin(v_f/\lambda)t \quad \text{.....(3.1)}$$

where, x_0 is the amplitude of excitation, v_f is the forward velocity and λ is the wave-length.

Although, there exists a small time delay between the input applied to front wheel and rear wheel for pitch plane vehicle model, for this study same in phase sinusodal input is applied to both front and rear wheel to simulate pure bounce excitation, and out of phase sinusoidal input to simulate pure pitch input .

3.3.2 Shock Input

Vehicles operating in road commonly encounter bumps, which sometimes can be severe for passengers as well as the freights carried by the vehicles. Vehicles are generally subjected to bump input for few seconds only. When a vehicle passes over a bump, vertical response of sprung mass (x_s), and pitch response of sprung mass (θ) shoots up. One of the major tasks of vehicle suspension system is to minimize damage to vehicle sprung mass, passenger and freights from the sudden shock from bumps. Thus, it is important for suspension not only to isolate vibrations, but also perform in the isolation of shock.

Bump inputs are generally presented by rounded step input (Wang *et al.*, 2003). It is the modification of the pure step input to represent the bumps. Rounded step input can be represented by the following equation –

$$x(t) = Xmax\{ 1 - e^{-\eta\omega_n t}(1+\eta\omega_n t)\} \quad \ldots\ldots (3.2)$$

where, $x(t)$ is the shock amplitude, $Xmax$ is the maximum amplitude of shock , η is the shock severity, and ω_n is the bounce natural frequency of the vehicle.

Since, vehicles are subjected to shock input at a lower velocity and higher amplitude, and for few seconds only, it is very important to consider the time delay

between front and rear wheels of the vehicle as it have significant effect in the bounce and pitch response of sprung mass in a pitch plane vehicle model.

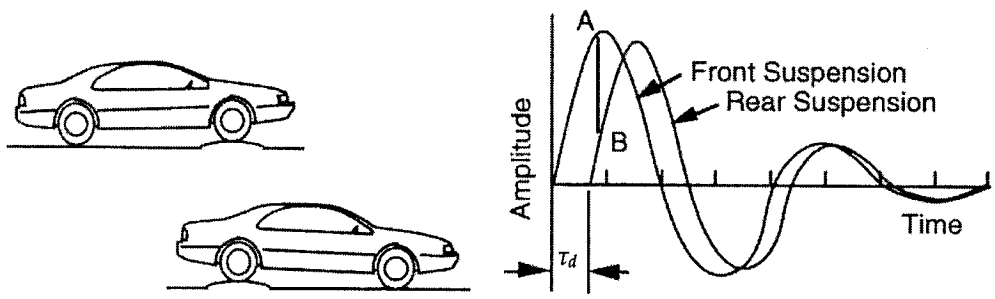

Figure 3.9: Oscillations of a vehicle passing over a road bump (Gillespie, 1992).

Figure 3.9 presents the oscillations at the front and rear of the car for bump input. It shows the vehicle at the worse condition of pitching after the wheels have passed over the bump, indicated by the points A and B in the figure. Point A corresponds to the front end of the car being in a maximum upward position, whereas the point B (rear end) is just beginning to move. As a result, the vehicle will pitch heavily (Gillespie, 1992). Furthermore, pitch is more annoying for human comfort than bounce.

The time lag (τ_d) between the front and rear wheels of the vehicle is given by -

$$\tau_d = L/v_f \ldots\ldots\ldots (3.3)$$

where, L is the wheel base (longitudinal distance between centers of front and rear axle of the vehicle) and v_f is the forward velocity of the vehicle.

Figure 3.10 and 3.11 presents samples of shock input given to front and rear wheels of a vehicle, respectively computed for a forward velocity of 30 km/h.

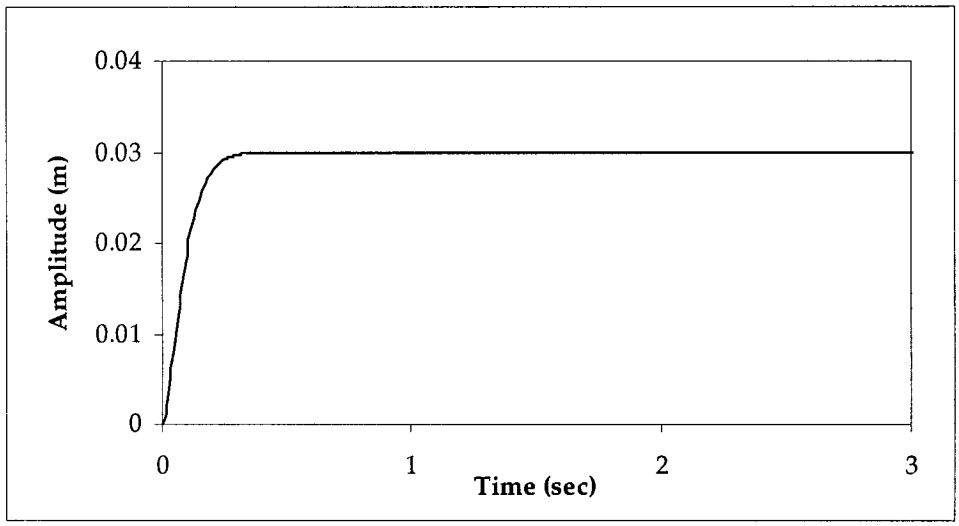

Figure 3.10: Shock (bump) input to the front axle.

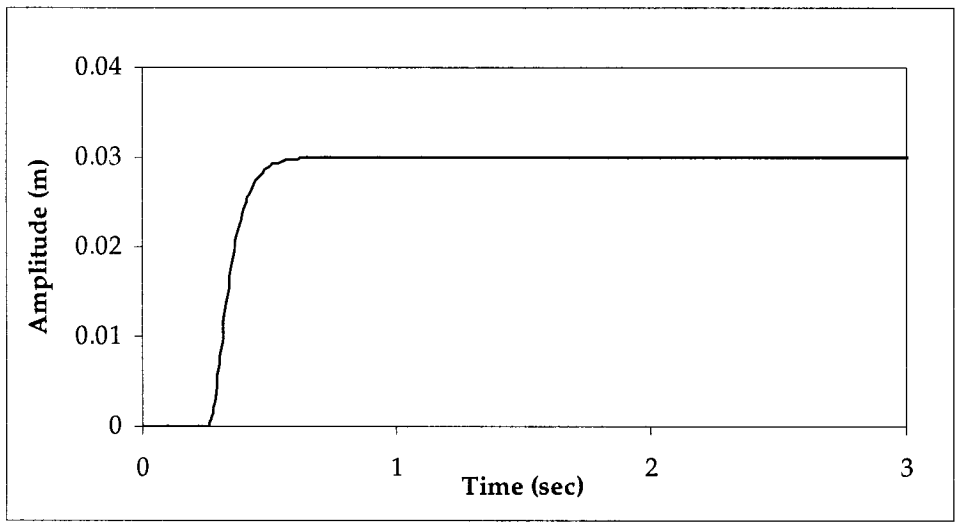

Figure 3.11: Shock (bump) input to the rear axle.

3.4 Performance Measures

The analysis of vibration and shock attenuation performances of suspension dampers used in road vehicles are based on performance of the vehicle under the influence of vibration and shock input from the road. Various performances are measured to determine the ability of the suspension dampers to isolate the vehicle from

steady-state road input. The performance measures include sprung mass displacement transmissibility, unsprung mass displacement transmissibility, sprung mass pitch displacement, suspension travel, relative velocity across the suspension, pavement load etc. (Ahmed 2001; Cole 2001; Wong, 2001; Hwang, 1998; Oueslati, 1990). Furthermore, ride height drift caused by asymmetric non-linear suspension dampers have been investigated by few researchers (Joarder, 2003; Warner, 1996). The investigations are based on simple quarter car model, which neglects possible effect of drifting in the pitch response of the vehicle. The pitch response to drifting is investigated in this study by using the 4 DOF pitch plane model (figure 3.12). A new performance measure, namely – angular drift of the sprung mass, is proposed to analyze the pitch response of the vehicle due to drifting phenomenon.

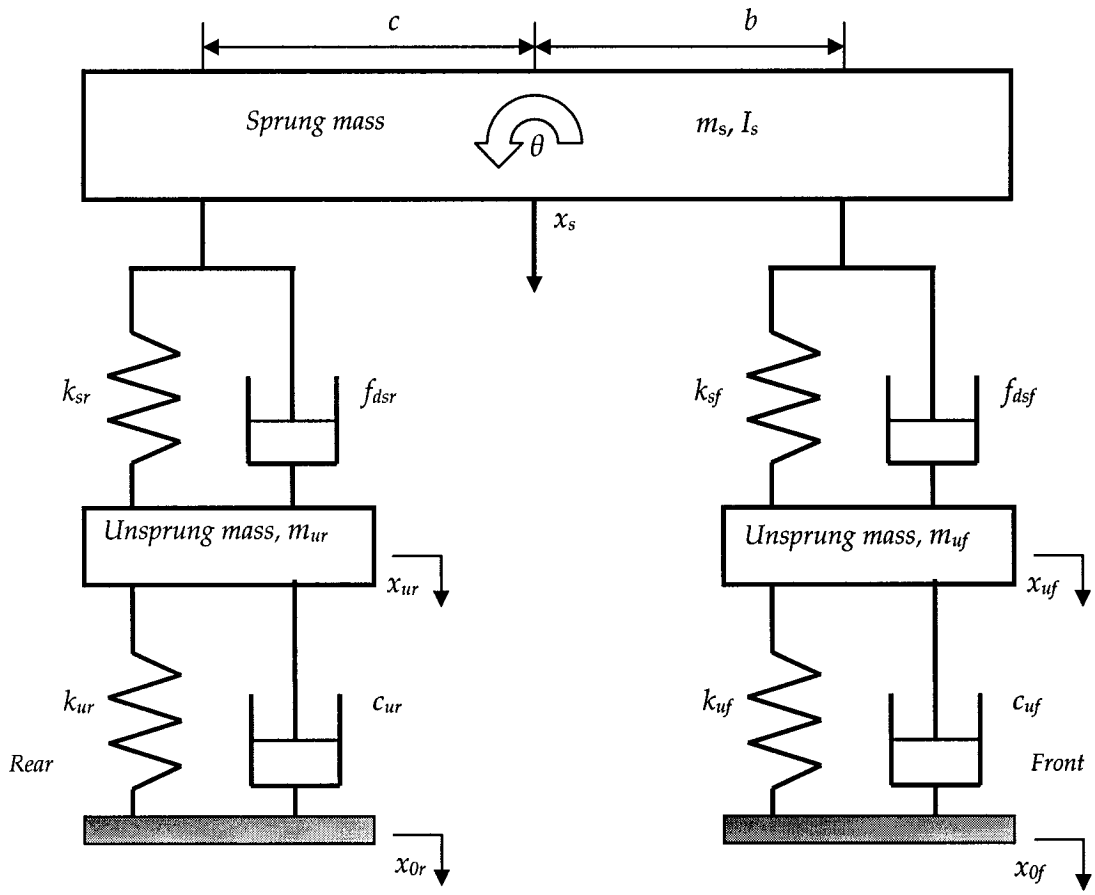

Figure 3.12: Schematic diagram of 4 DOF pitch plane model.

On the other hand, the performance of vehicle suspension subject to shock input can be measured by maximum percent overshoot, rise time and settling time (Sun *et al.*, 2002).

The purpose of this study is to compare the vibration and shock attenuation performances of four different suspension dampers using a small-size passenger car. The comparative analysis is based on a 4 DOF pitch-plane model. In order to compare the performance of the vehicle using different dampers, a set of performance measures, as discussed earlier, is proposed. The performance measures are descried in the following sections with the help of figure 3.12.

3.4.1 Performance measures for Sinusoidal Input

The performance measures considered for this study of a vehicle under sinusoidal input are – (i) sprung mass displacement transmissibility, (ii) unsprung mass displacement transmissibility, (iii) sprung mass pitch displacement, (iv) suspension travel, (v) relative velocity across the suspension, (vi) ride height drift, (vii) angular drift and (viii) pavement load. The performance measures are discussed in the following subsections.

3.4.1.1 Sprung Mass Transmissibility

Sprung mass displacement transmissibility ratio, also known as sprung mass transmissibility, is commonly used to determine the ability of vehicle suspension damper to isolate the sprung mass (m_s) of the vehicle from the road disturbances (x_0). Sprung mass transmissibility ratio is the ratio of vertical displacement of the sprung mass (x_s) to the excitation from the road (x_0). The road input is taken as x_{0f} for the front axle, and x_{0r} for the rear axle. Sprung mass transmissibility to bounce response is defined

as (X_s/X_0). As discussed earlier, for out of phase input the peak pitch angle of excitation computed from (X_{0f} - X_{0r})/L, where X_{0f} and X_{0r} are out of phase sinusoidal (pitch) excitations. The performance of a suspension is judged by its transmissibility performance over the entire frequency range.

3.4.1.2 Unsprung Mass Transmissibility

Similar to sprung mass displacement transmissibility ratio, unsprung mass displacement transmissibility ratio is commonly used to determine the response of the unsprung mass of vehicle (x_{uf} and x_{ur}) to vibration input from the road. Unsprung mass transmissibility ratio is the ratio of vertical displacement of the unsprung mass to the excitation from the road. For the front unsprung mass, it is the ratio of vertical displacement of the front unsprung mass (x_{uf}) to the excitation from the road (x_{0f}), and for the rear unsprung mass it is the ratio of vertical displacement of the rear unsprung mass (x_{ur}) to the excitation from the road (x_{0r}).

3.4.1.3 Sprung Mass Pitch Displacement

Sprung mass pitch displacement (θ) is the angular displacement of the sprung mass of the vehicle due to road input at the wheels. Higher values of pitch displacement might result in motion sickness to the occupants of the vehicle and might cause damage to freights carried by the vehicle. Hence, it is very important for the suspension dampers to minimize the pitch displacement of the sprung mass, by providing better isolation to the sprung mass. For this study, the angular motion in the counter-clockwise direction is assumed to be positive. It is desired that, pitch displacement of the vehicle is kept as low

as possible around pitch natural frequency, and has reasonable values at other frequencies, under both bounce and pitch excitations.

3.4.1.4 Suspension Travel

Suspension travel, also known as rattle space, is a measure of the relative displacement between the sprung and unsprung mass of the vehicle. It indicates the space required to accommodate the suspension spring motion. Rattle space is very important when it comes to determining the amount of payload that certain vehicle can carry without causing damage to the suspension system. Corresponding to figure 3.12, the quantities $(x_s - x_{uf})$ and $(x_s - x_{ur})$ represents the rattle space required by front axle suspensions and rear axle suspensions respectively.

3.4.1.5 Relative Velocity Across Suspension

Relative velocity across suspension, also known as damper piston velocity, is a measure of relative velocity between the sprung and unsprung mass. Since velocity of the damper's piston is limited to certain design value, it is important that the relative velocity is kept within the design limit. Corresponding to figure 3.12, the quantities $(\dot{x}_s - \dot{x}_{uf})$ and $(\dot{x}_s - \dot{x}_{ur})$ represents the relative velocity across the dampers of front axle and rear axle, respectively.

3.4.1.6 Ride Height Drift

Ride height drifting is a response of the suspension system which is generated from the asymmetry of the suspension dampers. Researchers often refer this phenomenon of drifting in the ride height as 'the packing down of the suspension'

(Warner, 1996) or as 'mean line shifting of the alternating amplitude response' (Rajalingham and Rakheja, 2003). Ride height of a vehicle is shown in figure 3.13.

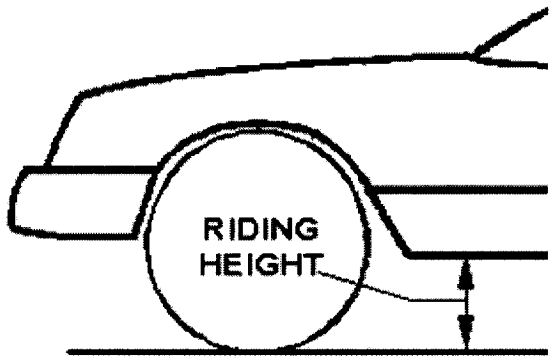

Figure 3.13: Ride height (Joarder, 2003).

An experimental investigation by Warner (1996) has demonstrated that the ride height is significantly influenced by the excitation frequency. It is also observed the variations in high rebound damping yields considerably larger variations in ride height than those caused by proportional changes in the compression damping. Rajalingham and Rakheja (2003) investigated the influence of a conceptual single-stage asymmetric damping on dynamic response of the sprung mass of a quarter car model. The numerical simulation based study suggested that, the damper non-linearity introduces a downward shifting in the mean position of the sprung mass in addition to the vibratory response. However, the response of the unsprung mass doesn't exhibit such a mean position shift. A comprehensive study on drifting is carried out by Joarder (2003) using a quarter car model. The study considered various damper model namely - linear, nonlinear symmetric, single stage asymmetric, and finally the two-stage asymmetric suspension properties. The study reveals that the 'ride height drifting' is the direct result of asymmetric properties of the suspension damper. The magnitude of the drift increases with an increase in asymmetry as well as amplitude of excitation, and it

approaches maximum corresponding to the wheel hop natural frequency. Figure 3.14 shows the effect of excitation amplitude on ride height drift.

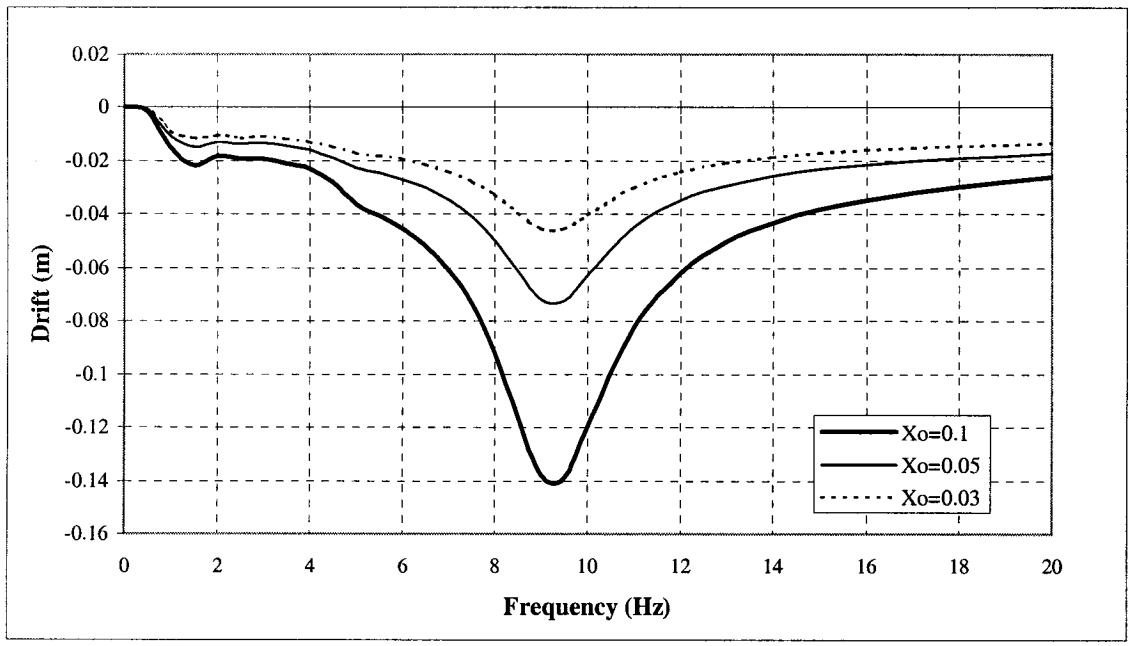

Figure 3.14: Frequency response of drift for a two-stage asymmetric damper model corresponding to different excitation amplitudes (Joarder, 2003).

It would be interesting to examine the ride height drift response in a pitch plane model as it may result in a pitch angle drift. Since no attempt has been so far regarding the effect of drifting on ER and MR based semi-active suspension system, it is necessary to study drifting for these dampers.

To should be mentioned that ride height drift is not a desired performance and is the result of certain damper parameters, namely asymmetricity. The drift is not desirable and may affect other vehicle performance. To rectify this problem, suspension manufacturer like ZF Sachs AG, Germany has designed Nivomat brand suspension systems which can control the ride height. Figure 3.15 represents the difference in ride

height observed by using such suspension system in Audi. Left side of the figure shows the vehicle with regular damper and right side shows the vehicle with Nivomat suspension system. It can be seen that, the drifting is reduced using the new suspension system.

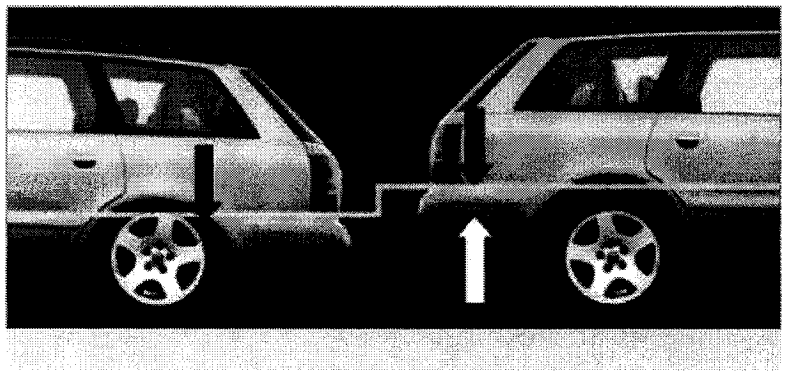

Figure 3.15: Difference in ride-height using Nivomat suspension in Audi (ZF Sachs AG, Germany).

The ride height drift is measured by the change in dynamic equilibrium of the sprung mass (m_s). It is done by measuring the average value of sprung mass displacement (x_s). An average of zero indicates the absence of drift, positive average means drift in downward direction (since downward motion of the vehicle is assumed positive for this study).

3.4.1.7 Angular Drift

The earlier investigations of drifting phenomenon based on simple quarter car model (Joarder, 2003; Warner, 1996), did not describe the effect of drifting in the pitch response of the vehicle. The 4 DOF pitch plane model used for this study analyzes the pitch response of the vehicle due to drifting. A new performance measure, namely –

angular drift of the sprung mass, is introduced to analyze the pitch response of the vehicle due to drifting phenomenon. Similar to ride height drift, angular drift is the change in the dynamic angular equilibrium of the vehicle. The angular drift may directly affects the lines of vision, line of head light dip, aerodynamics etc. to name a few. Thus it is desired that, suspension damper will produce no angular drift or very little drift throughout the operating frequencies of the vehicle. The angular drift is measured by the change in dynamic pitch equilibrium of the sprung mass (m_s). It is done by measuring the average value of sprung mass pitch displacement (θ). An average of zero indicates the absence of any drift, positive average means drift in counter-clockwise direction (since counter-clockwise pitch motion of the vehicle is assumed positive for this study).

3.4.1.8 Pavement Load

Modern suspension designs should not only consider the suspension performance in terms of vehicle and its occupants, but also should consider damages caused by dynamic motion of vehicle. The dampers of the vehicles are responsible to reduce the amount of force transmitted to road from the vehicle. The force transmitted to the road from the moving vehicle is known as pavement load. It is important to keep the pavement load as low as possible, as the longevity of the road depends on the amount of load transmitted to pavement by vehicles. Higher pavement road will require frequent maintenance of roads, which is expensive. Also, regulations are in place to limit the amount of pavement load vehicles can transfer to the road, so the roads suffer less damage. Pavement load is not really an issue for the vehicle size considered

in this investigation. However, it is included as a performance measure for comparative analysis.

Corresponding to figure 3.12, the quantities $[(\dot{x}_u - \dot{x}_{0f})c_{uf} + (x_u - x_{0f})\, k_{uf}]$ and $[(\dot{x}_u - \dot{x}_{0r})c_{ur} + (x_u - x_{0r})\, k_{ur}]$ represent the dynamic pavement load generated by front and rear axle suspensions of the vehicle respectively. For this study, the peak values of the pavement loads are considered at various operating frequencies of the vehicle. It is desired that, the peak values of pavement load be as low as possible to minimize the road damage caused by the dynamic motion of the vehicle.

3.4.2 Performance Measures for Shock Input

When a vehicle passes over a bump, vertical response of sprung mass (x_s), and pitch response of sprung mass (θ) shoots up. Generally, vehicles are subjected to shock (bump) input for few seconds only. Thus, sprung mass bounce and pitch displacement response are analyzed to understand the behavior of a vehicle subject to shock input. The sprung mass displacement response can be analyzed by three different parameter- (i) maximum percent overshoot, (ii) rise time and (iii) settling time (Sun *et al.*, 2002).

Corresponding to figure 3.12, maximum percent overshoot is the maximum vertical displacement of the sprung mass (x_s) as percentage of maximum amplitude of shock *Xmax* (equation 3.2). Rise time is the time required to reach the maximum vertical displacement (x_s) from *Xmax*, and settling time is the time required to reach 110% of the maximum amplitude of shock input (*Xmax*).

For the sprung mass pitch response, maximum pitch of sprung mass (θ) both in clockwise and counterclockwise direction, and the settling time required to reach certain

pitch value (Sun *et al.*, 2002) are measured. For this study, the time required to reach 0.005 radian is considered as settling time.

3.5 Summary

In this chapter, the damping characteristics of the candidate dampers have been discussed and formulated. They are modeled as block in the MATLAB® SIMULINK to incorporate in the 4 DOF vehicle model. Simulations are carried out to ensure that the models produce the damper characteristics that are being designed for. The road excitations, namely sinusoidal pure bounce, sinusoidal pure pitch and shock input of rounded step are explained at discussed. Finally, a set of performance measures are presented to study the comparative performance of the suspension dampers.

CHAPTER 4

A Comparative Study

4.1 General

The smart fluid based ER and MR dampers have gained widespread attention both in the academia and in industries for their attractive feature which overcomes the performance limitation of conventional dampers. Although there are several studies that investigate the vibration isolation performance of a specific advance concept with a set of parameters, there is a lack of comprehensive parametric study and investigation of isolation performance under shock excitations. Majority of the studies only compared either ER or MR damper with linear damper, despite the fact that asymmetric dampers are widely used in modern vehicles. Moreover, most of the studies used simple quarter car model, neglecting the pitch motion and bounce-pitch coupling in the vehicle motions. This work presents a comprehensive study of linear passive, two-stage asymmetric non-linear, ER and MR damper to analyze their vibration and shock isolation performance using a four degree-of-freedom pitch plane ride model and a set of performance measures.

The damper models presented in chapter 2, and the damper validation presented in chapter 3, clearly indicates that the simulation damper models are capable of generating desired damping characteristics. Thus, the damper model can be incorporated in vehicle models to study their comparative performance. This chapter is devoted to the comparative study of vibration and shock isolation performance of the dampers. The comparative performance of the dampers are investigated by

incorporating the damper models one at a time in a 4 DOF of pitch plane model, to analyze the performance measures presented in chapter 3 (section 3.4). Before analyzing the performance of the dampers using a 4 DOF pitch plane model, the performance of the dampers are studied by incorporating the dampers in a simple 2 DOF quarter car model. The 2 DOF system analyses provide brief understanding of the performance of the dampers. Most importantly, this model is used to tune the dampers for the vehicle parameters used such that reasonable and comparable performances are produced.

In order to evaluate the performance of the dampers using 2 DOF and 4 DOF systems, basic system parameters for the vehicle are proposed in this chapter. The vibration isolation performances of the dampers are compared at excitation amplitude of 10mm, which represents reasonable road input, over a wide sinusoidal (both in phase and out of phase) frequency range. The frequency range of 0.8 to 18 Hz is considered appropriate for vehicle ride performance analysis. Subsequently, the shock performances of the dampers are analyzed by applying rounded step input. Finally, the effect of higher amplitude excitation is studied by applying sinusoidal excitation (both in phase and out of phase) of 15 mm amplitude to examine the influence of amplitude on performances of the dampers.

For the convenience of discussion, in this chapter, the linear passive damper, two-stage asymmetric non-linear damper, Electro-Rheological damper, and Magneto-Rheological damper are short named as linear, asymmetric, ER and MR damper.

4.2 Basic System Parameters

In order to evaluate the performance of 2 DOF and 4 DOF model using different dampers, it is important to select sets of basic system parameters. The basic system

parameters represent the values of the parameters corresponding to equation 2.1 to 2.6. Basic system parameters for 2 DOF quarter car model and 4 DOF pitch plane model are adopted from literature (Ahmed, 2001) and are typical of those used for a small-size passenger car. Table 4.1 represents the parameters for 2 DOF quarter car model and table 4.2 presents the parameters for 4 DOF pitch plane model.

Table 4.1: Basic system parameters for 2 DOF quarter car model.

Parameter	*Value*	*Unit*
Sprung mass, m_{sq}	231	Kg
unsprung mass, m_{uq}	17	Kg
Suspension stiffness coefficient, k_s	12,800	N/m
Tire damping coefficient,c_u	750	Ns/m
Tire stiffness coefficient, k_u	150,000	N/m

Table 4.2: Basic system parameters for 4 DOF pitch plane model.

Parameter	*Value*	*Unit*
Sprung mass, m_s	754.6	Kg
Front unsprung mass, m_{uf}	34.2	Kg
Rear unsprung mass, m_{ur}	41.2	Kg
Sprung mass moment of inertia, I_s	1094	kg m^2
Distance between front axle and CG of the vehicle, b	0.87	M
Distance between rear axle and CG of the vehicle, c	1.29	M
Front tire damping coefficient (each tire),c_{uf}	750	Ns/m
Rear tire damping coefficient (each tire), c_{ur}	750	Ns/m
Front suspension stiffness coefficient (front axle), k_{sf}	25,600	N/m
Rear suspension stiffness coefficient (rear axle), k_{sr}	17,300	N/m
Front tire stiffness coefficient (each tire), k_{uf}	150,000	N/m
Rear tire stiffness coefficient (each tire), k_{ur}	150,000	N/m

4.3 Natural Frequencies of the Vehicle System

The sprung mass and unsprung mass natural frequencies of the quarter car model are estimated by using the following equations adopted from Ahmed (2001) -

Sprung mass natural frequency, $\omega_{ns}=\sqrt{(k_{ride}/m_{sq})}$ where, $k_{ride}= k_u k_s/(k_s+k_u)$

Unsprung mass natural frequency, $\omega_{nu} =\sqrt{(k_{effective}/m_{uq})}$ where, $k_{effective}= k_s+k_u$

By using the basic system parameter values of 2 DOF quarter car model presented in table 4.1, sprung mass natural frequency is found to be 1.14 Hz and unsprung mass natural frequency (also known as wheel hop frequency) is found to be 15.57 Hz.

Subsequently, using the equations 2.1 to 2.4 and basic parameters of 4 DOF pitch plane model presented in table 4.2, the dynamic matrix of undamped system as $[M]^{-1}[k]$ is established. The eigenvalue solution of the dynamic matrix and corresponding eigenvector (mode shape) is utilized to establish and identify the four natural frequencies. The natural frequencies are 1.16, 1.0, 15.57 and 13.97 Hz for bounce, pitch, front wheel hop and rear wheel hop respectively.

4.4 Vibration Isolation Performance Analysis Using 2 DOF Model

First step of the study is to examine the behavior of the dampers using a simplified 2 DOF model. The advantage of using 2 DOF model is that, one can easily observe the performance of the vehicle system equipped with different dampers and can identify the performance for comparison with widely available response signatures. The linear, asymmetric, ER and MR damper models, presented in section 2.4, and validated in chapter 3, are incorporated in the 2 DOF model to investigate their performance. The performance of 2 DOF model is evaluated using the data presented in table 4.1, and data

of damper parameters presented in table 2.1, 2.2, 2.3 and 2.4 are used to evaluate the performance of linear, asymmetric , ER and MR damper respectively. The performances of the vehicle model, using different dampers are investigated under sinusoidal excitations in the range of 0.8 Hz to 18 Hz with excitation amplitude of 10mm. The 2 DOF model study consists of two parts: (a) study of sprung mass response (e.g. displacement transmissibility); (b) study of unsprung mass response (e.g. displacement transmissibility).

4.4.1 Sprung Mass Transmissibility

The sprung mass displacement transmissibility ratios of the vehicle using 4 different dampers are presented in figure 4.1. The results represent sprung mass transmissibility of the candidate damper tuned such a way that they all produce similar ride quality for higher frequencies, while minimize the response at resonance. The figure indicates that, around the sprung mass natural frequency (1.1 Hz), the sprung mass displacement transmissibility ratios are highest.

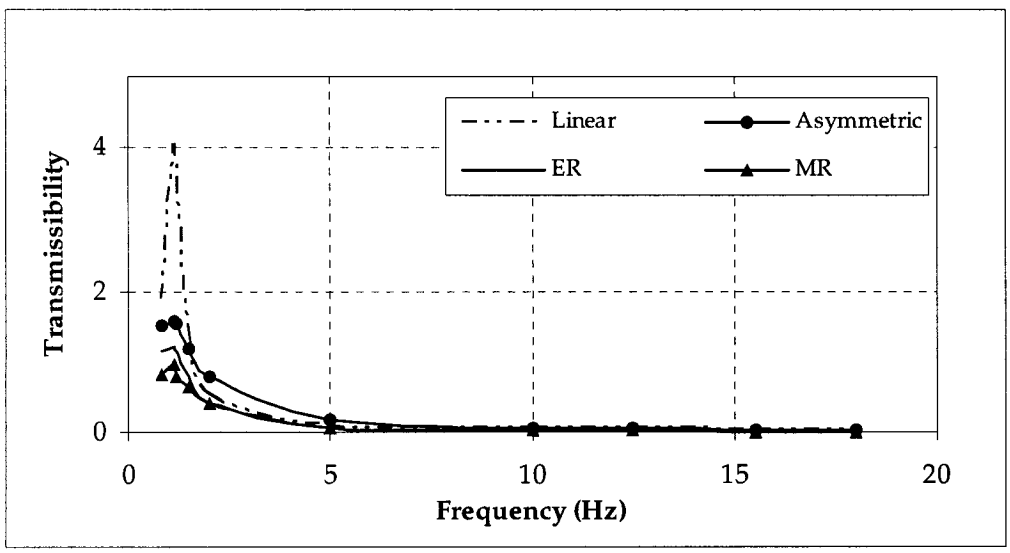

Figure: 4.1: Sprung mass transmissibility of 2 DOF model.

The transmissibility ratio is 4.02 with linear damper, 1.59 with asymmetric damper, 1.03 with ER damper, and 1.11 with MR damper. These responses are typical of those available in literatures. A comparison of the four dampers clearly reveals the superiority of asymmetric damper over linear, and the effectiveness of ER and MR over the entire frequency range. It is also been observed that, at frequencies above the sprung mass natural frequency, the transmissibility values decrease more rapidly for ER damper and MR damper compared to the asymmetric case.

4.4.2 Unsprung Mass Transmissibility

The unsprung mass displacement transmissibility ratios of the vehicle using 4 different dampers are presented in figure 4.2. The figure shows that, in the frequency range around the unsprung mass natural frequency (15.5 Hz), the unsprung mass displacement transmissibility ratio is highest. The transmissibility ratios of the system with linear damper is 1.51, with asymmetric damper is 1.38, with ER damper is 1.98 and with MR damper is 1.99. It is evident that, although ER and MR damper based system provides better vibration isolation to sprung mass compared to linear and asymmetric, they provide poor isolation to unsprung mass. The ER and MR dampers thus provide superior sprung mass transmissibility at the expense of performance for unsprung mass response.

An interesting aspect in the results shown in figure 4.2 is the fact that asymmetric damper provides superior performance compared to linear for both sprung and unsprung mass transmissibility over the entire frequency range. This can be attributed to better road holding capability of asymmetric damper. This can be easily verified by one simulation with reduced asymmetry. Figure 4.3 presents a comparison of

results showing unsprung mass transmissibility for asymmetric, symmetric and linear system. Here, the symmetric case is established by assuming C_1 value to C_3 and value of C_2 value to C_4 asymmetric damper model (equation 2.14). The results clearly reveal the influence of asymmetricity on transmissibility performance around unsprung mass natural frequency.

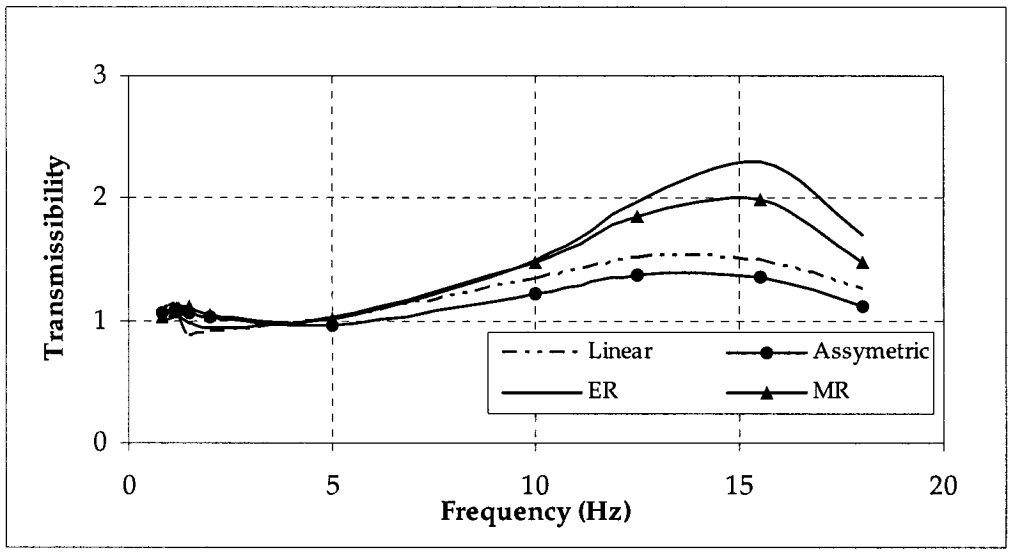

Figure 4.2: Unsprung mass transmissibility of 2 DOF model.

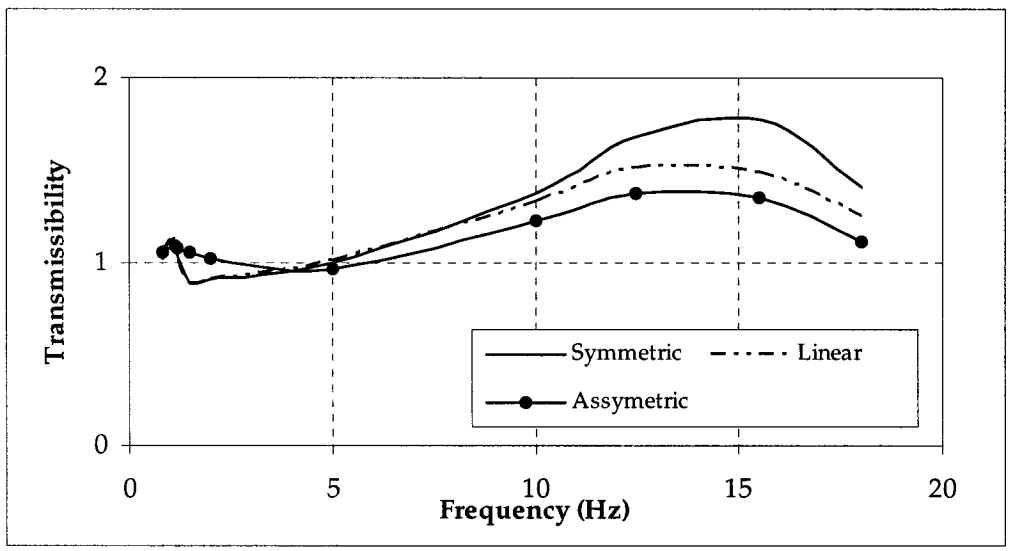

Figure 4.3: Comparison of symmetric vs. asymmetric damping at unsprung mass natural frequency.

4.5 Vibration and Shock Isolation Performance Analysis Using 4 DOF Pitch Plane Model

The damper validation results presented in chapter 3 and the responses of 2 DOF system in terms of sprung and unsprung mass transmissibility indicate that, the 4 damper models developed for this study are generating comparable results. Thus, linear, asymmetric, ER and MR dampers can be incorporated in a 4 DOF pitch plane model to study their comparative performance. The performance of 4 DOF pitch plane model is evaluated using the data presented in table 4.2, and data of damper parameters presented in table 2.1, 2.2, 2.3 and 2.4 are used to evaluate the performance of linear, asymmetric , ER and MR damper respectively. The comparative study of the dampers is based on the performance measures described section 3.4 of chapter 3.

The comparative study is divided into five sections. At first sample time history of various performance measures of the vehicle system due to sinusoidal input are presented to aid in the interpretation of results. It is followed by damper force-velocity and force-displacement characteristics extracted from the simulation model and are presented to aid the verification of actual damping force generated by the dampers over the cycle.

Comparative results in terms of frequency response are then presented for both bounce (in phase sinusoidal) and pitch (out of phase sinusoidal) excitations in the range of 0.8 to 18Hz with amplitude of 10mm. It is followed by analysis under the influence of shock excitation. Finally, the effect of higher excitation amplitude (15mm) is examined as it may have influence due to non-linear characteristics of the dampers considered.

4.5.1. Time History

In this section, the steady state sample time histories of selected performance parameters are presented for sinusoidal excitation (bounce) of 10 mm amplitude and at different frequencies. Figure 4.4 clearly shows the asymmetricity of the asymmetric damper. Figure 4.5 shows that unsprung mass responses for all the dampers are similar at low frequency.

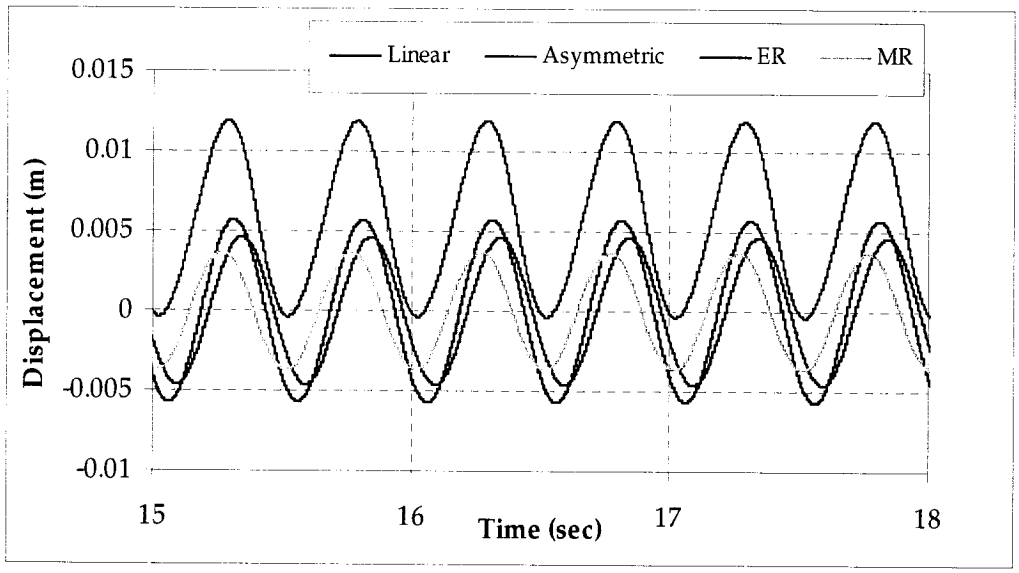

Figure 4.4: Steady state time history of sprung mass displacement (2Hz).

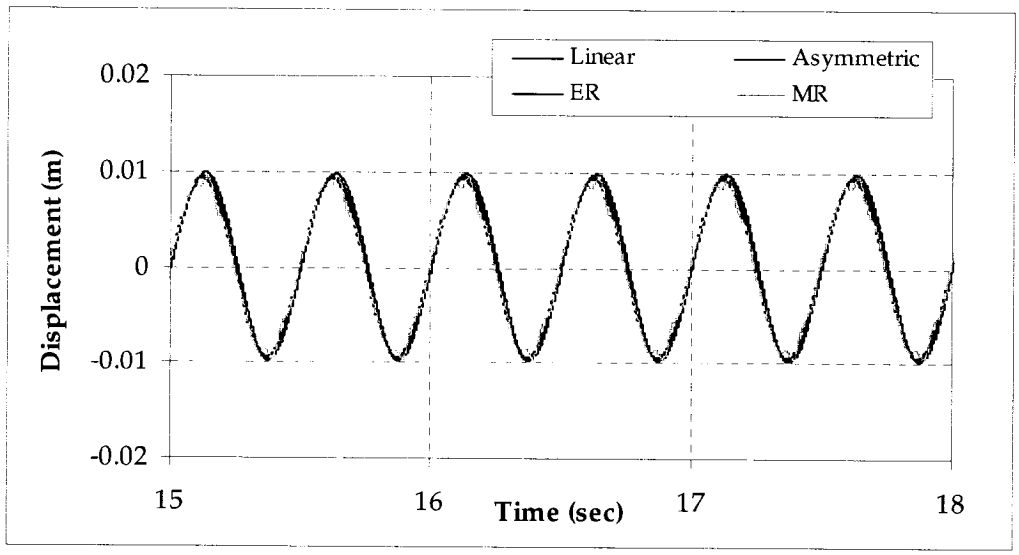

Figure 4.5: Steady state time history of front unsprung mass displacement (2 Hz).

Figure 4.6 and 4.7 reveal the poor performance of ER damper and MR damper around unsprung mass natural frequencies.

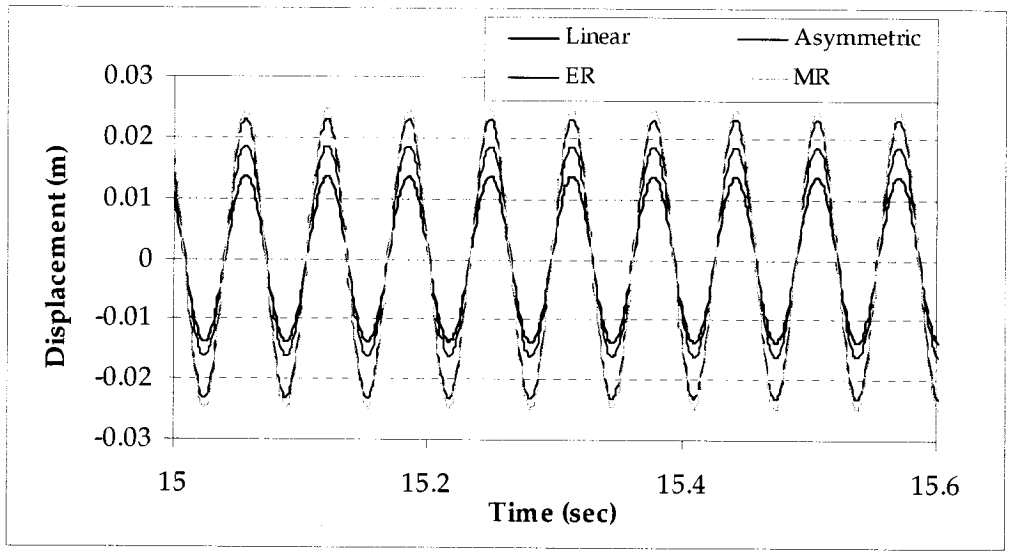

Figure 4.6: Steady state time history of front unsprung mass displacement (15.57 Hz).

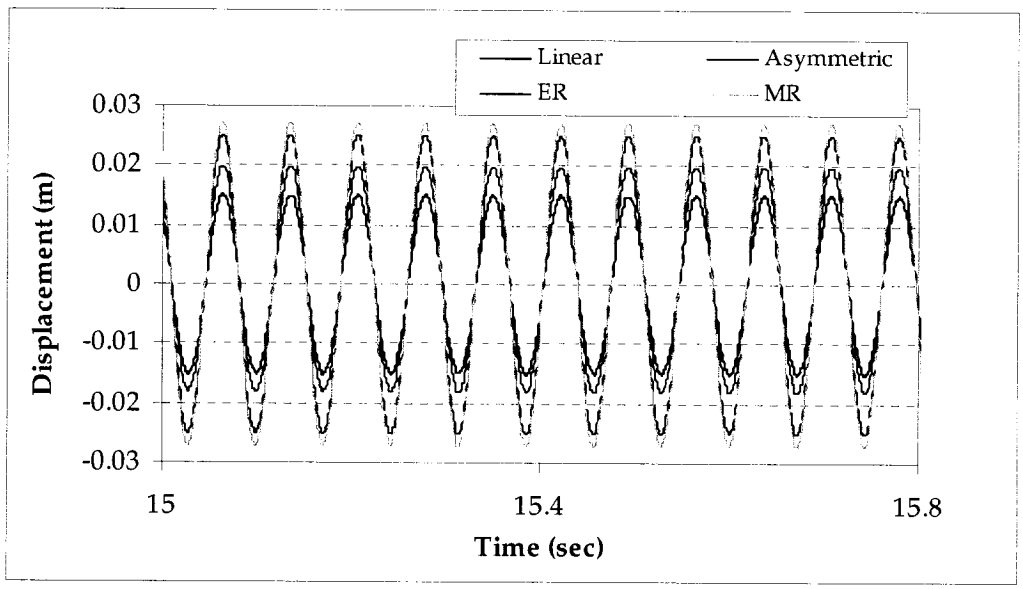

Figure 4.7: Steady state time history of rear unsprung mass displacement (13.96Hz).

Figure 4.8 shows the effect of asymmetricity in the pitch response of asymmetric damper.

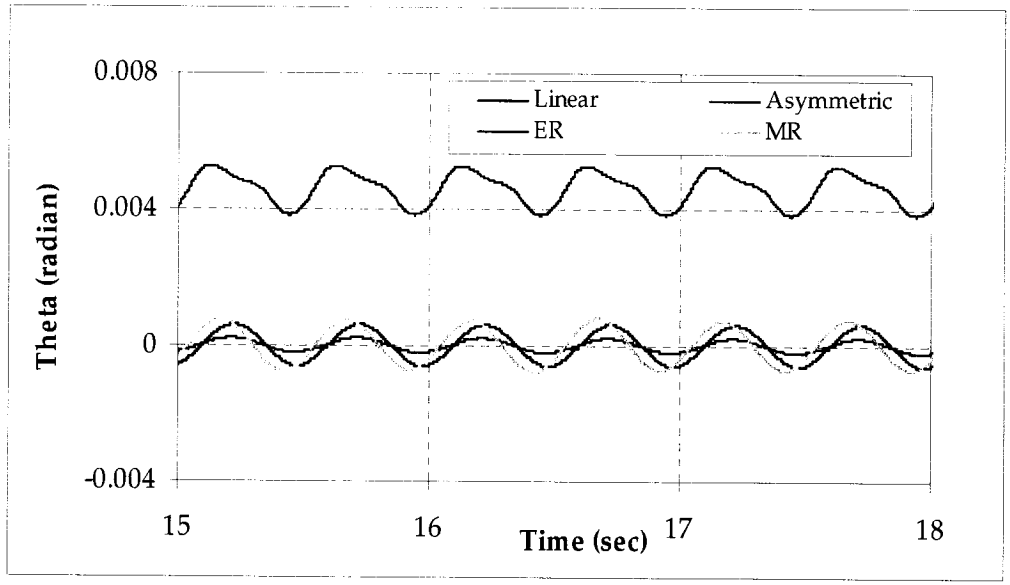

Figure 4.7: Steady state time history of pitch displacement (2Hz).

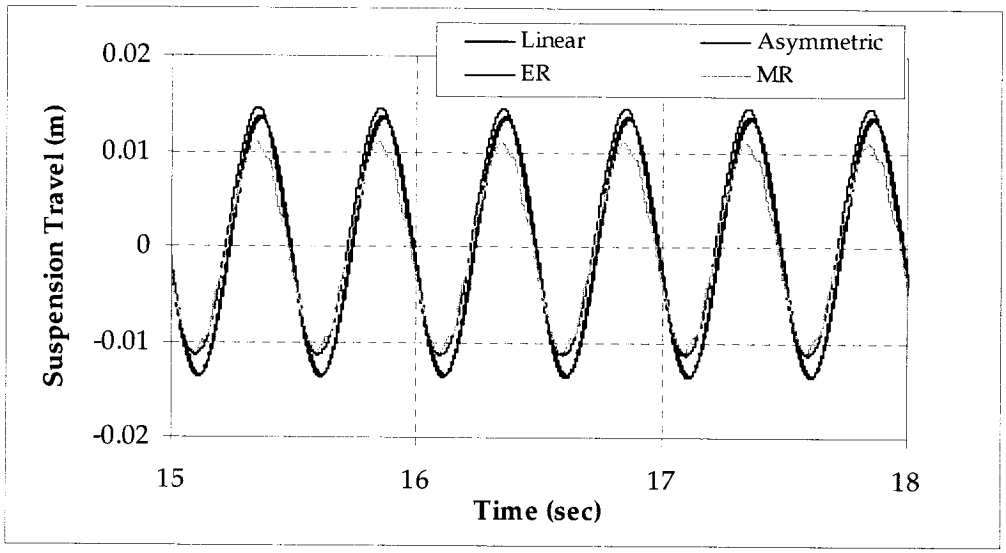

Figure 4.9: Steady state time history of suspension travel for front suspensions (2Hz).

Figure 4.10 indicates that suspension travel for ER damper and MR damper are high at higher frequency.

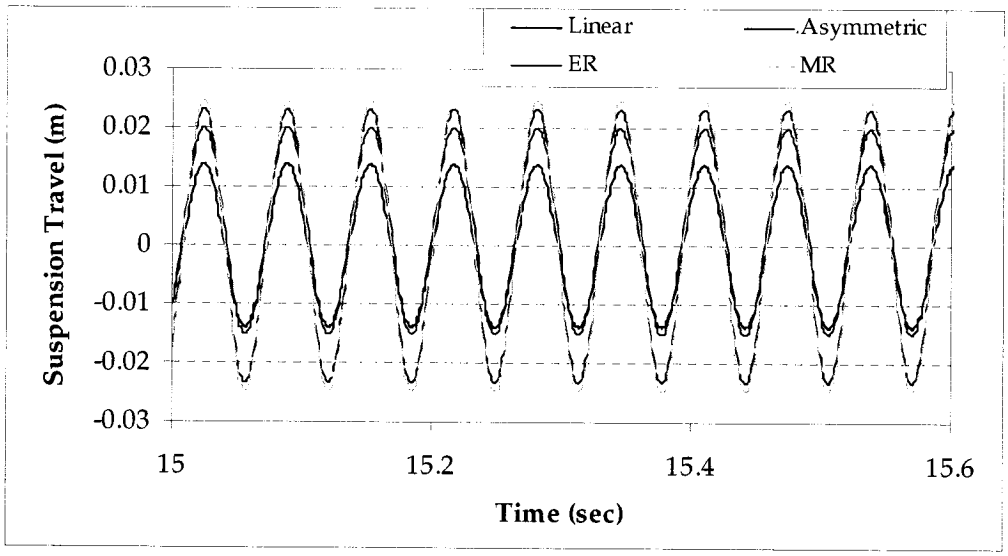

Figure 4.10: Steady state time history of suspension travel for front suspensions (15.57 Hz).

Figure 4.11 indicates that pavement load for ER damper and MR damper are high at higher frequency.

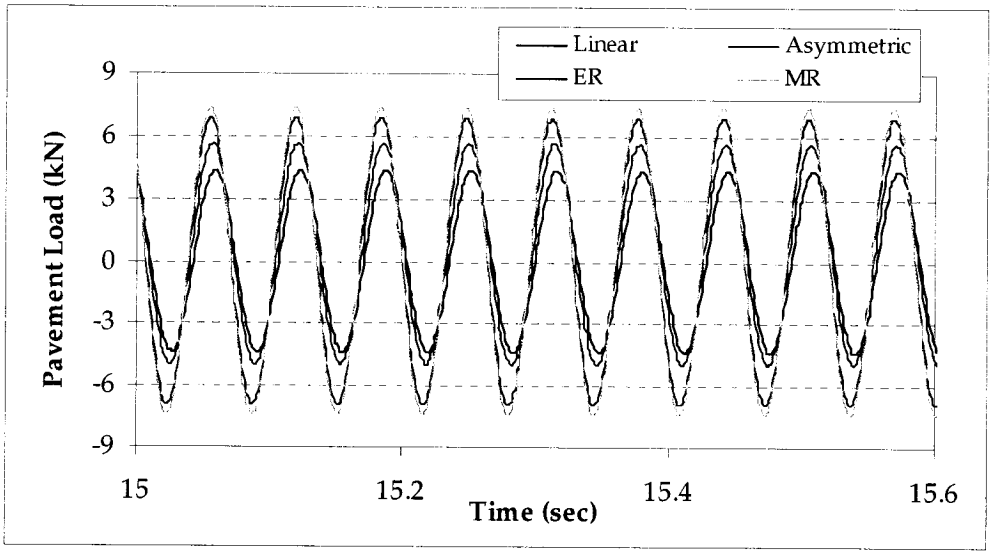

Figure 4.11: Steady state time history of pavement load of front axle (15.57 Hz).

4.5.2 Damping Characteristics of the Candidate Dampers

In this section, steady state damping characteristics of all the damper models are presented. The real time damping characteristics of the dampers, as applied to the vehicle model are examined under an excitation frequency of 5 Hz and excitation amplitude of 10mm.

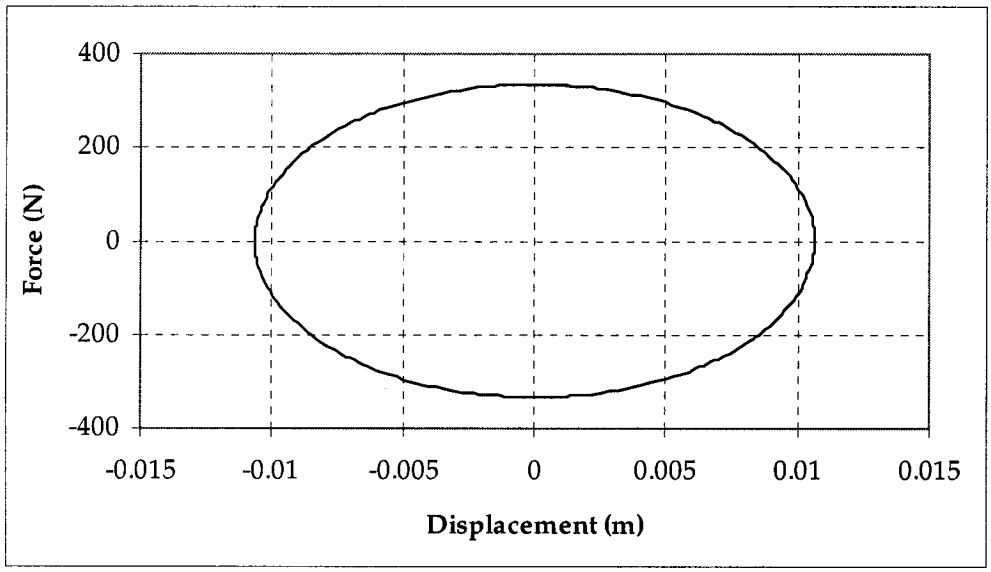

Figure 4.12: Force-displacement characteristics of linear damper.

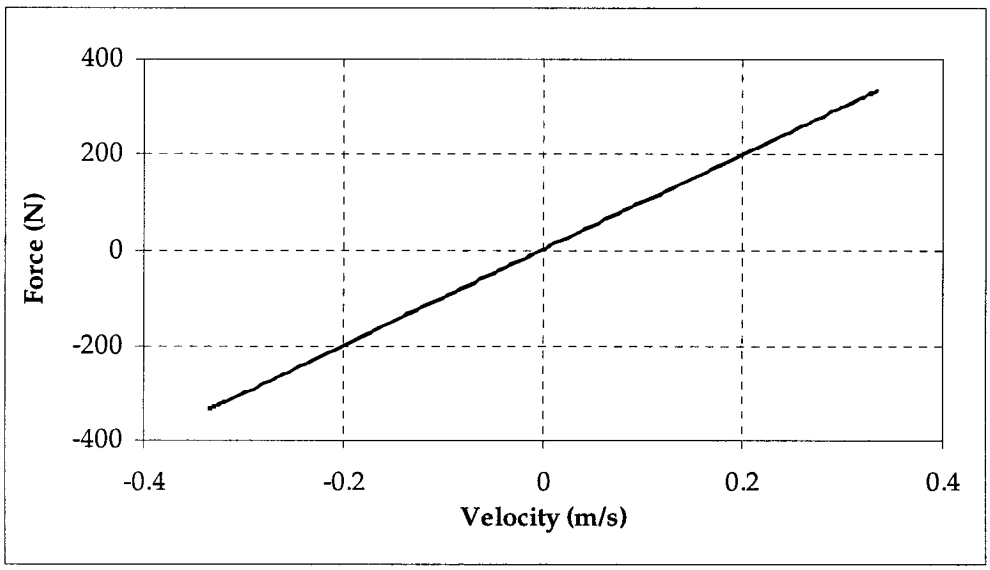

Figure 4.13: *f*-v characteristics of linear damper.

Figure 4.12, 4.14, 4.16, 4.18 presents force-displacement characteristics, and figure 4.13, 4.15, 4.17, 4.19 presents force-velocity (*f-v*) characteristics of linear, asymmetric, ER and MR damper respectively.

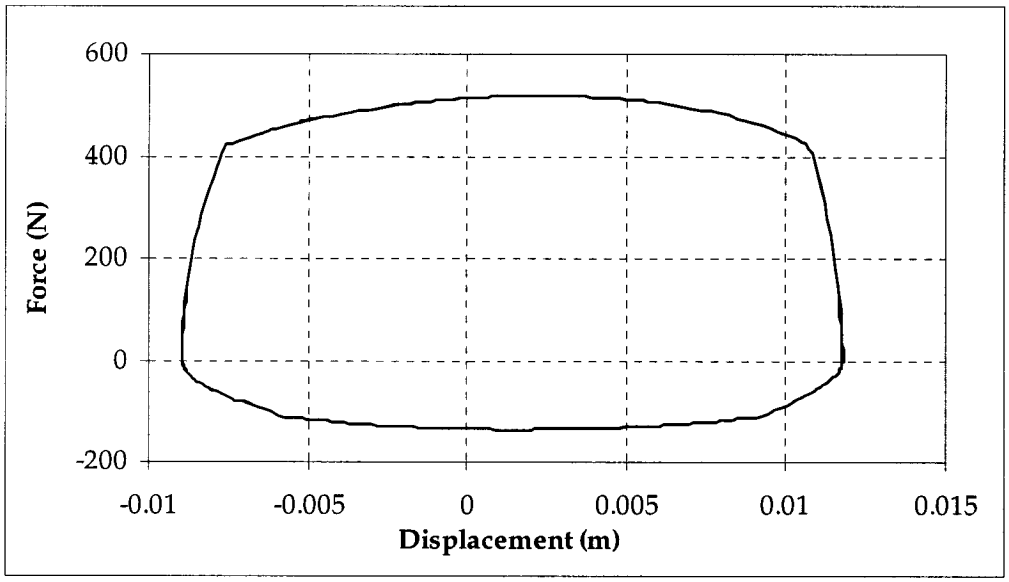

Figure 4.14: Force-displacement characteristics of asymmetric damper.

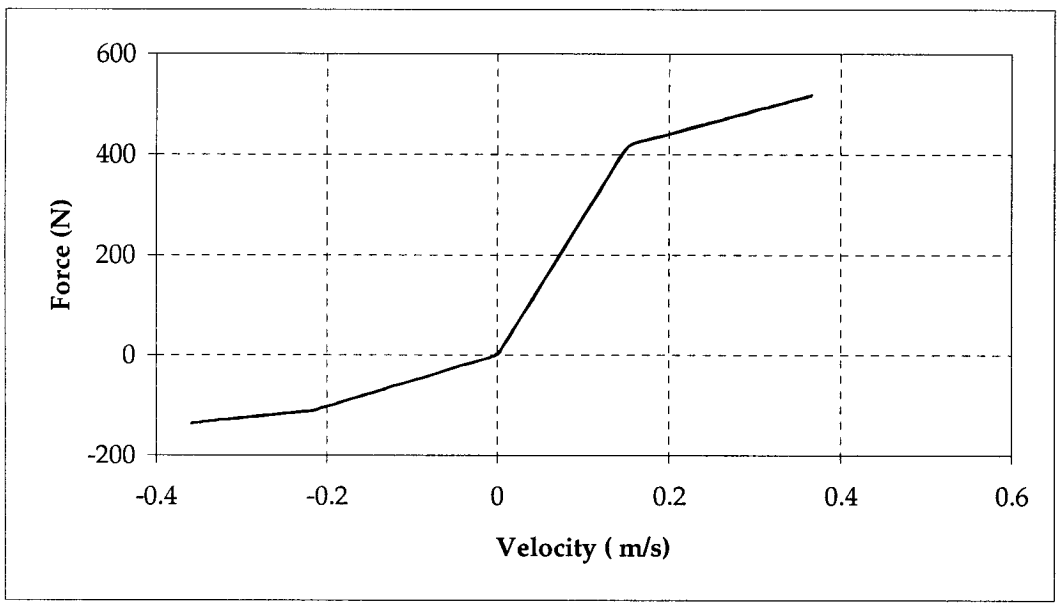

Figure 4.15: *f*-v characteristics of asymmetric damper.

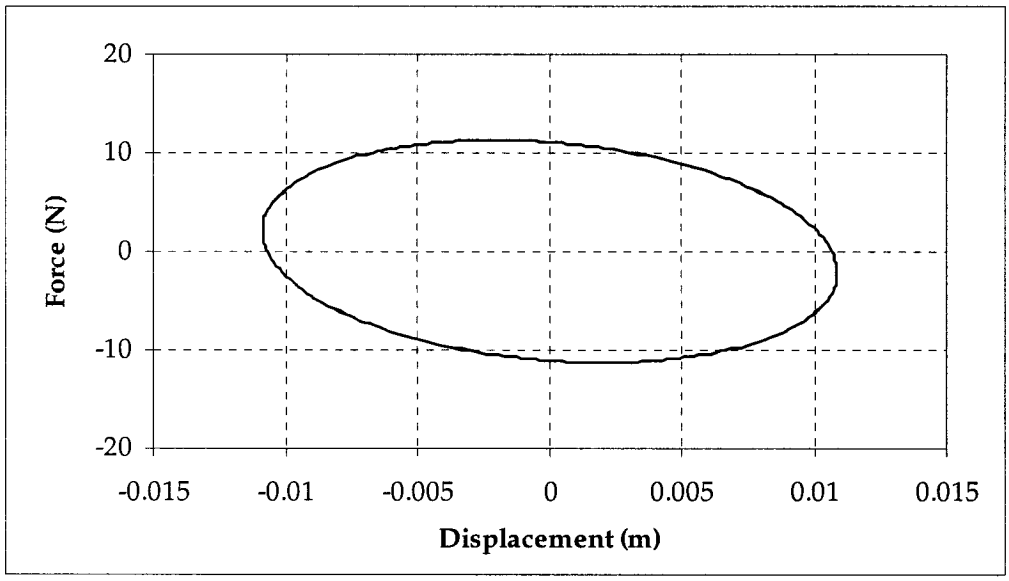

Figure 4.16: Force-displacement characteristics of ER damper.

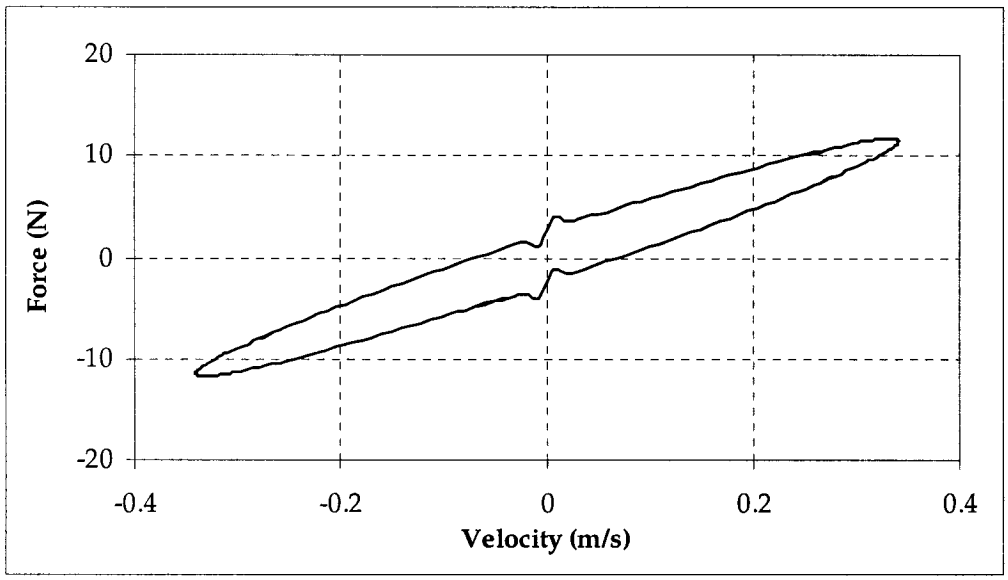

Figure 4.17: *f*-v characteristics of ER damper.

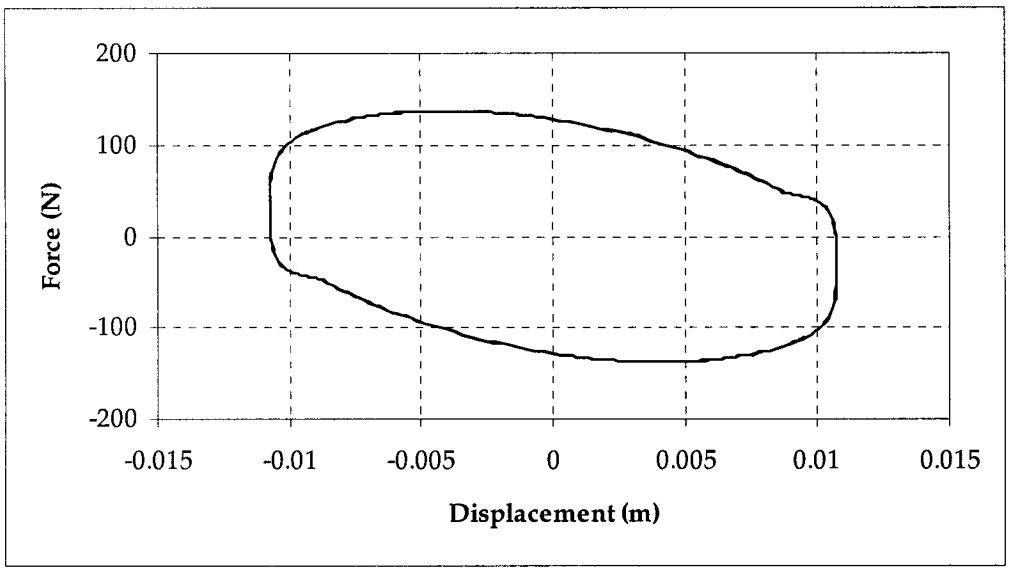

Figure 4.18: Force-displacement characteristics of MR damper.

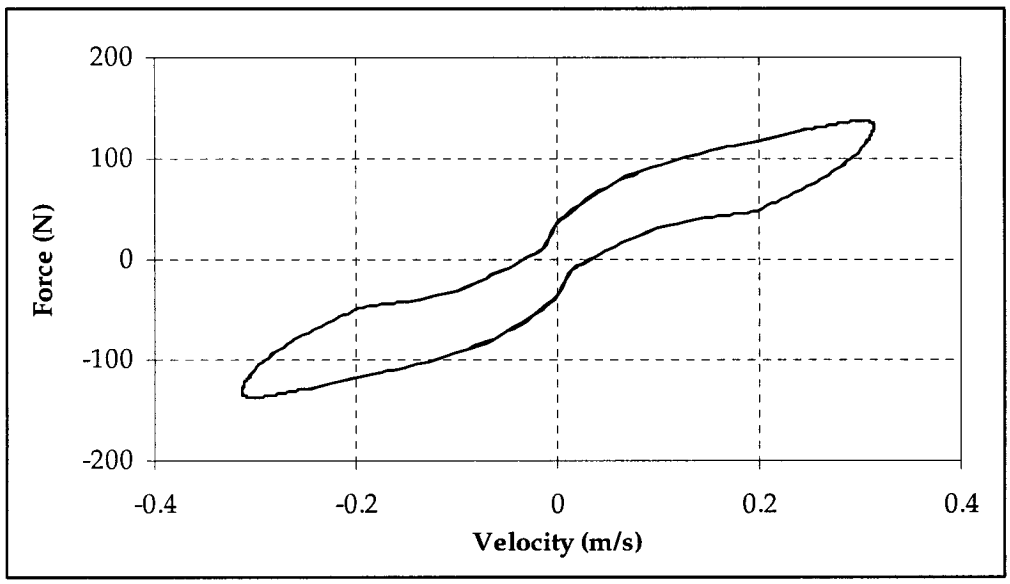

Figure 4.19: *f*-v characteristics of MR damper.

4.5.3 Comparative Performance

4.5.3.1 Sprung Mass Transmissibility

The sprung mass displacement transmissibility ratios of the vehicle using 4 different dampers for bounce excitations are presented in figure 4.20. Similar to 2 DOF system, the sprung mass transmissibility of the candidate dampers are tuned such a way that they all produce similar ride quality for higher frequencies, while minimize the response at resonance. The figure indicates that, around the sprung mass natural frequency (1.16 Hz), transmissibility ratios for all the dampers are maximum. Maximum values are 3.3, 2.22, 1.62 and 1.06 for linear, asymmetric, ER and MR damper respectively.

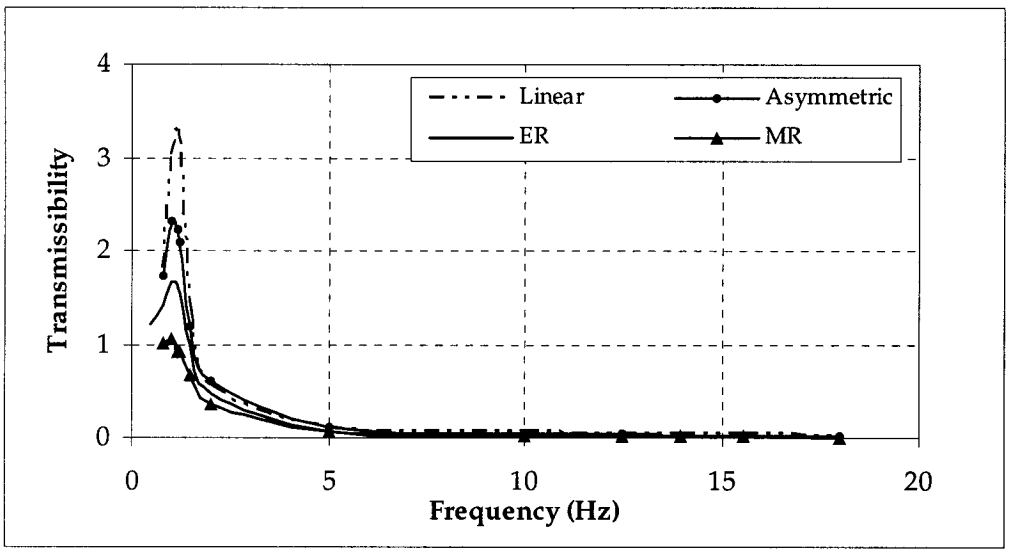

Figure 4.20: Sprung mass transmissibility to bounce excitations.

A comparison of four dampers clearly reveals the superiority of asymmetric damper over linear, and the effectiveness of ER and MR over the entire frequency range. Among all dampers, MR damper provides best performance over the entire frequency range.

Figure 4.21 presents sprung mass displacement transmissibility ratios of the vehicle using 4 different dampers for pitch excitations. Similar to bounce excitations, the dampers provide similar ride performance at higher frequencies and minimize pitch effect at pitch natural frequency. Maximum values of transmissibility are 1.5, 0.99, 1.28, and 0.67 for linear, asymmetric, ER and MR damper respectively.

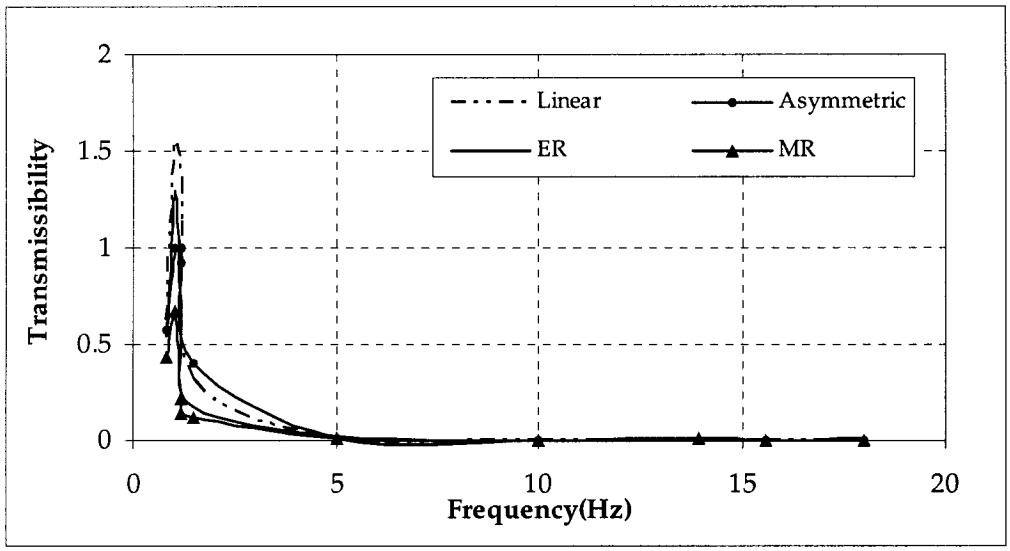

Figure 4.21: Sprung mass transmissibility to pitch excitations.

The results clearly indicate superior performance of asymmetric damper over linear and ER damper, and best performance of MR damper over entire frequency range. It is also been observed that, at frequencies above the pitch natural frequency, the transmissibility values decrease sharply for ER and MR dampers when compared to the asymmetric and linear damper.

A comparison between the performance of the dampers under bounce and pitch excitations reveals that, although ER damper has superior performance over asymmetric damper under bounce excitations, it has inferior performance under pitch excitations. This is due to fact that the dampers are tuned to provide better performance under bounce excitations. As a result performance under pitch might not be as good as that

under bounce. However, this problem can be rectified by tuning the dampers in a manner that they perform better for both bounce and pitch excitations.

4.5.3.2 Unsprung Mass Transmissibility

The unsprung mass transmissibility ratios for front and rear unsprung mass to bounce excitations for 4 different dampers are presented in figure 4.22 and 4.23 respectively. The figures indicate that, around unsprung mass natural frequencies the transmissibility ratios are maximum and around 1 at other frequencies.

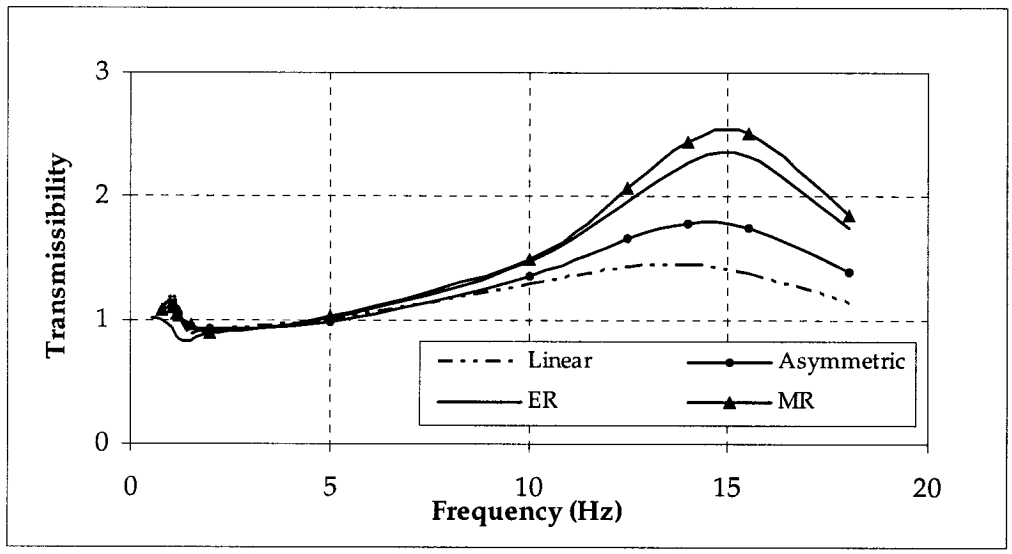

Figure 4.22: Front unsprung mass transmissibility for bounce excitations.

Maximum values are 1.42, 1.74, 2.32 and 2.52, for linear, asymmetric, ER, and MR damper respectively for front unsprung mass and are 1.5, 1.9, 2.51 and 2.71 for linear, asymmetric, ER, and MR damper respectively for rear unsprung mass. The ER and MR dampers hence provide superior performance for sprung mass at the expense of performance for unsprung mass response. Among all the dampers, MR provides best performance for sprung mass and worse performance for unsprung mass.

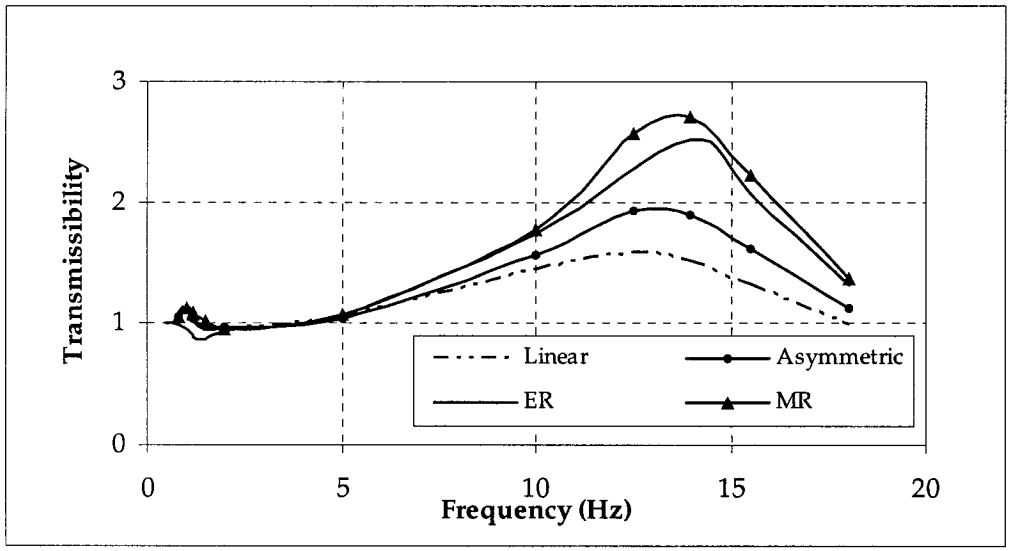

Figure 4.23: Rear unsprung mass transmissibility for bounce excitations.

Comparing the transmissibility of the asymmetric damper obtained in using 2 DOF model (figure 4.2) with that of 4 DOF system (figure 4.22), it can be seen that although asymmetric damper has superior performance over linear in the 2 DOF model, it has inferior performance in the 4 DOF model. The reason is the presence of bounce-pitch coupling in the asymmetric damper for 4 DOF model.

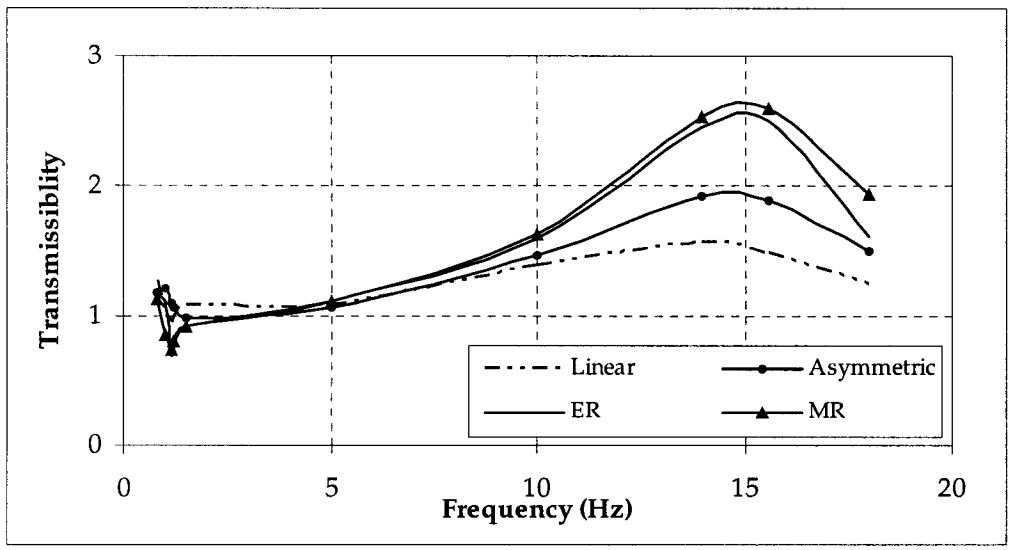

Figure 4.24: Front unsprung mass transmissibility to pitch excitations.

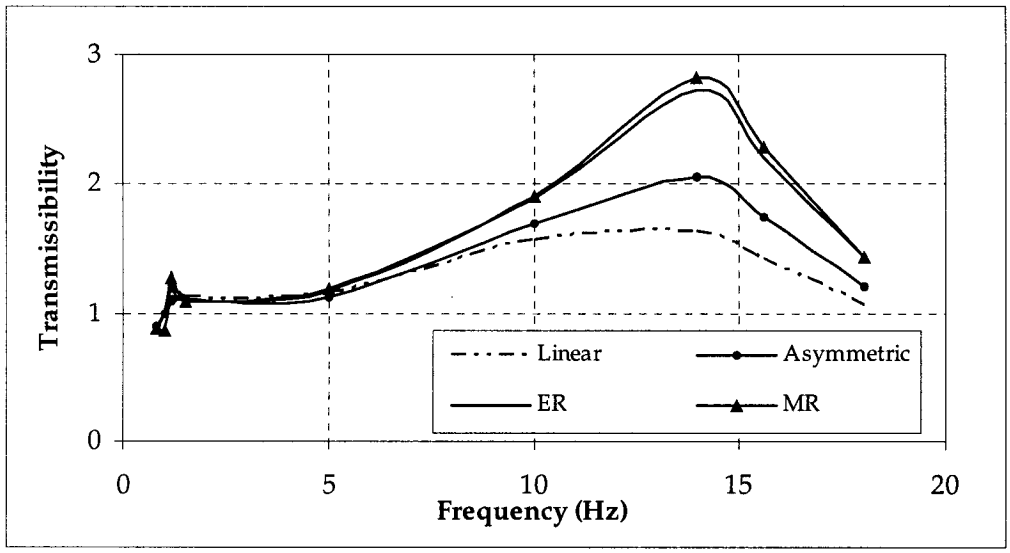

Figure 4.25: Rear unsprung mass transmissibility to pitch excitations.

Similar to bounce excitations, the ratio is highest around unsprung mass natural frequencies and is around 1 at other frequencies. The maximum values are 1.37, 1.74, 2.3 and 2.4 for linear, asymmetric, ER and MR damper respectively for front unsprung mass, and 1.5, 1.9, 2.5, 2.6 for linear, asymmetric, ER and MR damper respectively for rear unsprung mass. The results presented for sprung mass and unsprung mass indicate that superior performance for sprung mass results in inferior performance for unsprung mass.

4.5.3.3 Sprung Mass Pitch Displacement

The sprung mass pitch (angular) displacements using 4 different dampers for bounce excitations are presented in figure 4.26. It can be seen that, pitch values are tuned to be low at higher frequencies and to have minimal value around the pitch natural frequency (1.0Hz). Maximum values are 0.005, 0.0035, 0.0022 and 0.004 radian for linear, asymmetric, ER, and MR damper respectively. The results reveal that under bounce

excitations, ER damper has superior performance over other three and linear has worst performance.

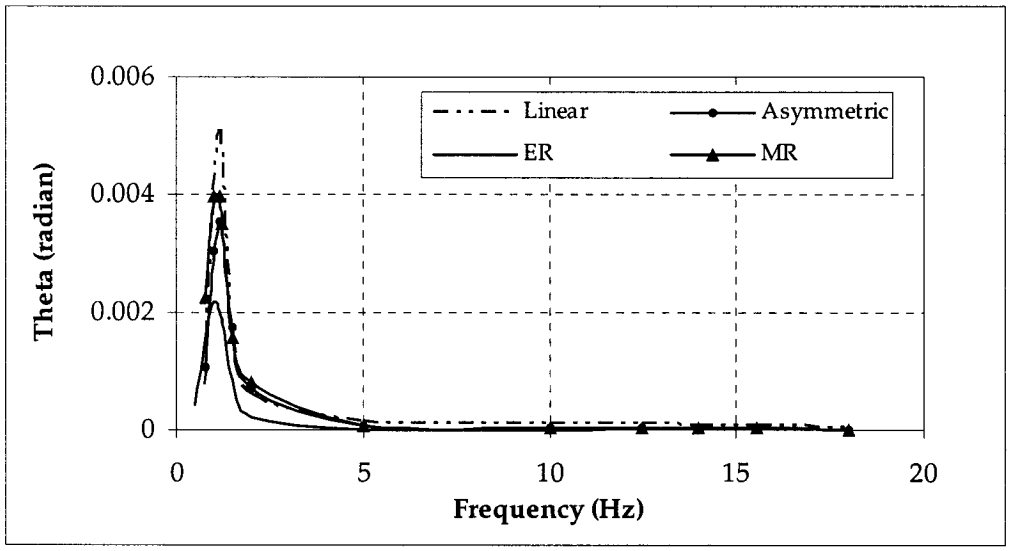

Figure 4.26: Pitch response of sprung mass to bounce excitations.

Figure 4.27 shows the pitch response of the sprung mass to pitch input. Similar trends as seen for bounce excitaions are seen here too. The maximum values around pitch natural frequency are 0.032, 0.021, 0.056, 0.056 radian for linear, asymmetric, ER and MR damper resepectively.

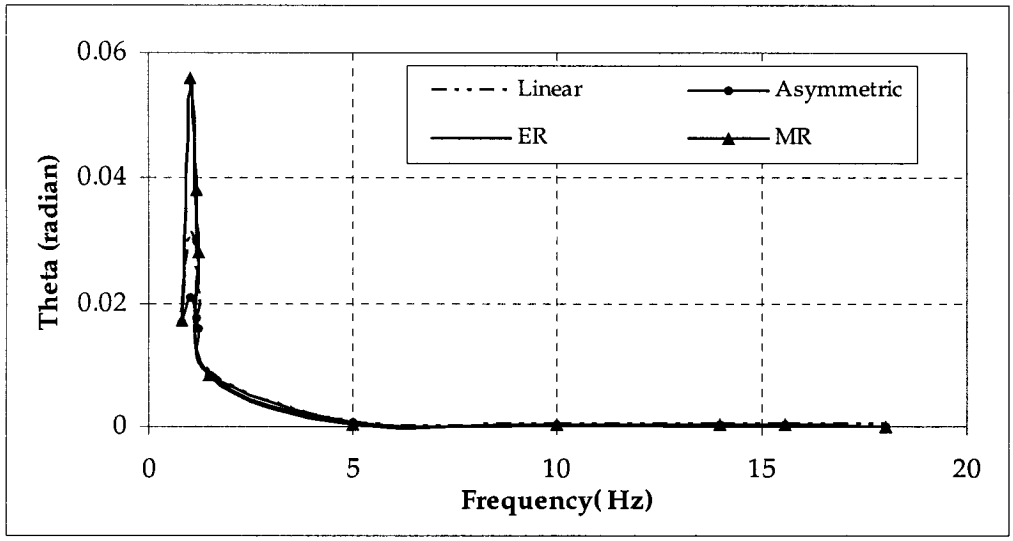

Figure 4.27: Pitch response of sprung mass to pitch excitations.

The results clearly indicate that linear and asymmetric dampers have superior pitch performance compared to ER and MR dampers under pitch excitations. A comparison between the performance of the dampers under bounce and pitch excitations reveals that performance of ER and MR damper worsens under pitch compared to bounce. Also, linear and asymmetric have better performance under pitch compared to that under bounce.

4.5.3.4 Suspension Travel

The suspension travel (rattle space) for the front axle suspensions and rear axle suspensions under bounce excitations are presented in figure 4.28 and 4.29. It is evident that around natural frequencies all the dampers require higher rattle space. For front suspensions, around sprung mass natural frequency, rattle space requirements are 0.032, 0.022, 0.019 and 0.014m, and around front unsprung mass natural frequency 0.015, 0.018, 0.023 and 0.025m for linear, asymmetric, ER, and MR damper respectively.

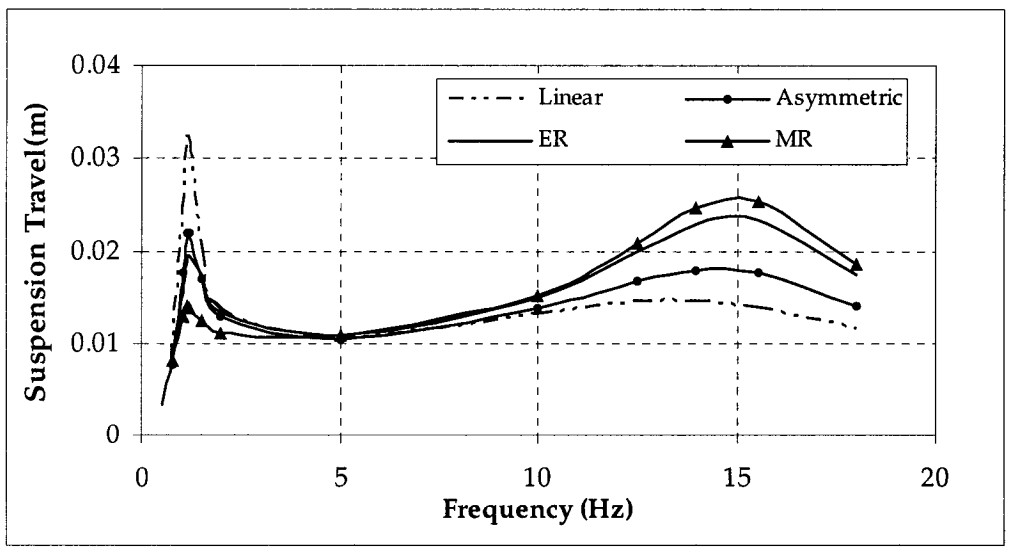

Figure 4.28 : Suspension travel of front suspensions for bounce excitations.

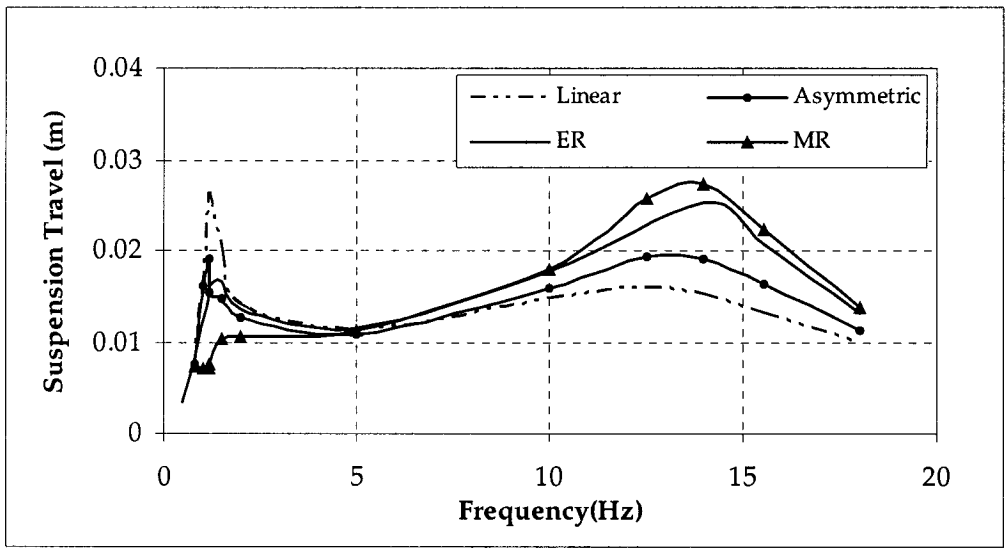

Figure 4.29: Suspension travel of rear suspensions for bounce excitations.

The results indicate that ER and MR damper based systems require low rattle space around sprung mass natural frequency, while around unsprung natural frequencies they require higher rattle space compared to linear and asymmetric damper. Thus low suspension travel around sprung mass natural frequency results in higher suspension travel at unsprung mass natural frequencies. Similar trends are observed for the rear axle, with maximum travel of 0.025, 0.019, 0.016 and 0.01m around sprung mass natural frequency, and 0.016, 0.019, 0.025 and 0.027m around rear unsprung mass natural frequency for linear, asymmetric, ER, and MR damper based suspension, respectively.

Figure 4.30 and 4.31 show suspension travel under pitch excitations for front and rear suspensions respectively. Similar to bounce input, the rattle space required is higher around natural frequencies. For the front axle suspensions, the values are 0.035, 0.02, 0.054, 0.045 m around sprung mass natural frequency and 0.0145, 0.018, 0.023, 0.024 m around front unsprung mass natural frequency for linear, asymmetric, ER and MR damper respectively. The results clearly reveal superior performance of linear and

asymmetric damper over ER and MR damper over entire frequency range. For the rear axle suspensions, the values are 0.025, 0.017, 0.061, 0.067 m around sprung mass natural frequency and 0.015, 0.019, 0.025, 0.026 m around rear unsprung mass natural frequency for linear, asymmetric, ER and MR damper respectively. For this case also ER and MR have inferior performance compared to other two.

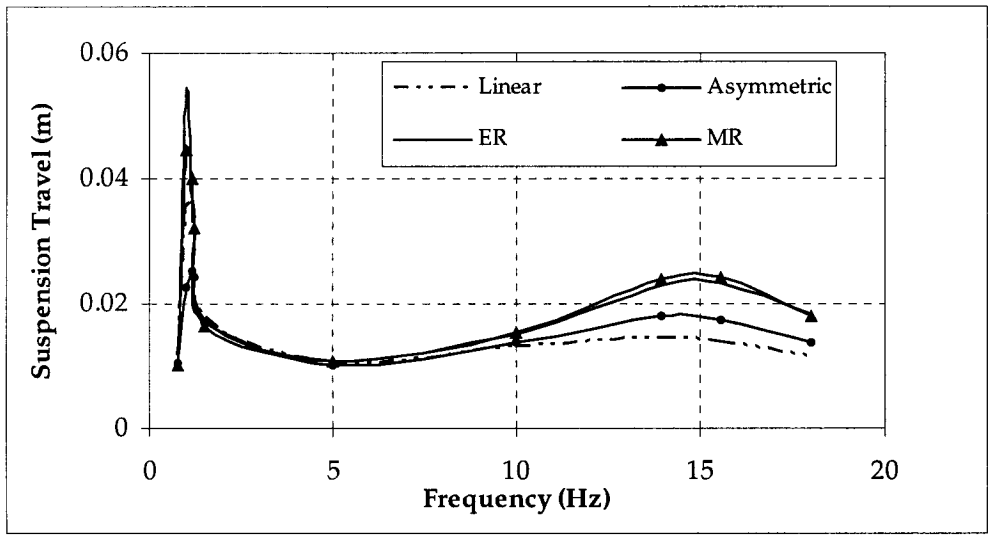

Figure 4.30 : Suspension travel of front suspensions for pitch excitations.

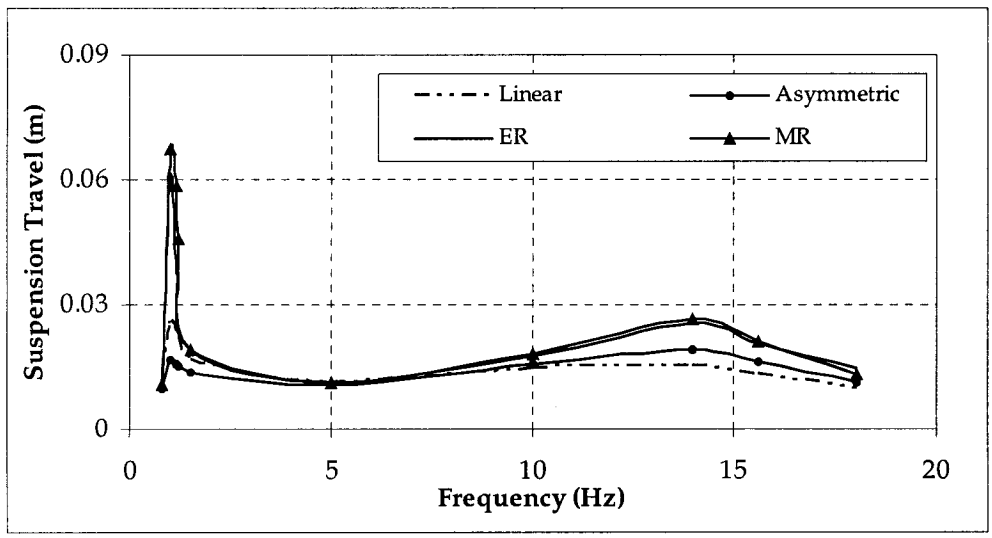

Figure 4.31: Suspension travel of rear suspensions for pitch excitations.

A comparison between suspension travel under bounce and pitch excitations indicates that around sprung mass natural frequencies ER and MR dampers have superior performance under bounce, but have inferior performance under pitch compared to linear and asymmetric damper. Interestingly, the asymmetric damper performs better both under bounce and pitch excitations over the entire frequency range.

4.5.3.5 Relative Velocity Across Suspension

The relative velocities across suspension for front and rear axle under bounce input are presented in figure 4.32 and 4.33. It is evident from the plots that, for all the damper models, maximum relative velocity is seen around unsprung mass natural frequencies.

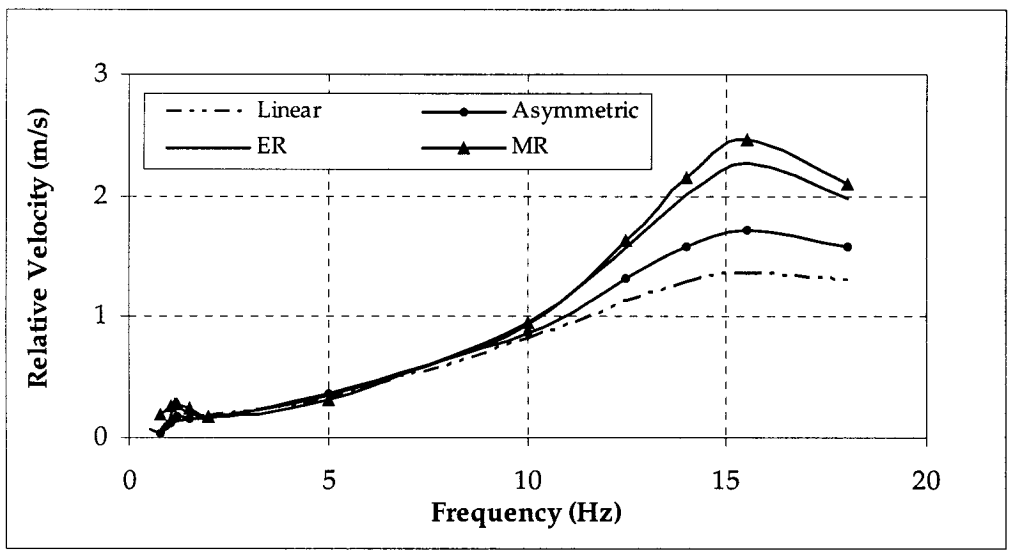

Figure 4.32: Relative velocity across front suspensions for bounce excitations.

For front suspensions the maximum values are 1.35, 1.72, 2.27, 2.47 m/s for linear, asymmetric, ER, and MR damper respectively, and for rear suspensions the maximum values are 1.33, 1.67, 2.22 and 2.4 m/s for linear, asymmetric, ER, and MR

damper based system respectively. The results indicate that linear and asymmetric damper have lower relative velocity across the suspension compared to ER and MR damper.

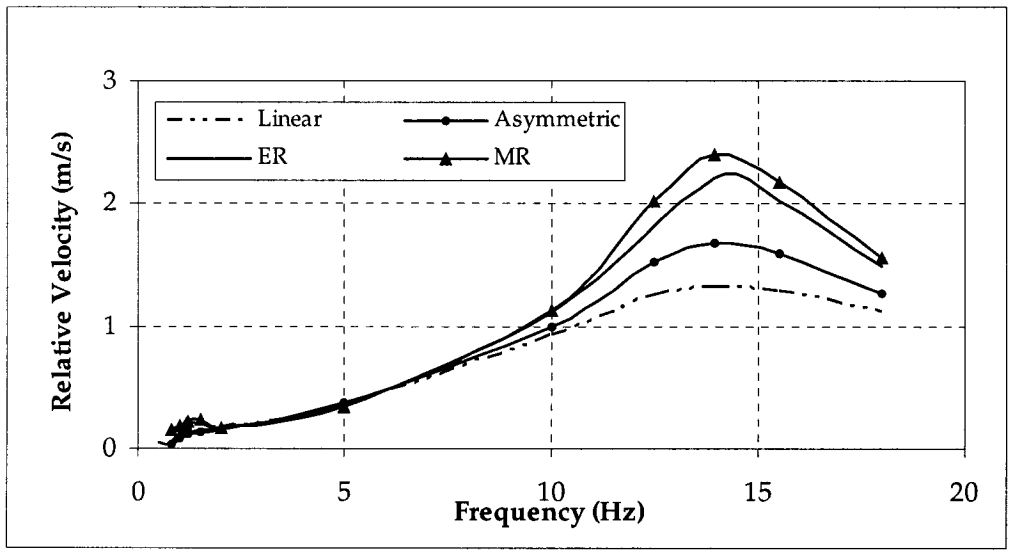

Figure 4.33: Relative velocity across rear suspensions for bounce excitations.

Figure 4.34 and 4.35 presents the relative velocity across front and rear suspensions under pitch excitations.

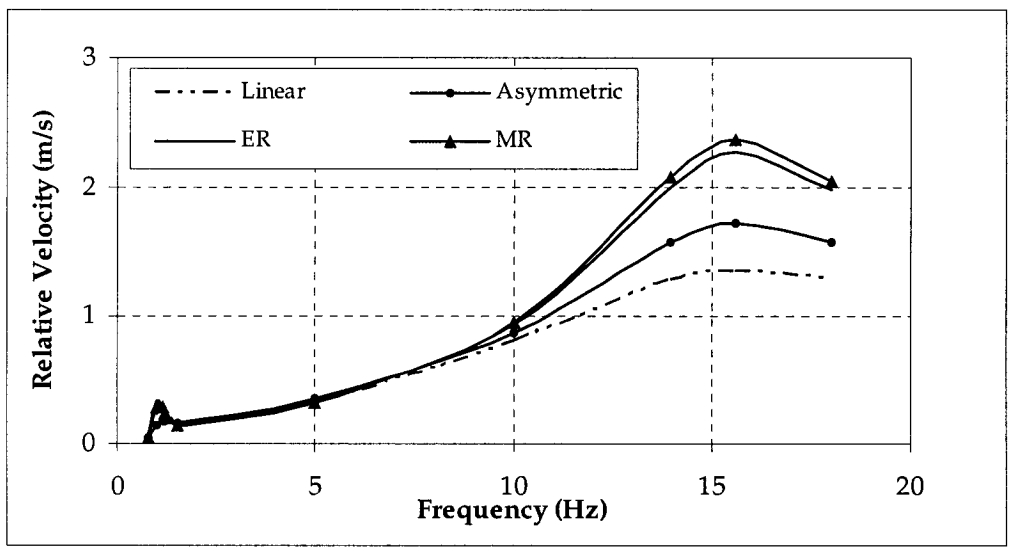

Figure 4.34: Relative velocity across front suspensions for pitch excitations.

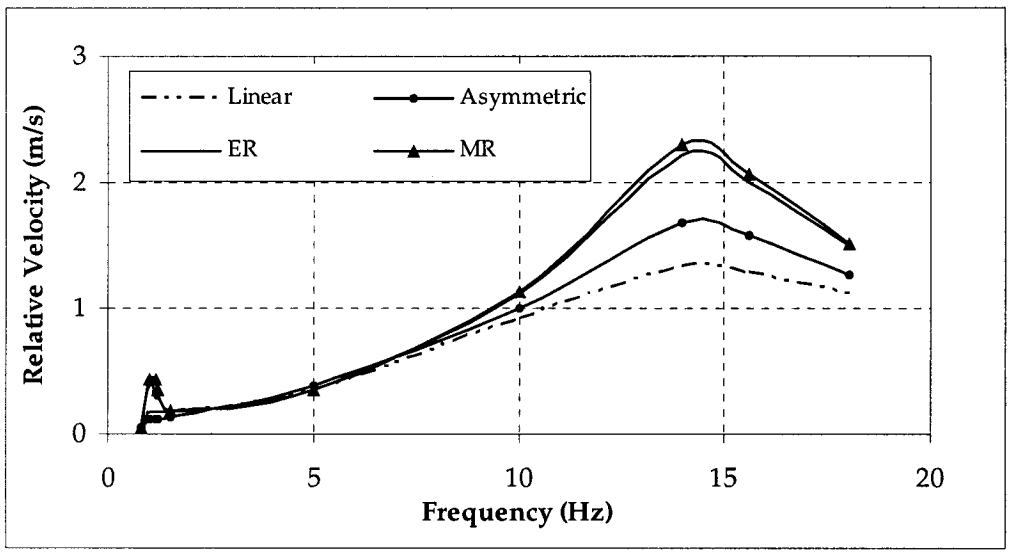

Figure 4.35: Relative velocity across rear suspensions for pitch excitations.

Similar trends as seen for bounce input are also seen here. Relative velocity is highest around unsprung mass natural frequencies. The values are 1.35, 1.71, 2.27, 2.36 m/s for front suspensions and 1.33, 1.68, 2.22 and 2.30 m/s for rear suspensions for linear, asymmetric, ER and MR damper respectively.

4.5.3.6 Ride Height Drift

As discussed in chapter 3, ride height drift is the shift of dynamic equilibrium of the sprung mass and is the direct result of asymmetric damping properties. All the damper models expect asymmetric damper have symmetric *f-v* characteristics in compression and rebound as seen from plots presented in section 4.5.2. Hence it is expected that linear, ER and MR damper will show no drift or negligible drift. The simulation results indicated that linear, ER and MR damper model have either negligible drift or no drift at all. The ride height drifting problem is only seen in asymmetric damper. For asymmetric damper, the drift is low at lower frequencies and maximum

around unsprung mass natural frequencies. For 10mm input under bounce input asymmetric damper shows maximum drift of 14.26 mm. It means that, around unsprung mass natural frequency, a vehicle with asymmetric damper will move down 14.26 mm from its dynamic equilibrium. Figure 4.36 shows the ride height drift of asymmetric damper under bounce input.

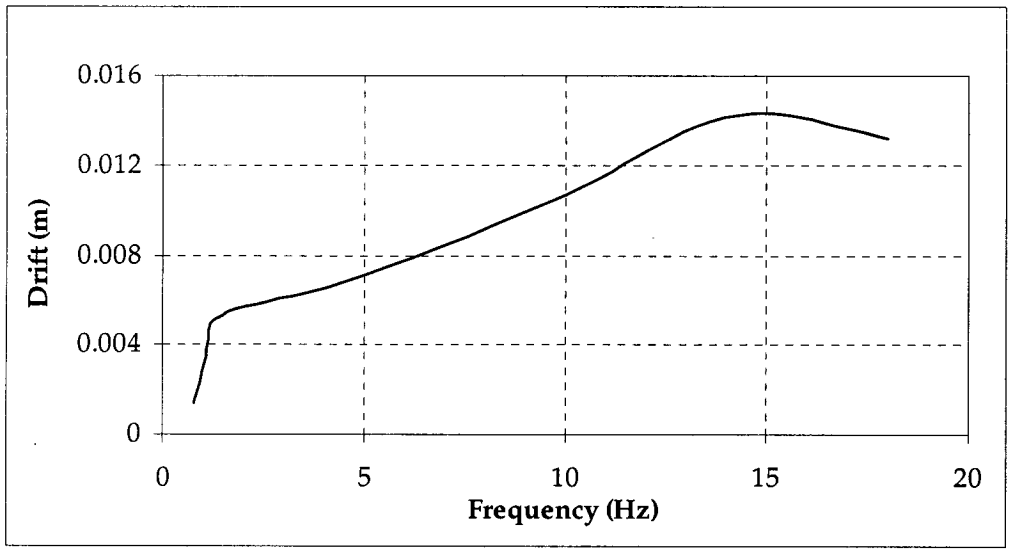

Figure 4.36: Ride height drift of asymmetric damper for bounce excitations.

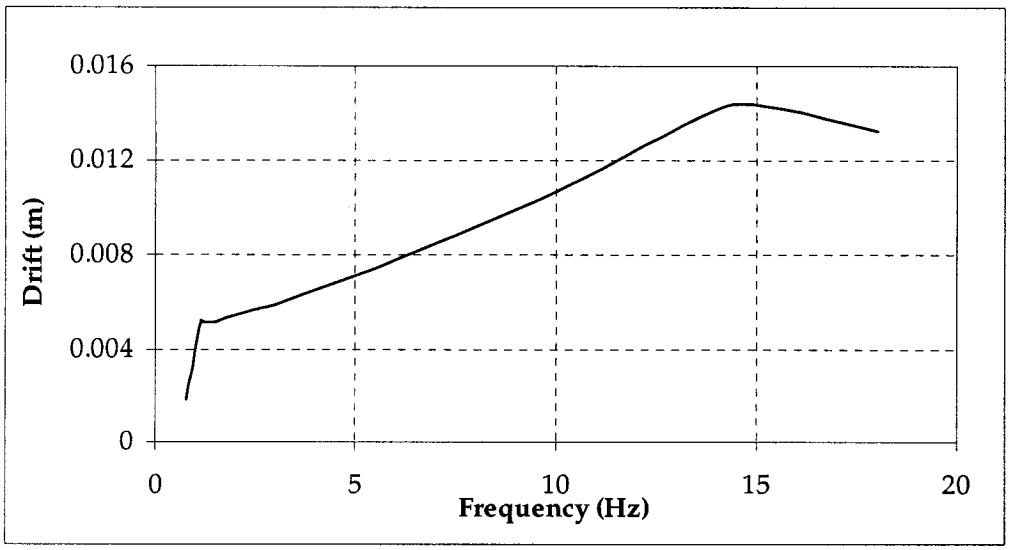

Figure 4.37: Ride height drift of asymmetric damper for pitch excitations.

Similar trend is seen for pitch excitations. The drift is higher around unsprung mass natural frequencies. The maximum value is 14.24 mm under pitch excitations. Figure 4.37 shows the drift under pitch excitations. The results indicate that ride height drift under bounce and pitch are almost the same.

4.5.3.7Angular Drift

Similar to ride height drift, angular drift is the change of the pitch dynamic equilibrium of the sprung mass. Similar to ride height drift, only asymmetric damper shows angular drift. Rest of the damper has no angular drift at all. For 10mm input under bounce excitation, asymmetric damper based system shows maximum angular drift of 0.012 radian. Since, the counter-clockwise angular motion of the sprung mass is assumed positive for this study, this means that around unsprung mass natural frequency, a vehicle with asymmetric damper will move 0.012 radian counter-clockwise from its dynamic pitch equilibrium. Figure 4.38 shows the angular drift for the asymmetric damper based vehicle system.

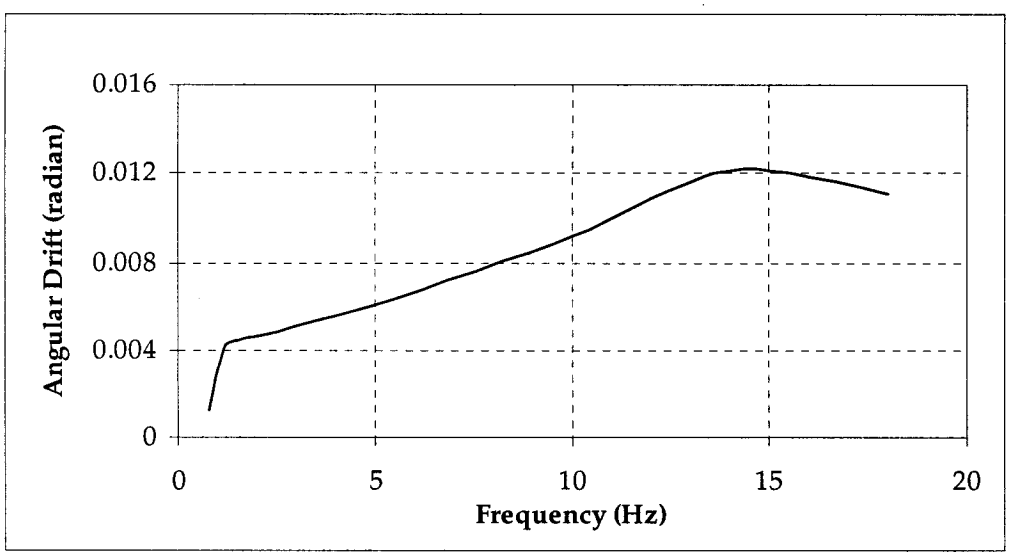

Figure 4.38: Angular drift of asymmetric damper for bounce excitations.

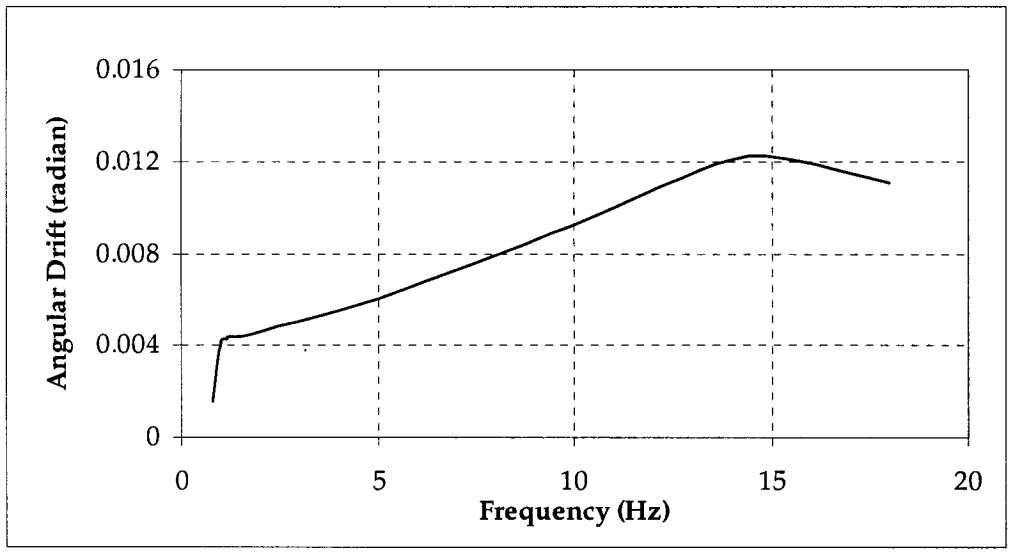

Figure 4.39: Angular drift of asymmetric damper for pitch excitations.

Similar trend is seen for pitch excitations. The drift is higher around unsprung mass natural frequencies. The maximum value is 0.012 radian under pitch excitations. Figure 4.39 shows the drift under pitch excitations. The results indicate that the angular drift under bounce and pitch excitations are the same for 10 mm amplitude.

4.5.3.8 Pavement Load

All the candidate dampers of this study transfer highest load to the pavement around unsprung mass natural frequencies of the vehicle. The pavement load of the front and rear axle for the dampers under bounce excitations are presented in figure 4.40 and 4.41 respectively. Maximum values of peak pavement loads for the front axle are 4.9, 5.76, 7.1 and 7.57 kN for linear, asymmetric, ER, and MR damper respectively, and for rear axle 5.13, 6.11, 7.67 and 8.23 kN for linear, asymmetric, ER, and MR damper respectively. It is evident from the results that ER and MR damper will cause more damage to road than linear and asymmetric damper. The higher pavement load results

from low damping force generated by ER and MR damper at higher frequencies compared to linear and asymmetric damper.

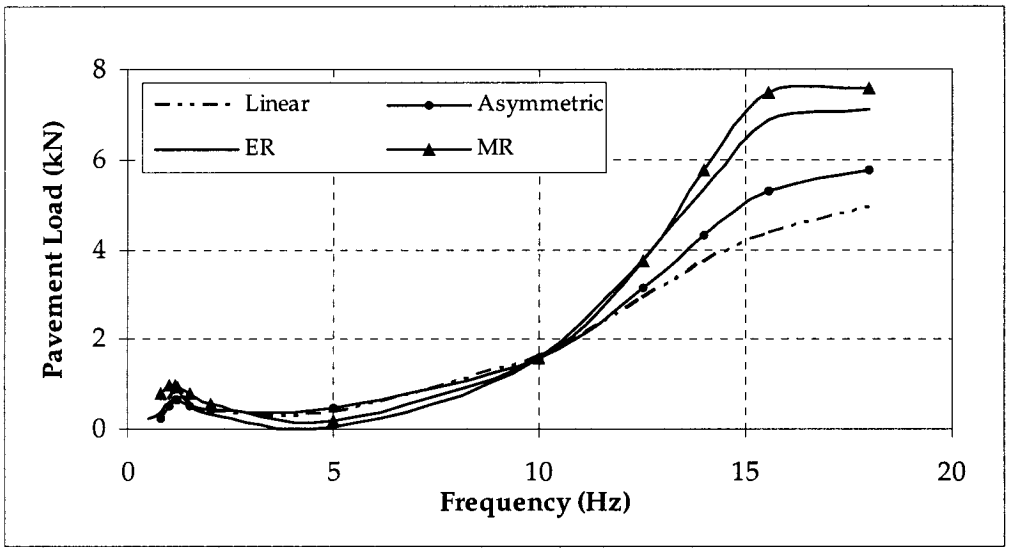

Figure 4.40: Pavement load of front axle for bounce excitations.

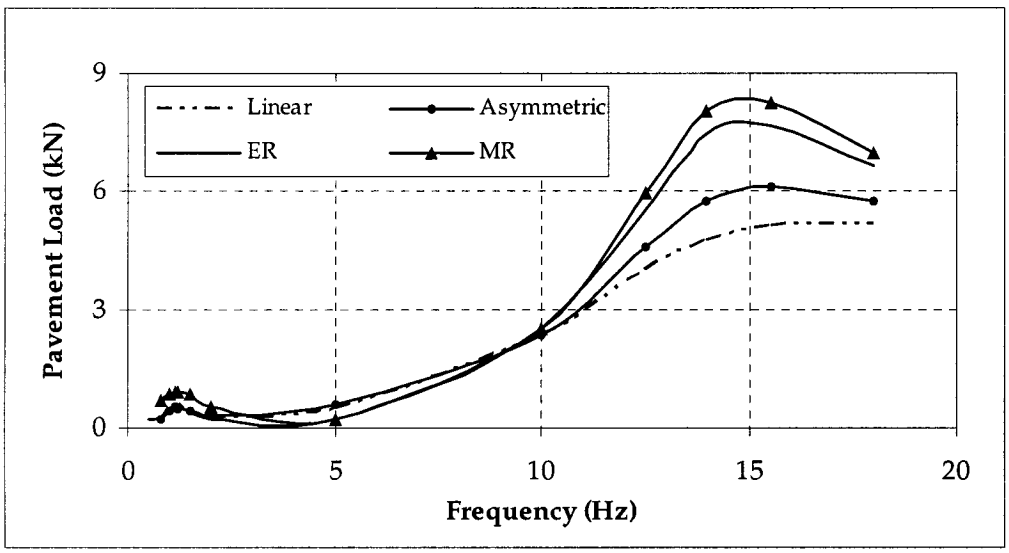

Figure 4.41: Pavement load of rear axle for bounce excitations.

Figure 4.42 and 4.43 presents the pavement load for front and rear axle under pitch excitations. Similar to bounce input, maximum values are seen around unsprung mass natural frequencies. The values are 4.91, 5.76, 6.90, 7.39 kN for front axle, and are

5.19, 6.12, 7.71, 7.97 kN for rear axle for linear, asymmetric, ER and MR damper respectively.

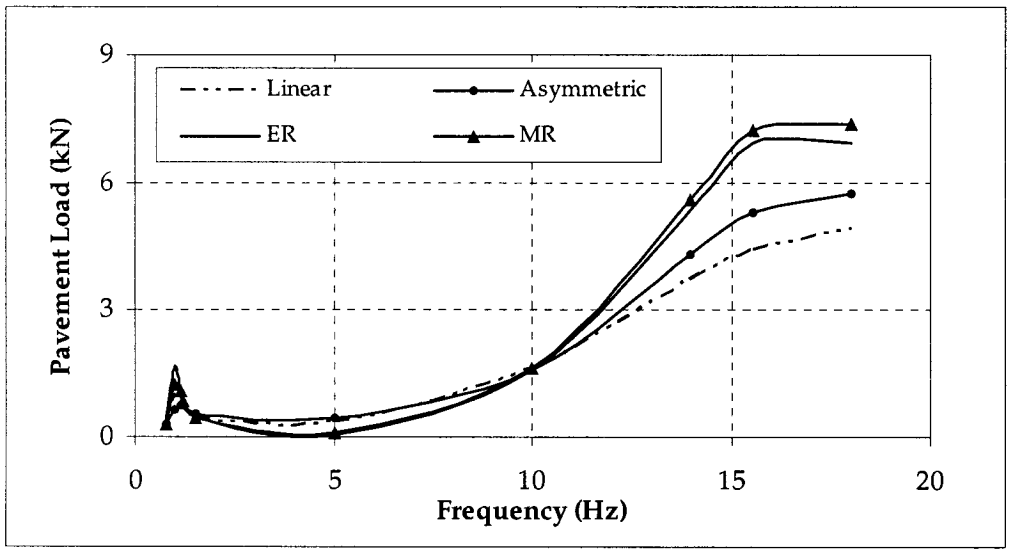

Figure 4.42: Pavement load of front axle for pitch excitations.

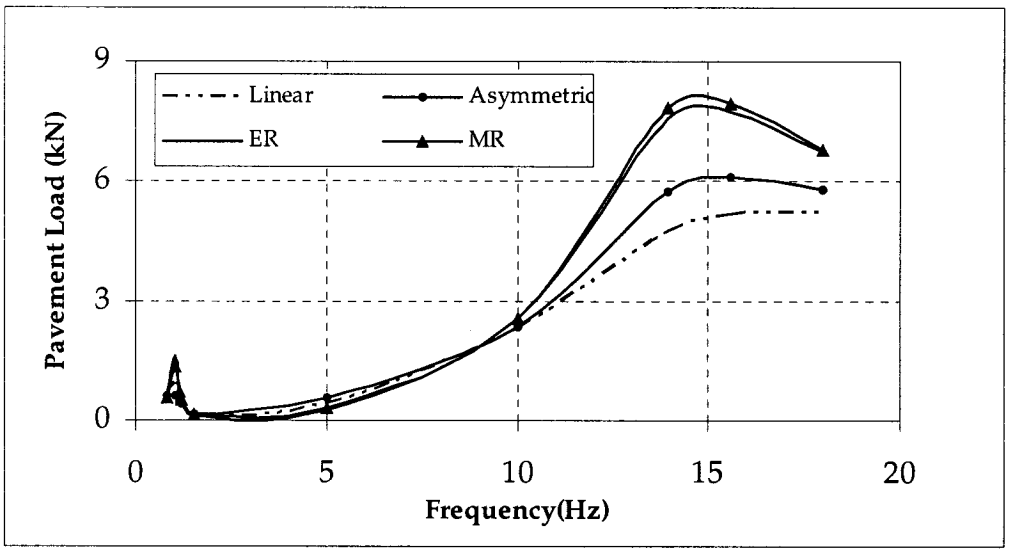

Figure 4.43: Pavement load of rear axle for pitch excitations.

The results indicate that ER and MR damper will cause more damage to road compared to other two, for the reasons explained earlier.

4.5.4 Response to Shock

Under the influence of shock input (bump), vertical and pitch responses of the vehicle shoot up. As discussed earlier in chapter 3, the shock inputs are generally presented by rounded step input (Wang *et al.*, 2003). Bump inputs are generally presented by rounded step input. As described in section 3.2.2, rounded step input can be represented by the following equation –

$$x(t) = Xmax\{1 - e^{-\eta\omega_n t}(1+\eta\omega_n t)\} \quad \ldots\ldots (4.1)$$

where, $x(t)$ is the shock amplitude, $Xmax$ is the maximum amplitude of shock , η is the shock severity, and ω_n is the bounce natural frequency of the vehicle.

For this study, $Xmax$ is considered to be 30 mm with shock severity (η) of 3, and bounce natural frequency (ω_n) of 1.15 Hz. The vehicle is considered to cross the bump at a speed of 30km/h. At this velocity, the rear wheels of the vehicle are subjected to the same input after a time delay (τ_d) of 0.2592 sec. Figure 4.44 and 4.45 represents the shock input given to the front and rear axle of the vehicle respectively.

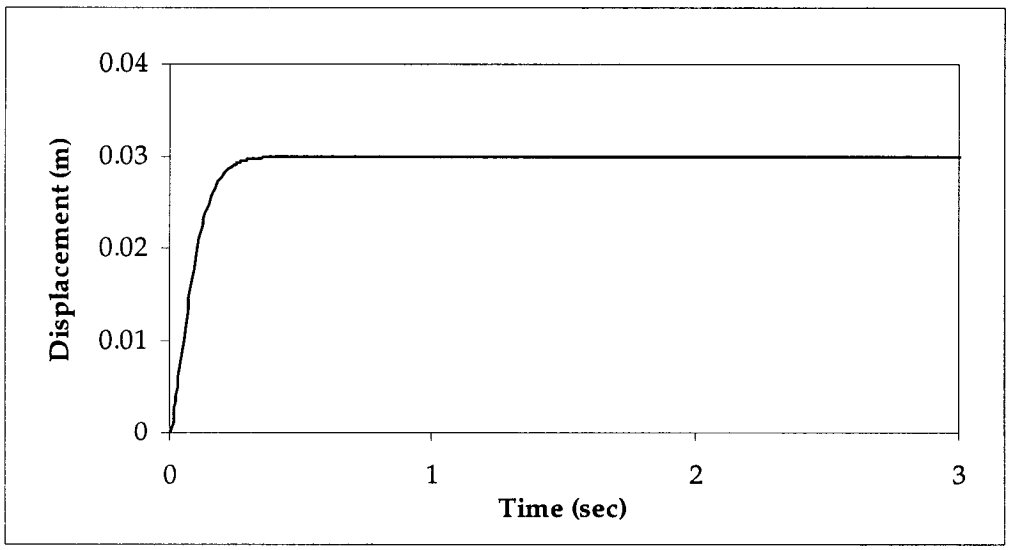

Figure 4.44: Shock input to the front axle.

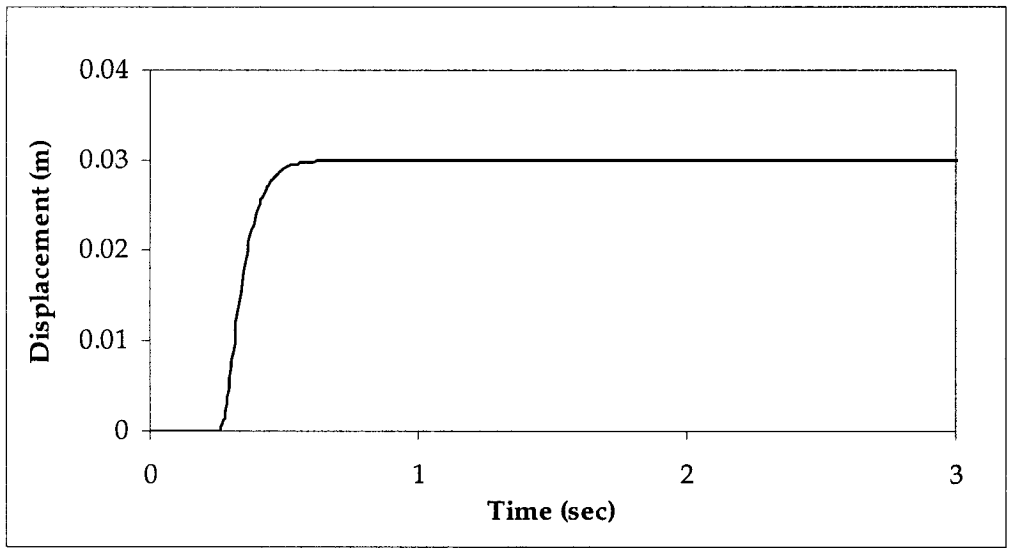

Figure 4.45: Shock input to the rear axle.

The bounce and pitch response of the sprung mass are analyzed to observe the shock performance of the vehicle. Figure 4.46 and 4.47 presents the bounce and pitch displacement of the sprung mass under the application of shock. To compare the sprung mass vertical displacement response of vehicle to the shock input, maximum percent overshoot, rise time and settling time are analyzed.

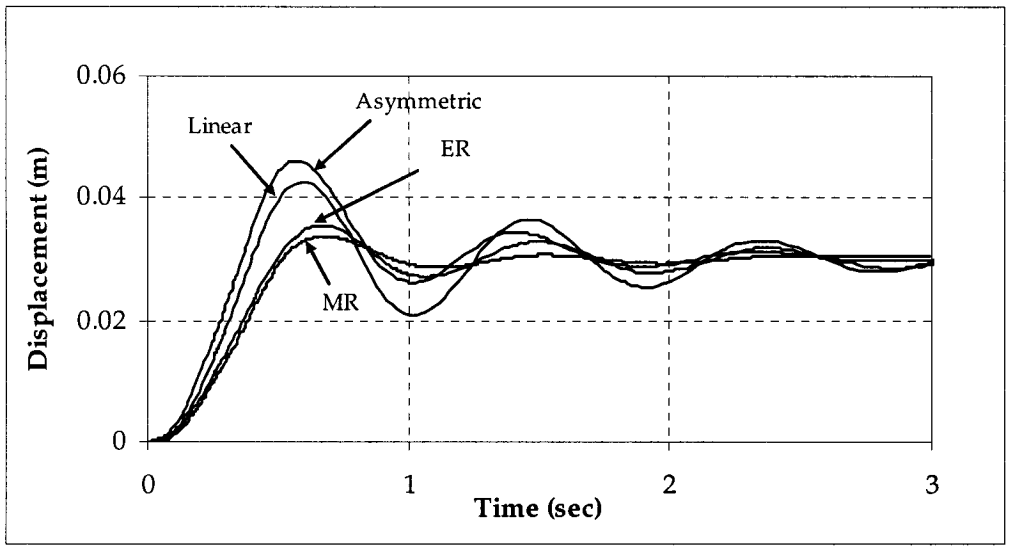

Figure 4.46: Sprung mass vertical response to shock input.

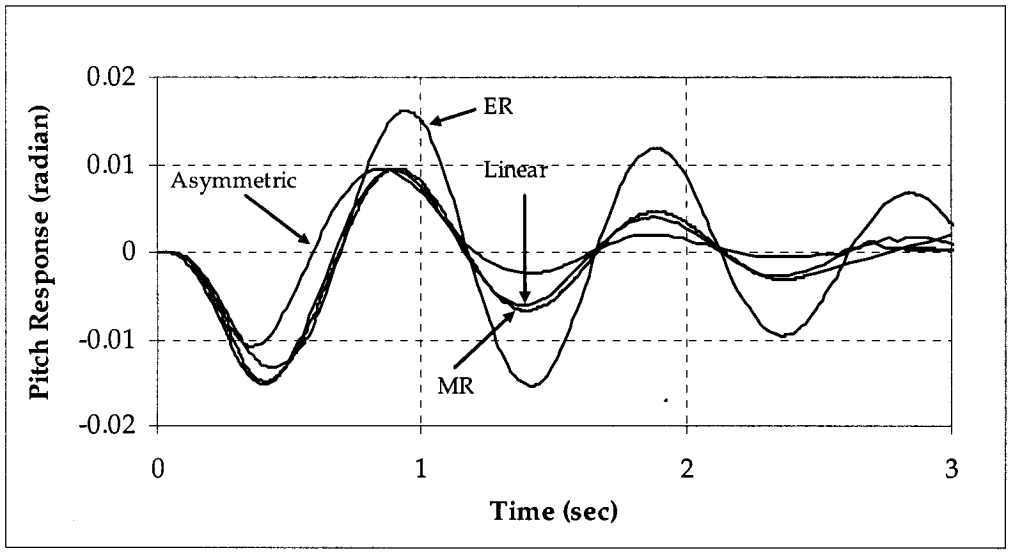

Figure 4.47: Sprung mass pitch response to shock input.

The values of the parameters for sprung mass vertical response and pitch response for all the dampers are presented in table 4.3 and 4.4. The results presented in table 4.3 and 4.4 indicate that ER and MR damper based systems provide better vertical shock isolation at bumps, as the maximum overshoot and settling time for these kinds of damper based systems are low compared to asymmetric and linear damper based systems.

Table 4.3: Sprung mass vertical displacement response analysis.

Damper Type	*Maximum Overshoot (%)*	*Rise Time (sec)*	*Settling Time (sec)*
Linear	42.0	0.19295	2.374
Asymmetric	53.2	0.22489	1.5351
ER	17.4	0.2138	0.79133
MR	11.1	0.2188	0.76083

Table 4.4: Sprung mass pitch response analysis.

Damper Type	*Maximum Pitch (radian)*		*Settling Time (sec)*
	Counter-Clockwise	*Clockwise*	
Linear	0.00937	0.0152	1.49
Asymmetric	0.00942	0.0108	1.778
ER	0.0161	0.0152	2.75
MR	0.00949	0.0149	1.51

In terms of pitch response at bumps, except ER damper, all the dampers have similar performances. ER damper causes high pitch and requires more time to settle compared to the other dampers. This means that at bumps ER damper will cause more discomfort to occupants of the vehicle as well as might damage the freights carried by the vehicle.

4.5.5 Effect of Higher Amplitude Excitation

Vehicles operating in roads are subject to different excitation conditions wide various amplitudes. The road conditions like roughness, potholes etc. have direct effect the excitation amplitude of the vehicle. The analyses presented in previous section are for bounce and pitch excitation input of 10 mm. Since, all the dampers except linear damper have non-linear characteristics, it is important to investigate the performance of the dampers at higher amplitude excitation to observe the performance trends. To investigate the performances of the dampers at higher amplitude excitation, the vehicle model is subjected to bounce and pitch excitation of 15mm amplitude. The responses of

the dampers resulting from higher amplitude excitations are presented in the following subsections.

4.5.5.1 Sprung Mass Transmissibility

The sprung mass displacement transmissibility ratios for bounce excitations using 4 different dampers are presented in figure 4.48. Similar trends, as seen for 10mm amplitude (shown is figure 4.20) are also seen here, i.e. the dampers provide better ride at higher frequencies and minimizes performance at resonance.

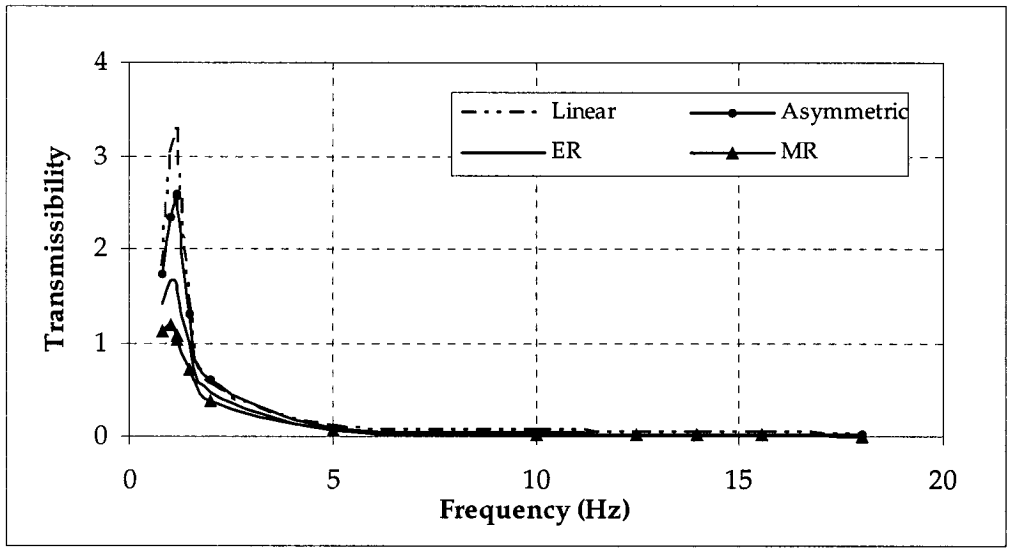

Figure 4.48: Sprung mass transmissibility to bounce excitations.

Maximum values of transmissibility ratios are 3.3, 2.56, 1.66 and 1.19 for linear, asymmetric, ER, and MR damper respectively. The results reveal that performance of linear remains the same and while performances deteriorate by 1% for ER, 11% for MR and 15% for asymmetric damper compared to 10mm input. This indicates that ER and linear damper can provide consistent performance over a wide range of input amplitude compared to asymmetric and MR damper. Figure 4.49 presents the sprung mass displacement transmissibility ratios for pitch excitations using 4 different dampers.

Similar trends, as seen for 10mm amplitude (shown is figure 4.21) are also seen here. The maximum values are 1.51, 1.92, 1.28 and 0.66 for linear, asymmetric, ER and MR damper respectively. Comparing the results with 10mm input, it is found that performance of linear, ER and MR dampers remains almost same, while deteriorates for asymmetric damper. This indicates that asymmetric damper can not maintain consistent performance at higher amplitude under pitch excitations.

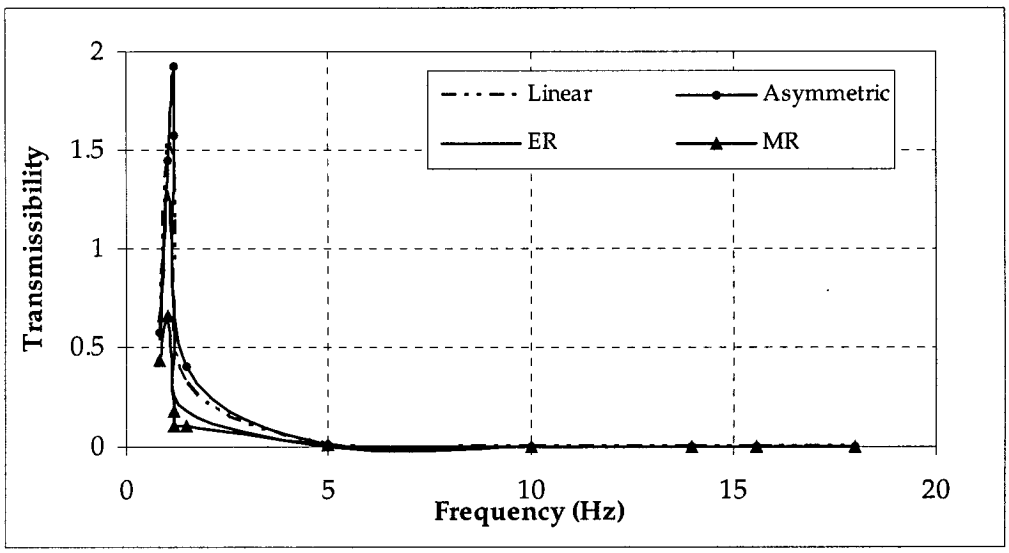

Figure 4.49: Sprung mass transmissibility to pitch excitations.

A comparison between performance under bounce and pitch excitations reveals that linear damper and ER damper have consistent performance under bounce and pitch excitations.

4.5.5.2 Unsprung Mass Transmissibility

The unsprung mass transmissibility for front and rear unsprung mass of the vehicle, using 4 different dampers under bounce excitations are presented in figure 4.50 and 4.51 respectively. Similar trends as observed at 10mm (figure 4.22 and 4.23) are

observed here too. For front unsprung mass maximum values are 1.43, 1.82, 2.32 and 2.63, for linear, asymmetric, ER, and MR damper based system respectively.

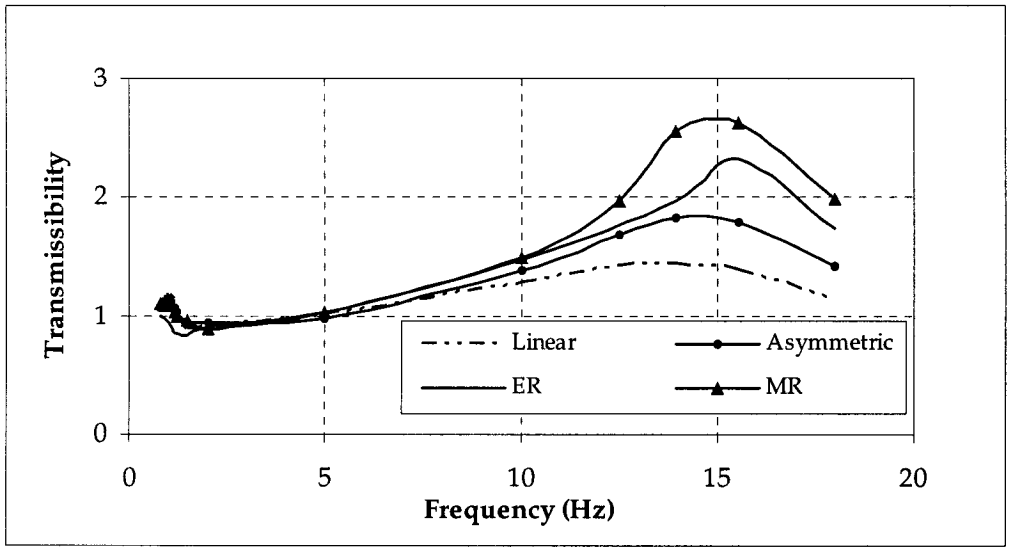

Figure 4.50: Front unsprung mass transmissibility to bounce excitations.

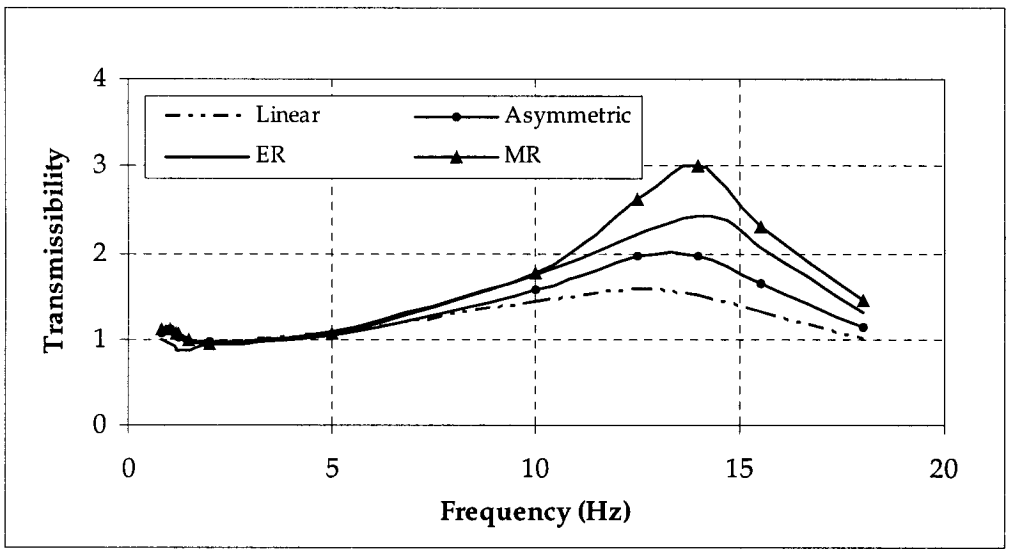

Figure 4.51: Rear unsprung mass transmissibility to bounce excitations.

A comparison between the results obtained for 10 mm and 15 mm indicates that under pitch excitations the performance of all the dampers remains almost same. Similar responses are seen for rear unsprung mass transmissibility.

Figure 4.52 and 4.53 presents the front and rear unsprung mass displacement transmissibility ratios for pitch excitations using 4 different dampers. Similar trends, as seen for 10mm amplitude (shown is figure 4.24, 4.25) are also seen here. For the front unsprung mass the maximum values are 1.36, 1.79, 2.31 and 2.44 for linear, asymmetric, ER and MR respectively.

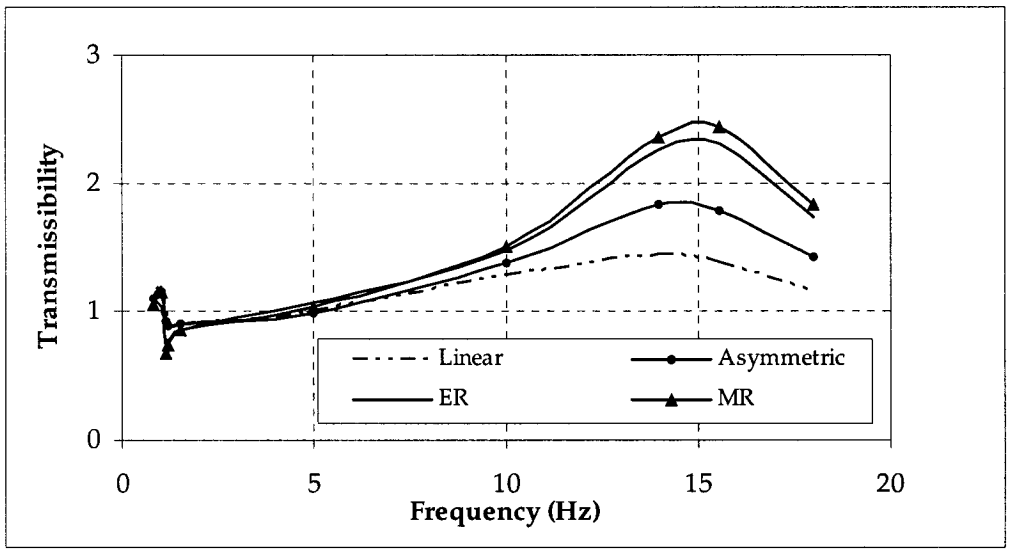

Figure 4.52: Front unsprung mass transmissibility to pitch excitations.

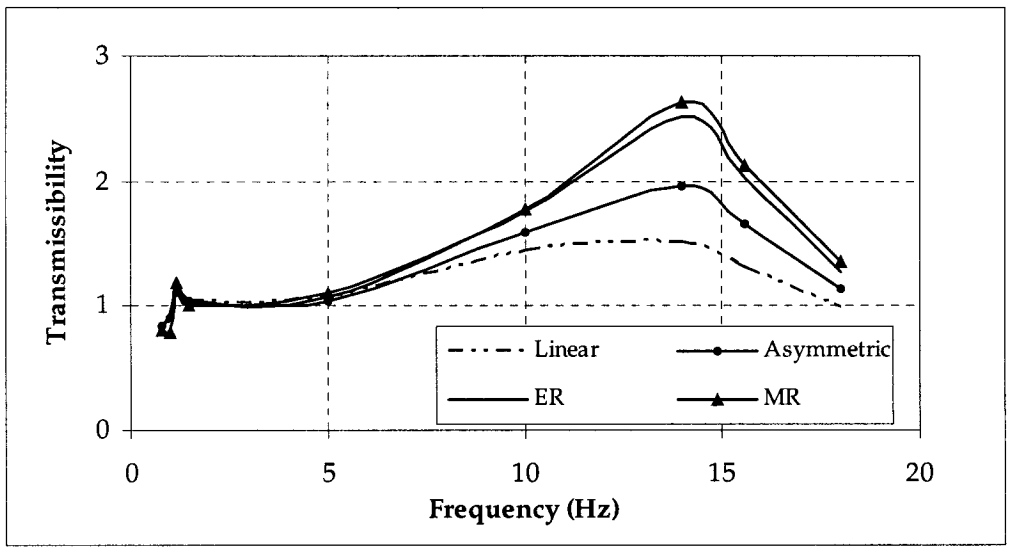

Figure 4.53: Rear unsprung mass transmissibility to pitch excitations.

A comparison between the results obtained for 10 mm and 15 mm indicates that under pitch excitations the performance of all the dampers remains almost the same. Similar responses are seen for rear unsprung mass transmissibility.

4.5.5.3 Sprung Mass Pitch Displacement

The pitch response or the angular displacements of the sprung mass under bounce input using 4 different dampers are presented in figure 4.54. Similar trends as seen for 10mm input (figure 4.26) are seen here too, i.e. around the pitch natural frequency (1.0Hz), values of angular displacement for all the dampers are maximum. Maximum values are 0.00765, 0.00499, 0.00326 and 0.00577 radian for linear, asymmetric, ER, and MR damper based system respectively. Compared to 10mm input, the angular displacement increases by 53%, 42.5%, 63% and 44% for linear, asymmetric, ER, and MR damper based system respectively. The results indicate that at higher amplitude asymmetric and MR damper have superior performances over linear and ER damper.

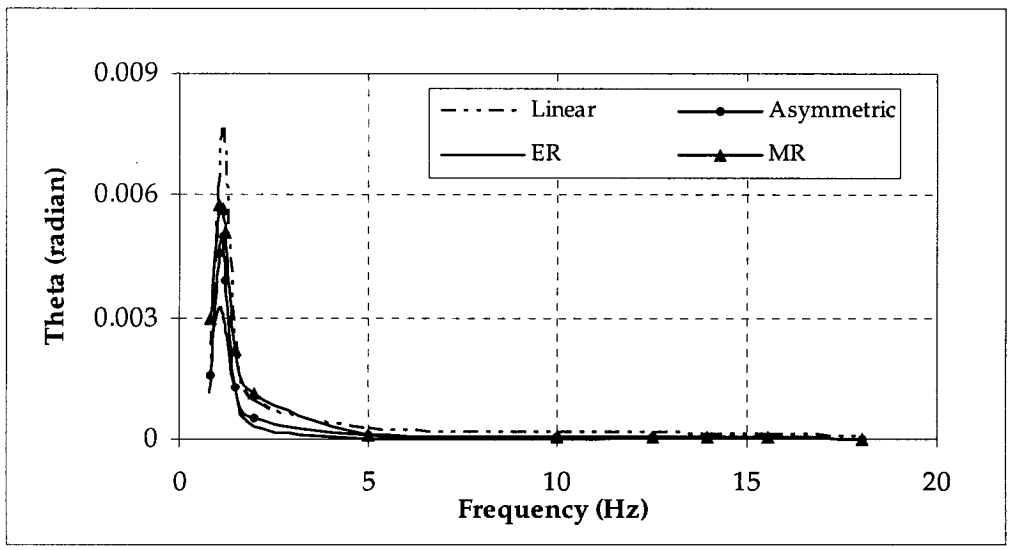

Figure 4.54: Pitch response of sprung mass to bounce excitations.

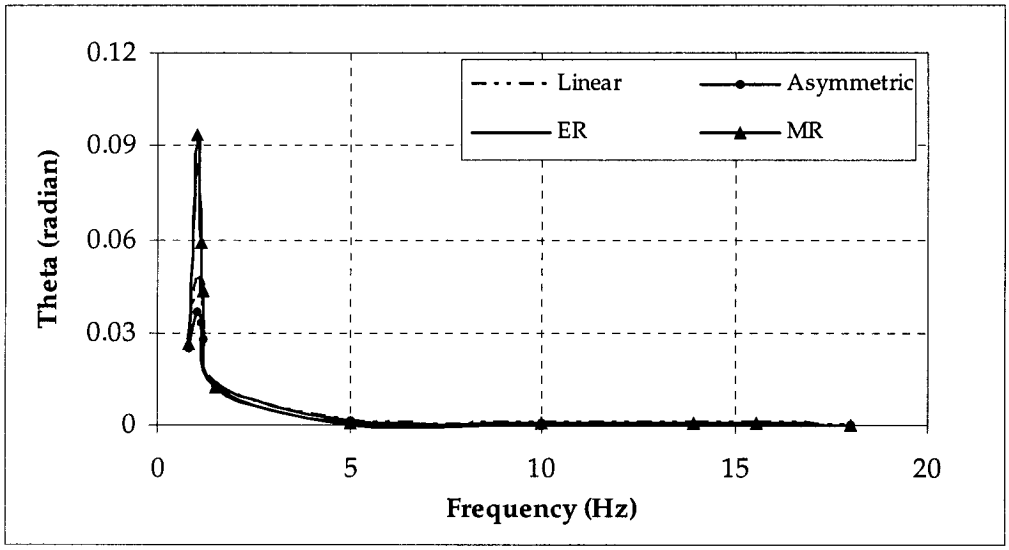

Figure 4.55: Pitch response of sprung mass to pitch excitations.

Figure 4.55 shows the pitch response of the sprung mass under pitch excitations. The maximum values are 0.047, 0.036, 0.084 and 0.093 radian for linear, asymmetric, ER and MR damper respectively. Compared to 10 mm input (figure 4.27), the angular displacement increases by 47%, 71%, 50% and 66% for linear, asymmetric, ER and MR damper respectively. The results indicate that at higher amplitude linear and ER damper have superior performance over asymmetric and MR damper.

A comparison between response under bounce and pitch inputs at higher amplitude indicates that performances of asymmetric and MR are superior under bounce, while linear and ER have superior performances under pitch.

4.5.5.4 Suspension Travel

Similar to low input, all the dampers require higher rattle space around sprung mass and unsprung mass natural frequencies. Figure 4.56 and 4.57 presents the suspension travel for front and rear suspensions under bounce excitations. For front

suspensions, around sprung mass natural frequency, rattle space requirements are 0.0474, 0.0381, 0.0289 and 0.02145 m, and around front unsprung mass natural frequency 0.0219, 0.0276, 0.0384 and 0.0396 m for linear, asymmetric, ER, and MR damper based system respectively.

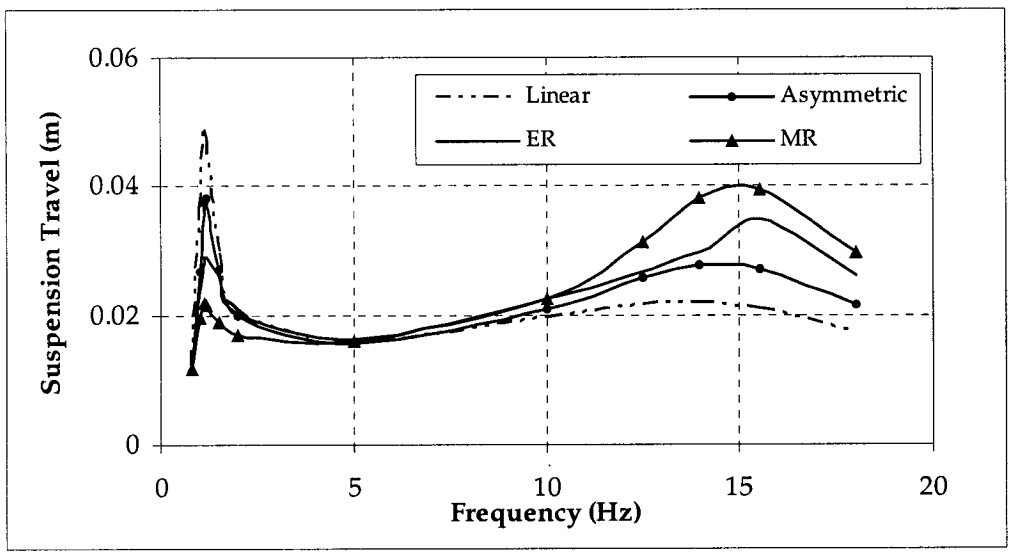

Figure 4.56 : Suspension travel of front suspensions for bounce excitations.

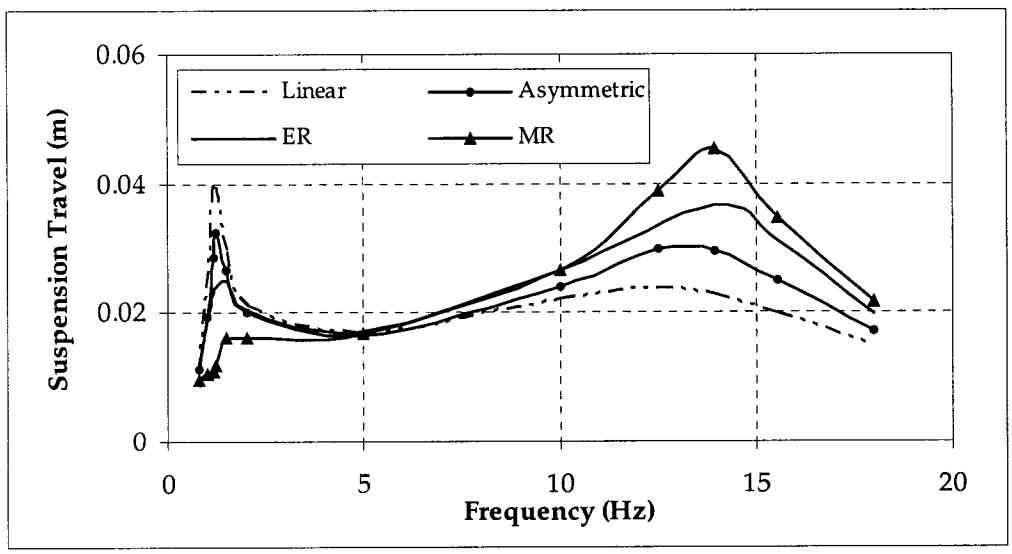

Figure 4.57: Suspension travel of rear suspensions for bounce excitations.

Compared to 10mm (figure 4.28) input, around sprung mass natural frequency, suspension travel increases by 48%, 73%, 52%, 53% and around front unsprung mass natural frequency suspension travel increases by 46%, 53%, 51%, 58% for linear, asymmetric, ER, and MR damper based system respectively, for the front axle. The results indicate that around sprung mass natural frequency suspension travel for asymmetric damper is higher compared to other three. Similar trends are observed for rear axle too.

Figure 4.58 and 4.59 presents the suspension travel for front and rear axle suspensions under pitch excitations. Maximum suspension travel is seen around sprung mass natural frequency. The maximum values are 0.053, 0.058, 0.08 and 0.073m for front suspensions, and 0.038, 0.058, 0.091 and 0.11m for rear suspensions for linear, asymmetric, ER and MR damper based system respectively. A comparison with 10 mm input reveals that increase in suspension travel for ER and MR damper are higher compared to linear and asymmetric damper.

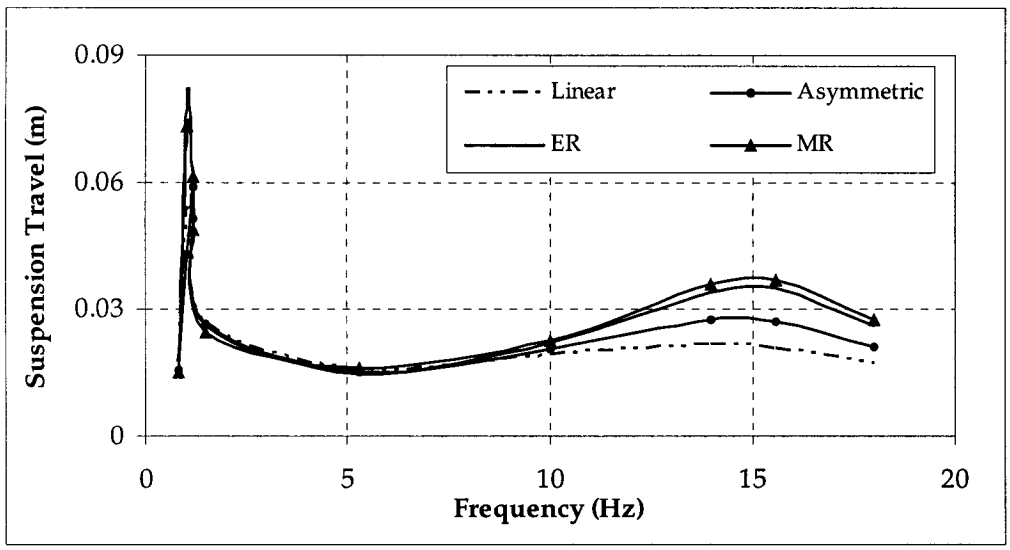

Figure 4.58 : Suspension travel of front suspensions for pitch excitations.

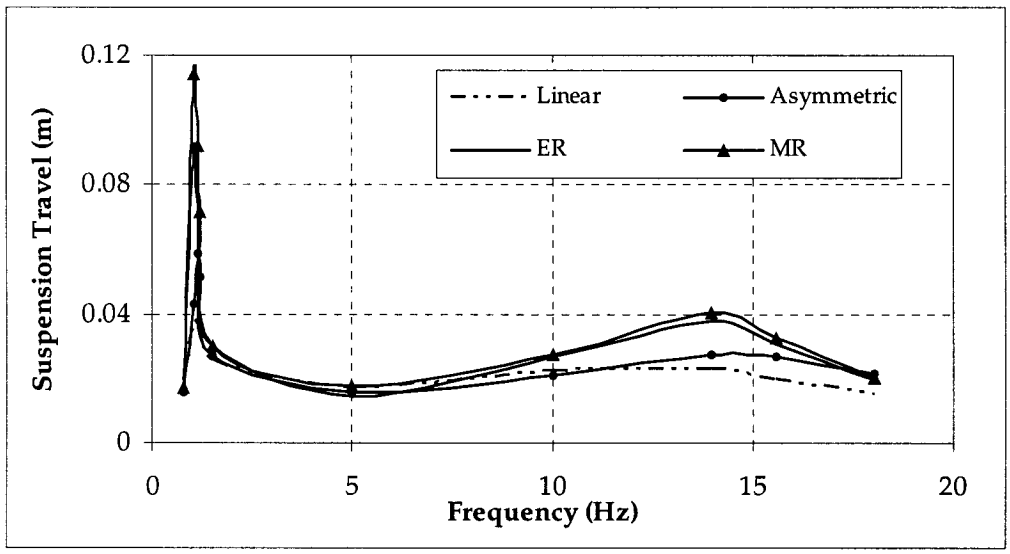

Figure 4.59: Suspension travel of rear suspensions for pitch excitations.

4.5.5.5 Relative Velocity Across Suspension

Figure 4.60 and 4.61 present relative velocity across suspension for front and rear suspensions under bounce excitations.

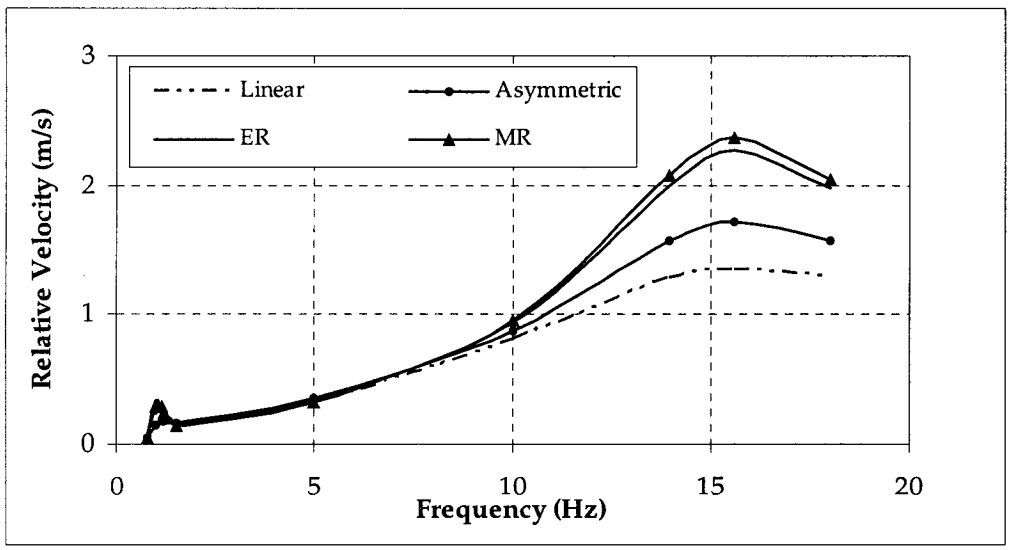

Figure 4.60: Relative velocity across the front suspensions for bounce excitations.

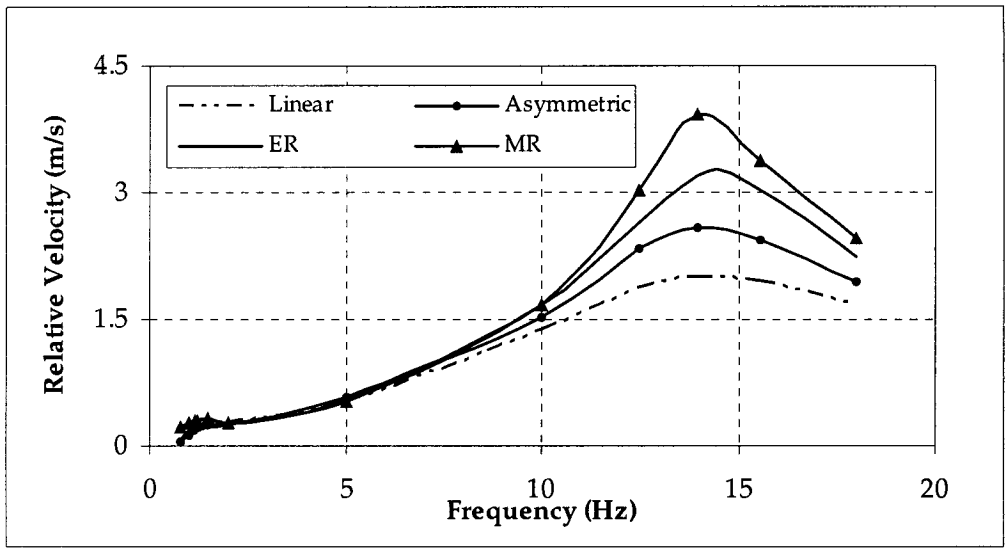

Figure 4.61: Relative velocity across the rear suspensions for bounce excitations.

For 5 mm change in input, from 10mm (figure 4.32, 4.33) to 15mm, the relative velocity at the front axle increases by an amount of 49%, 54%, 49% and 56%, and at the rear axle by 49%, 55%, 44% and 63% for linear, asymmetric, ER and MR damper based system respectively. It can be seen that the increase in relative velocity for MR damper occurs at a higher rate than other three.

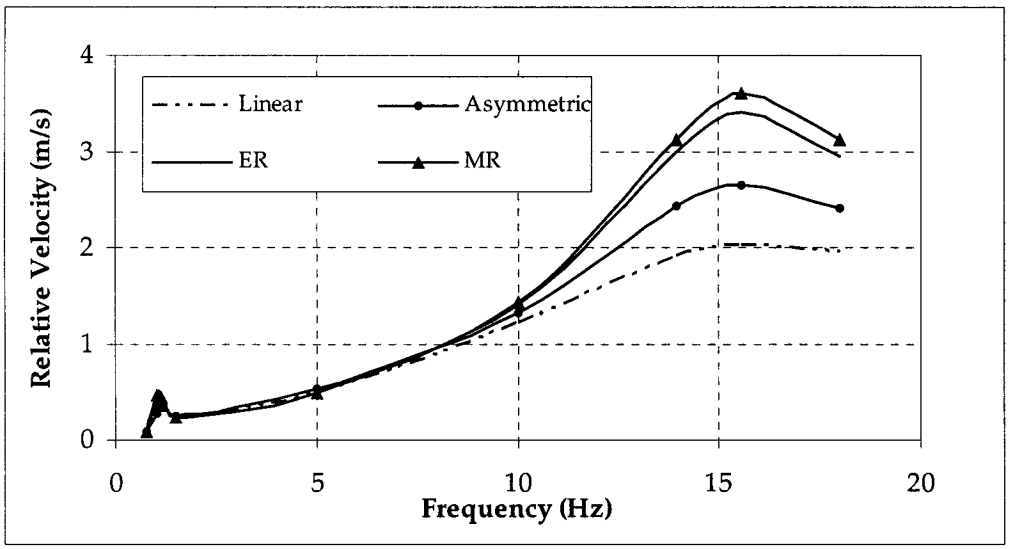

Figure 4.62: Relative velocity across front suspensions for pitch excitations.

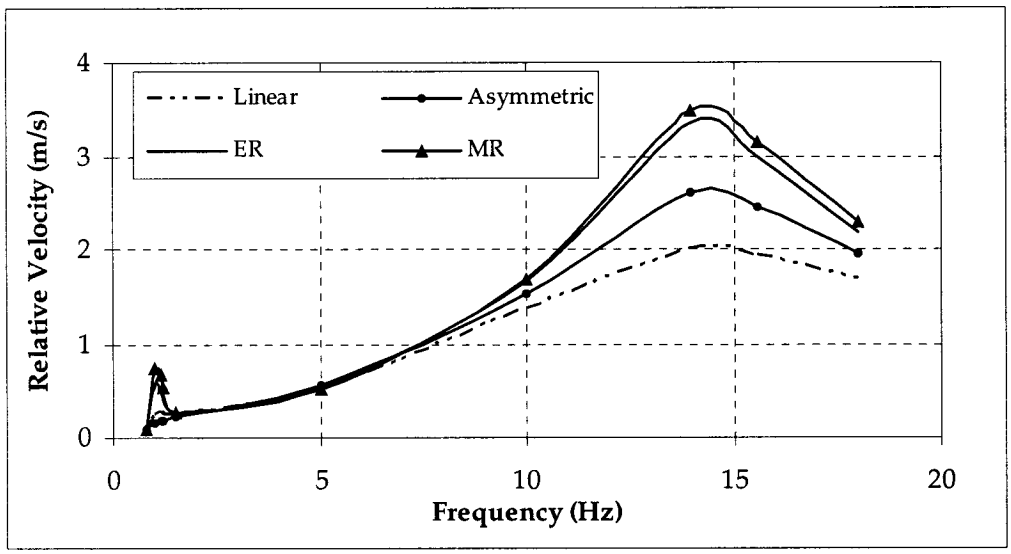

Figure 4.63: Relative velocity across rear suspensions for pitch excitations.

Figure 4.62 and 4.63 present relative velocity across suspension for front and rear suspensions under pitch excitations. Compared to 10mm (figure 4.34, 4.35), the relative velocity at the front axle increases by 49%, 54%, 50% and 52%, and at the rear axle by 49%, 54%, 50% and 51% for linear, asymmetric, ER and MR damper based system respectively. It is evident from the results that the change in relative velocity for all the dampers under pitch excitations changes in a similar manner.

4.5.5.6 Ride Height Drift

With the increase of excitation amplitude the drift for asymmetric damper increases. As seen before, rest of the dampers do not show any drift at all. The ride height drift of the asymmetric damper under bounce excitations is presented in figure 4.64. For 15mm input, asymmetric damper based system shows maximum drift of 18.4mm. In case of 10mm input, the maximum drift was 14.26mm. So drift increases with the increase of input amplitude.

Similar trend is seen for pitch excitations. The drift is higher around unsprung mass natural frequencies. The maximum value is 18.38 mm under pitch excitations. Figure 4.65 shows the drift under pitch excitations. The results indicate that ride height drift under bounce excitations and pitch are almost the same.

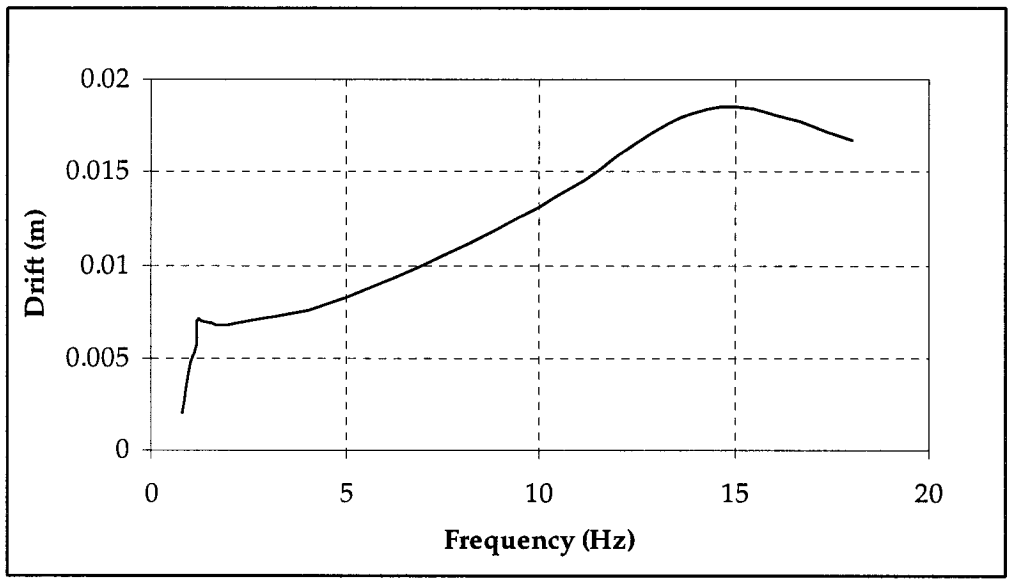

Figure: 4.64: Ride height drift of asymmetric damper for bounce excitations.

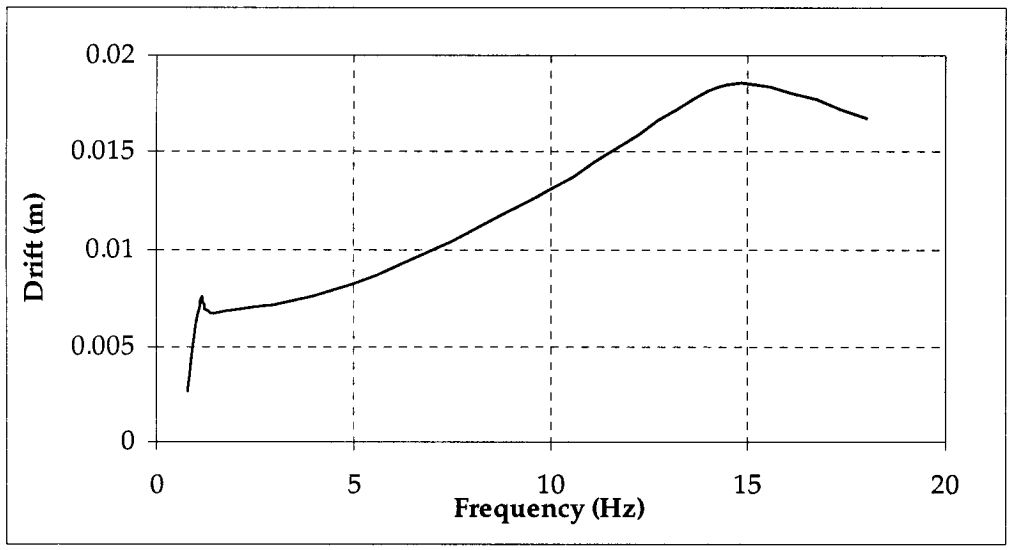

Figure: 4.65: Ride height drift of asymmetric damper for pitch excitations.

4.5.5.7 Angular Drift

Similar to ride height drift, angular drift increases with higher amplitude excitation. Figure 4.66 shows angular drift for the asymmetric damper for bounce excitations. As seen before, rest of the dampers does not show any angular drift.

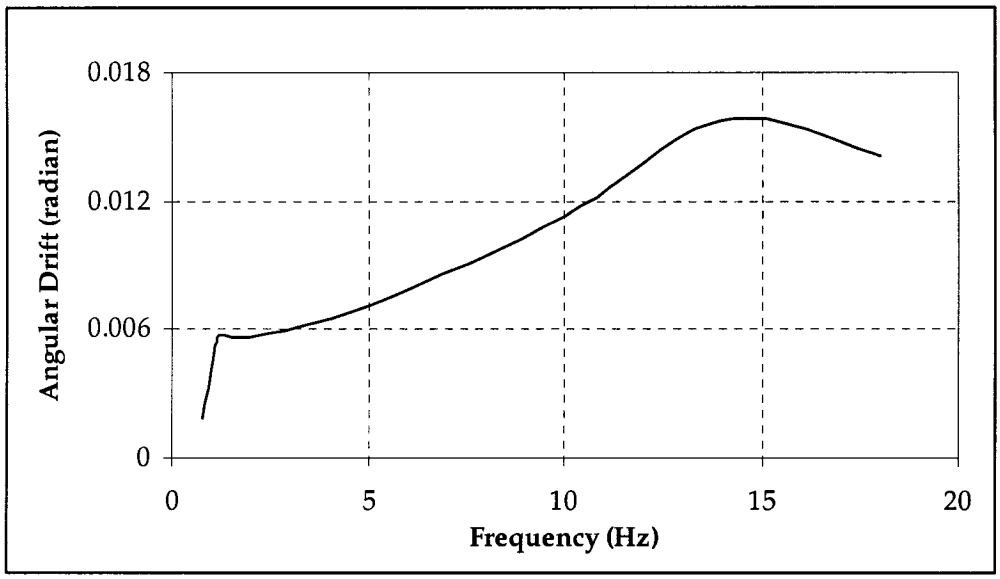

Figure 4.66: Angular drift of asymmetric damper for bounce excitations.

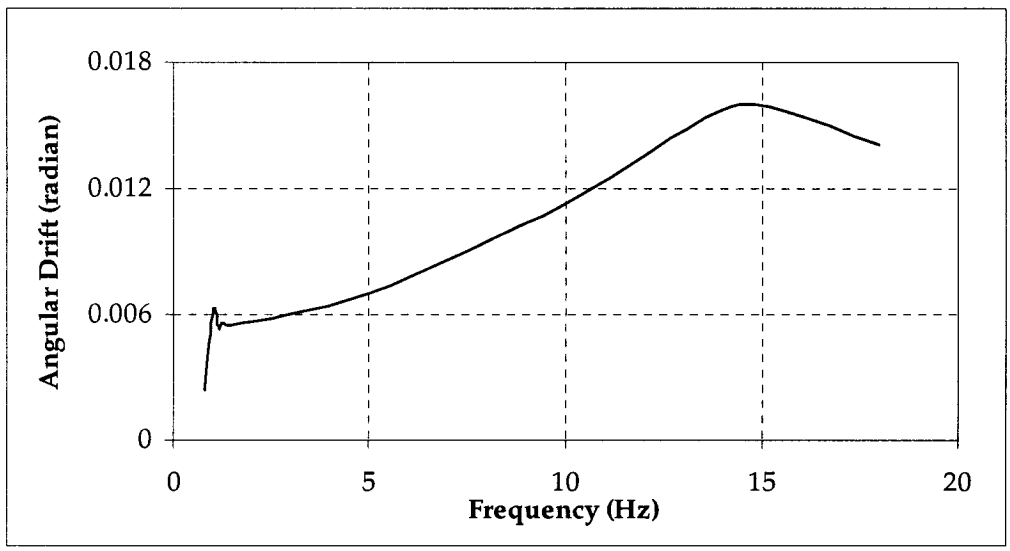

Figure 4.67: Angular drift of asymmetric damper for pitch excitations.

For 15 mm input, asymmetric damper based system shows maximum angular drift of 0.0157 radian. For 10mm input, maximum angular drift was 0.012 radian. Thus, it can be said that angular drift of the asymmetric damper increases with increase in excitation amplitude.

Similar trend is seen for pitch excitations. The drift is high around unsprung mass natural frequencies. The maximum value is 0.0157 radian under pitch excitations. The results indicate that ride height drift under bounce and pitch are almost the same. Figure 4.67 shows the drift under pitch excitations.

4.5.5.8 Pavement Load

Similar trends as seen for 10 mm input (figure 4.40, 4.41) are seen here too, i.e. ER and MR dampers cause more damage to the road than asymmetric and linear dampers.

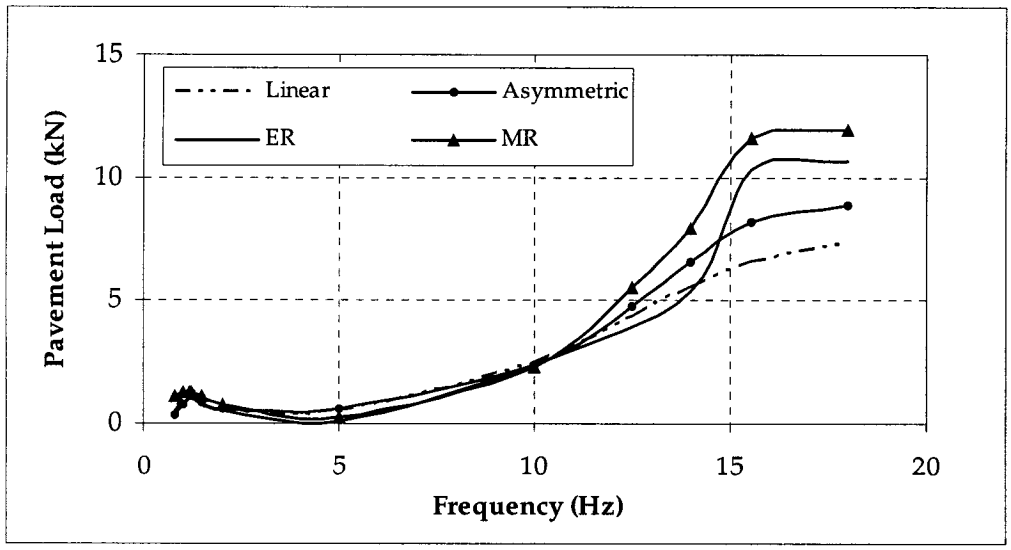

Figure 4.68: Pavement load of front axle for bounce excitations.

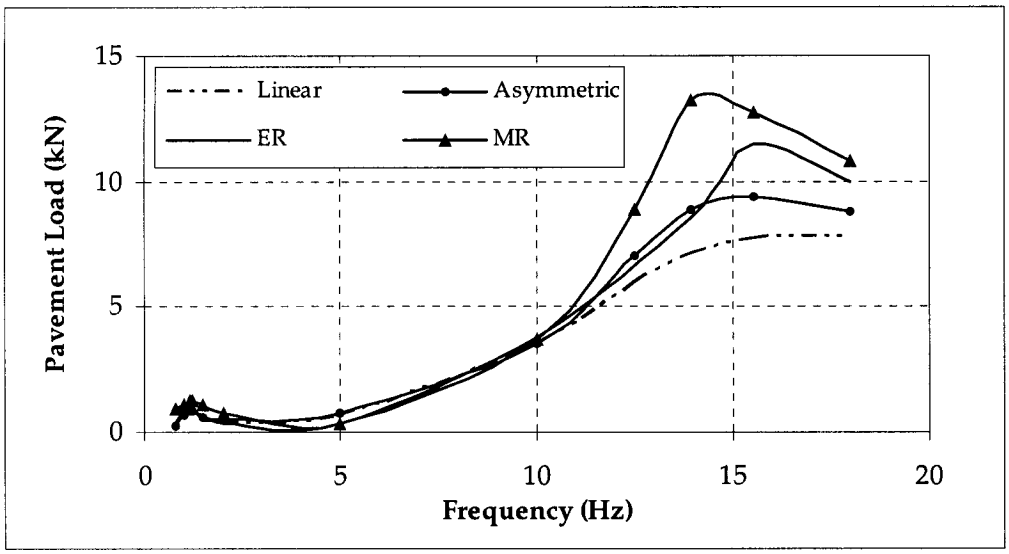

Figure 4.69: Pavement load of rear axle for bounce excitations.

Figure 4.68 and 4.69 present pavement load generated by front and rear axle for bounce excitations. For 5 mm change in input, from 10mm to 15mm, the pavement load at the front axle increases by 50%, 53%, 50% and 57% and at the rear axle by 50%, 53%, 50% and 60% for linear, asymmetric, ER and MR damper based system respectively.

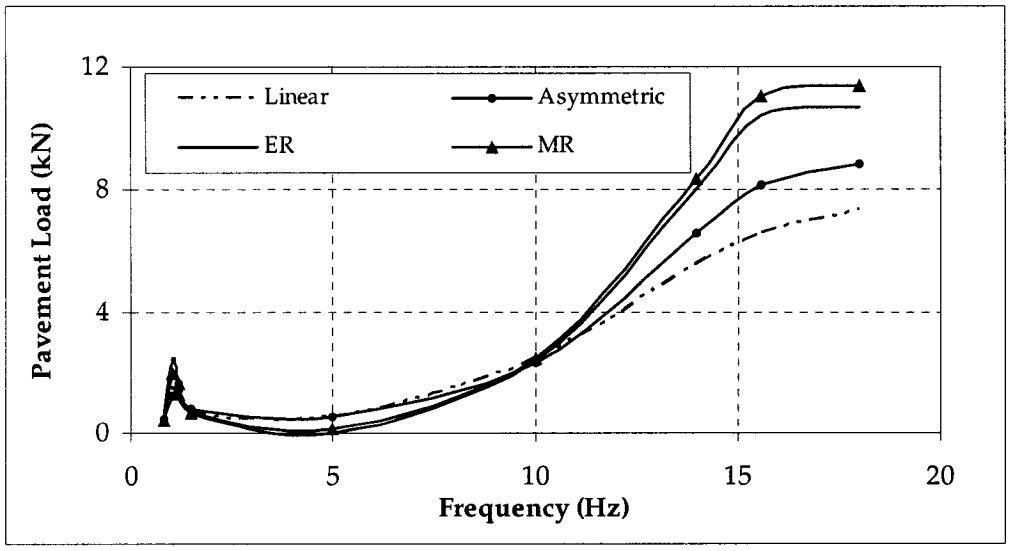

Figure 4.70: Pavement load of front axle for pitch excitations.

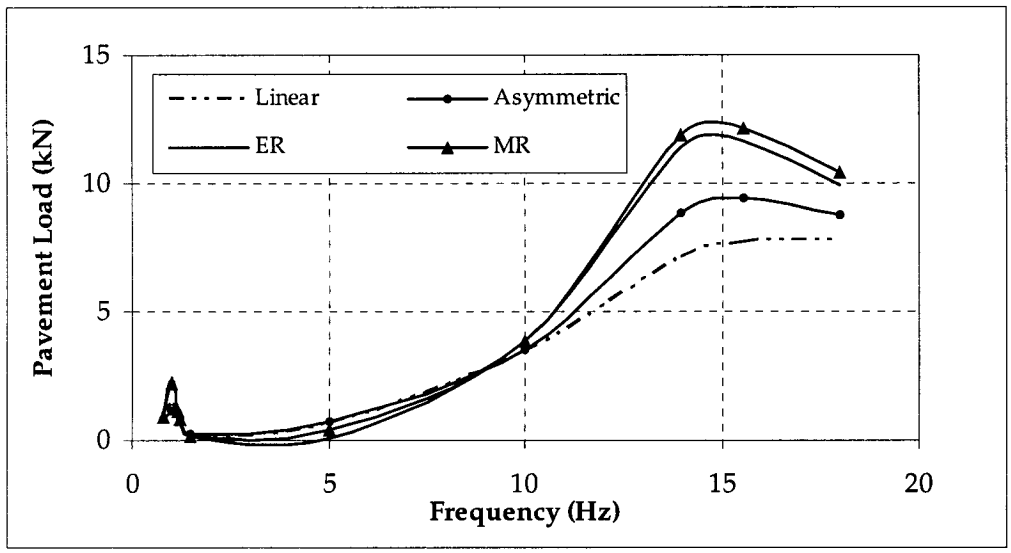

Figure 4.71: Pavement load of rear axle for pitch excitations.

Figure 4.70 and 4.71 represents pavement load generated by front and rear axle for pitch excitations. Compared to 10 mm input (figure 4.42, 4.43) the pavement load at the front axle increases by 50%, 53%, 55% and 53% and at the rear axle by 50%, 53%, 50% and 52% for linear, asymmetric, ER and MR damper based system respectively.

The results clearly indicate that increase in pavement load is similar for all the dampers for both bounce and pitch.

4.6 Summary

In this chapter, a set of basic system parameters are proposed for 2 DOF and 4 DOF model. The vibration isolation performances of the candidate damper are first analyzed using a 2 DOF quarter car model. Subsequently, the dampers are incorporated in a 4 DOF pitch-plane model to investigate the vibration and shock isolation performance of the dampers. Finally, the effects of higher amplitude of excitation on the performances of the dampers are investigated.

CHAPTER 5

Conclusions and Recommendations for Future Work

5.1 General

Electro-Rheological (ER) and Magneto-Rheological (MR) fluid based advanced suspension dampers are emerging to be the next generation of suspension dampers. ER damper and MR damper have gained wide spread attention in academia as well in auto industries with their attractive features and promising performance potential to overcome the limitations of existing dampers in market.

Although there exists several studies that investigate the vibration isolation performance of a specific advance concept with a set of parameters, there is a lack of comprehensive parametric study and investigation of isolation performance under shock excitations. Majority of the studies only compared either ER or MR damper with linear passive damper, despite the fact that asymmetric dampers are widely used in modern vehicles. Moreover, most of the studies used simple quarter car model neglecting the pitch motion and bounce-pitch coupling in the vehicle motions. Furthermore, the performance measures used for most of the studies are limited to sprung mass vibration isolation performance of the damper, neglecting the performance like unsprung mass isolation, relative motion, pavement load, drift and shock isolation performance.

This work presents a comprehensive study of vibration and shock isolation performance of linear passive, two-stage-asymmetric non-linear, ER and MR damper. The damper models are selected form works published in literature. The models are

incorporated in a 4 degree-of-freedom (DOF) pitch-plane vehicle model to investigate the comparative performance. The models are initially subjected to sinusoidal in phase and out of phase (bounce and pitch excitations) road input frequency range of 0.8-18 Hz. Subsequently, the dampers are subjected to shock input to analyze their performance at bumps. A wide range of performance measure is considered in this investigation, namely – sprung and unsprung mass responses, relative motions, ride height drift, and pavement load. A new performance measure namely angular drift is proposed to study the effect of drifting in angular dynamic equilibrium of the vehicle. Finally, the effects of higher amplitude excitation are investigated. The investigation is performed by simulating the vehicle models in the time domain using MATLAB® SIMULINK.

The major conclusions drawn from the simulation results and a list of recommendation for future works are presented in the following subsections.

5.2 Major Conclusions

The study investigated the comparative performance of linear passive, asymmetric non-linear, Electro-rheological and Magneto-rheological dampers using a 4 DOF pitch-plane model. The major conclusions drawn from the results and observations are as follows -

1. The damper models developed for this study are valid and are capable of providing reasonable vibration and shock isolation performance. The results generated by the models are similar to the results published in literature.
2. The comparative study of four dampers under bounce excitations clearly indicates that ER and MR damper provides superior vibration isolation to sprung mass over entire frequency range compared to linear passive and

asymmetric non-linear damper. Among all the dampers, MR damper provides best sprung mass vibration isolation performance over the entire frequency range. It also reveals the superiority of asymmetric non-linear damper over linear passive damper. Under the pitch excitations, asymmetric damper has superior performance over linear and ER damper. MR damper shows best isolation under pitch input too. ER damper has superior performance over asymmetric damper under bounce excitations but has inferior performance under pitch excitations.

3. However, the superior performances of the ER and MR dampers for sprung mass are achieved at the expense of performances for unsprung mass response. The study indicates the superior performance for sprung mass results in interior performance for unsprung mass. Linear passive damper provides best unsprung mass response compared to rest of the dampers. Same trends are observed for bounce and pitch excitations.
4. MR and ER dampers have superior performance in terms of pitch response over linear and asymmetric damper under bounce excitations, while have inferior performance under pitch excitations. Hence superior performance under bounce results in inferior performance under pitch.
5. Rattle space required for ER damper and MR damper are low around sprung mass natural frequency and are high around unsprung mass natural frequencies compared to linear and asymmetric damper under bounce excitations. Under pitch excitations ER and MR dampers require higher rattle space over entire frequency range compared to other two. Asymmetric damper provides best performance under bounce and pitch excitations over the entire frequency range.

6. ER and MR dampers have higher relative velocity across the suspension compared to other two for bounce and pitch.
7. ER and MR dampers are immune from drifting problem as they are symmetric in nature. Ride height drift for asymmetric damper under bounce and pitch excitations are almost same.
8. Angular drift is maximum around unsprung mass natural frequencies. Angular drift under bounce and pitch have same trends.
9. ER damper and MR damper transmit more dynamic load to pavement compared to asymmetric and linear passive damper for both bounce and pitch excitations. The low damping force generated by ER damper and MR damper at higher frequencies are to blame for this. However the pavement loads generated by the candidate vehicle are not significant. Higher pavement load is an issue for heavy vehicles. Thus modifications of the dampers are required to use them in heavy vehicles.
10. ER damper and MR damper have superior shock isolation performance compared to linear passive and asymmetric damper. The shock performance study reveals that vertical displacement and settling time of sprung mass for these dampers are low compared to linear passive and asymmetric non-linear. In terms of pitch response at bumps, except ER damper, all the dampers have similar performance. ER damper has high pitch response and requires more time to settle compared to the other dampers.

5.2.1 Effect of Higher Amplitude Excitation

The study further investigates the effect of higher amplitude excitation to the performance of the dampers. Some general and specific conclusions drawn from the study are as follows -

1. At higher amplitude the sprung mass isolation performance of linear and ER damper are consistent while the performance of asymmetric and MR damper deteriorate for both bounce and remain same for pitch input. Hence it can be concluded that asymmetric and MR damper presented in the study requires further tuning to maintain consistent performance at higher amplitudes or within a range of excitation amplitude. Despite having deteriorating performance at higher amplitude, MR damper performs best among all the dampers.
2. Unsprung mass response of all the dampers remains almost the same at higher amplitude for both bounce and pitch excitations.
3. Pitch response of sprung mass under bounce and pitch excitations at higher amplitude indicate that performance of asymmetric and MR dampers are superior under bounce, while linear and ER have superior performance under pitch.
4. Around sprung mass natural frequency increase in suspension travel for asymmetric damper is higher compared to other three under bounce excitations. On the other hand increase in suspension travel for ER and MR damper are higher compared to linear and asymmetric damper under pitch excitations. Despite deteriorating performance by asymmetric damper, it remains the best

damper in terms of suspension rattle space requirement under bounce excitations.

5. Relative velocity across the suspension at higher amplitude increases in similar manner for all the dampers under bounces and pitch excitations.
6. Ride height drift at higher frequency increases for both excitations. Similar to lower amplitude the ride height drift is same for both bounce and pitch excitations. Thus it can be concluded that pitch has no significant effect of ride height drift rather it affects the angular drift. The angular drift increases at higher amplitude for both excitations and has different values.
7. At higher amplitude all the dampers transmit more force to the pavement. The increase is similar for all the dampers.

The study reveals that asymmetry is needed for suspension to perform better for sprung and unsprung mass. The ER and MR fluid based dampers have symmetric properties in compression and rebound. Asymmetric properties should be included in ER and MR damper model to achieve improved performance for sprung and unsprung mass. It can be done by modifying the controllers for such dampers to monitor the compression and rebound and change the gain accordingly instead of having the same gain for the whole operating range.

The automotive application of ER damper is difficult due to the fact that ER dampers require very high voltage. On the other hand MR dampers can deliver improved isolation performance with reasonable current supply. Thus a properly tuned MR damper has potential to provide superior isolation performance over entire operation cycle of the vehicle. The tuning of such damper should be done to ensure performance both under bounce and pitch, as well as under shock. It can be done by

using sophisticated controllers and sensors to monitor various performances of the vehicle.

5.3 Recommendations for Future Work

The present work presents the comparative performance of the dampers to provide basic insight to the performance of the advanced suspensions using a 4 DOF pitch-plane plane and commonly used performance measures. The knowledge gained from this investigation is a starting point for the study of advance suspension systems for road vehicles and establishes the direction for future works -

1. A full vehicle model may be studied with the proposed dampers to further study the performance of the dampers.
2. Experimental validation of the results obtained may be under taken by laboratory and field testing of an instrumented vehicle.
3. This study considered symmetric ER and MR damper model. Future study may consider asymmetricity in ER and MR damper for improved performance for sprung and unsprung mass.
4. Current study considers simple controller to modulate the damping force. Future studies may consider more sophisticated controllers to achieve improved performance.
5. The present study is based on sinusoidal excitations with constant amplitude to analyze the performance of the dampers. But, real life vehicles are subjected to random vibration rather than sinusoidal excitations. So, future study may investigate the performance of the dampers using random road excitation.

6. The present investigation examined the performance of dampers as applied to a small size car. Future work may investigate vehicles of different size to further investigate the performance of the dampers. Also the effect of variations in sprung and unsprung mass of the vehicles may also be investigated to analyze the performance of the dampers.
7. The current study considers damping properties of only one kind of tire and unsprung mass associated with it to avoid complications. Future study may investigate different types of tires to determine best tire properties.
8. The suspension springs are considered to be linear for this study. But in real life vehicles, different types of non-linear springs are used. Future work may incorporate the spring non-linearity in the suspension design.
9. Commercial feasibility of the smart fluid based dampers might be studied to explore the possibilities of mass production.
10. As voltage requirement for ER damper is very high, future study might include regenerative units to reduce the voltage required from the vehicle. Moreover, new ER fluid might be developed to reduce higher voltage requirement.
11. The present study investigated only one kind of ER and MR damper. Future study may investigate different types of ER and MR dampers. Also dampers with different types of ER and MR fluids may also be investigated.
12. Possible use of smart fluid based suspension as vehicle seat suspension and engine mount may also be investigated to explore the new avenues of use for smart fluid dampers.

References:

1. Ahmed, A. K. W. (2001). Ground Transportation Systems, Encyclopedia of Vibration, Academic Press, USA, ISBN 0-12-227085-1, pp. 603-620.
2. Bacon, M. E. (1988). Automotive Steering, Suspension, and Wheel Alignment, McGraw-Hill Book Company, ISBN 0070795770.
3. Bastow D. (1993). Car Suspension and Handling, 3rd Edition, Pentech Press, UK, ISBN 0-7273-0318-x.
4. Bayer AG (1994). Publicity Material on 'Rheobay' Electro-Rheological Fluids and a Valve-Controlled Shock Absorber, Leverkusen, Germany.
5. Bert, C.W. (1973). Material Damping: An Introductory Review Of Mathematical Models, Measures and Experimental Techniques, Journal of Sound and Vibration. Vol. 29(2), pp. 129-153.
6. Bloodworth, R., Wendth, E. (1995). Materials for ER Fluids, Proceedings of the Fifth International Conference on Electro-rheological Fluids, Magnetorheological Suspensions and Associated Technology , Sheffield, UK, pp. 118-131.
7. Brooks, D.A. (1982). Electro-Rheological Devices, Charted Mechanical Engineer, September, pp. 91-93.
8. Bitman, L., Choi, Y., Wereley, M. (2001). Electrorheological Damper Analysis Using an Eyring Constitutive Model, Proceedings of the Eighth International Conference on Electrorheological Fluids and Magnetorheological Suspensions, Nice, France, pp. 77-83.
9. Carlson, J. D., Weiss, K. D. (1994). A Growing Attraction to Magnetic Fluids, Machine Design, Aug 8, pp. 61–64.

10. Carlson, J.D., Catanzarite, D.M., Clair, K.A.St. (1995). Commercial Magnetorheological Fluid Devices, Proceedings of the Fifth International Conference on Electro-rheological Fluids, Magnetorheological Suspensions and Associated Technology, Sheffield, UK, pp. 20-28.
11. Carlson, J.D. (1999). Magnetorheological Fluid Actuators, Adaptronics and Smart Structures: Basics, Materials, Designs and Applications, Springer-Verlag, Germany, ISBN: 3540614842, pp. 180-195.
12. Carlson, J.D. (2000). Implementation of Semi-Active Control Using Magneto-Rheological Fluids, Mechatronic System: A Proceeding Volume from the IFAC Conference, Darmstadt, Germany, pp. 905-910.
13. Carlson, J. D., Jolly, M. R. (2000). MR Fluid, Foam and Elastomer Devices, Mechatronics, Vol. 10, 555–569.
14. Carlson, J.D., Sproston, J.L. (2000). Controllable Fluids in 2000- Status of ER and MR Fluid Technology, Proceedings of Seventh International Conference on New Actuator, Berman, Germany, pp. 126-130.
15. Carlson, J.D. (2001). What Makes a Good MR Fluid?, Proceedings of the Eighth International Conference on Electrorheological Fluids and Magnetorheological Suspensions, Nice, France, pp. 63-69.
16. Causemann, P. (2000). Automotive Shock Absorber, Verlag Moderne Industrie AG & Co. KG, Landsberg, Germany.
17. Cebon, D. (1999). Handbook of Vehicle-Road Interaction, Swets & Zeitlinger, The Netherlands, ISBN 90-265-1554-5.
18. Chen, S.H., Yang, G., Liu, X.H. (2001). Response Analysis of Vibration System with ER Dampers, Smart Materials and Structures, Vol.10 (5), pp. 1025-1030.

19. Choi, S.B., Lee, S.K., Park, Y.P. (1997). A Hysteresis Model for the Field-Dependent Damping Force of a Magnetorheological Damper, Journal of Sound and Vibration, Vol. 245 (2),pp.375-383.

20. Choi, S.B., Kim, W.K. (2000). Vibration Control of a Semi-Active Suspension Featuring Electrorheological Fluid Dampers, Journal of Sound and Vibration, Vol. 234(3), pp. 537-546.

21. Choi, S.B., Lee, H.K., Chang, E.G. (2001). Field Test Results of a Semi-active ER Suspension System Associated with Skyhook Controller, Mechatronics, Vol.11 (3), pp. 345-353.

22. Choi, S.B., Lee, H.S., Park, Y.P. (2002). H_∞ Control Response Performance of a Full-Vehicle Suspension Featuring a Magneto-Rheological Damper, Vehicle System Dynamics, Vol. 38 (5), pp. 341-360.

23. Choi, S.B., Han, Y.M. (2003). MR Seat Suspension for Vibration Control of a Commercial Vehicle, International Journal of Vehicle Design, Vol. 33 (1-3), pp.202-215.

24. Choi, Y.T., Wereley, N.M. (2001). Comparative Analysis of the Time Response of Electrorheological and Magnetorheological Dampers Using Nondimensional Parameters, Proceedings of the Eighth International Conference on Electrorheological Fluids and Magnetorheological Suspensions, Nice, France, pp. 187-193.

31. Chaudhary, S. (1998). Ride and Roll Performance Analysis of a Vehicle with Spring Loaded Interconnected Hydropneumatic Suspension, M. A. Sc. Thesis, Concordia University, Montreal, Canada.

32. Cole, D.J. (2001). Fundamental Issues in Suspension Design for Heavy Road Vehicles, Vehicle System Dynamics, Vol. 35 (4-5), pp. 319 – 360.

33. Ellinger, H.E.,Hathaway, R.B. (1989). Automotive Suspension and Steering Theory and Service, Prentice Hall, New Jersey, USA.

34. Ericksen, E.O., Gordaninejad, F. (2003). A Magneto-Rheological Fluid Shock Absorber for Off-Road Motorcycle, International Journal of Vehicle Design, Vol. 33 (1-3), pp.139-152.

35. Ficher, D., Isermaan, R. (2004). Mechatronic Semi-active and Active Vehicle Suspensions, Control Engineering Practice Vol.12, pp. 1353-1367.

36. Gavin, H.P., Hanson, R.D., Filisko, F.E. (1996). Electrorheological Dampers, Part I: Analysis and Design, Journal of Applied Mechanics, Vol.63 (3), pp. 669-675.

37. Gavin, H.P., Hanson, R.D., Filisko, F.E. (1996). Electrorheological Dampers, Part II: Testing and Modeling, Journal of Applied Mechanics, Vol.63 (3), pp. 676-682.

38. Gavin, H. P. (1998). Design Method for High-Force Electrorheological Dampers, Smart Materials and Structure, Vol. 7(5), pp. 664–673.

39. Genç¸S, Phulé, P.P. (2002). Rheological Properties of Magnetorheological Fluids, Smart Materials and Structures, Vol.11 (1), pp.140-146.

40. Gillespie, T.D. (1992). Fundamental of Vehicle Dynamics, ISBN 1-56091-199-9, Society of Automotive Engineers, PA, USA.

41. Gilbert, R., Jackson, M. (2002). Magnetic Ride Control, GM TechLink 4.

42. Gilliomee, C.L., Els, P.S. (1998). Semi-active Hydropneumatic Spring and Damper System, Journal of Terramechanics, Vol. 35, pp. 109-117.

43. Ginder ,J. M., Davis, L. C. (1994). Shear Stresses in Magnetorheological Fluids: Role of Magnetic Saturation, Appl. Phys. Lett. , Vol. 65, pp. 3410–3412.

44. Gordaninejad, F., Breese, D.G. (1999). Heating of Magnetorheological Fluid Dampers: An Experimental Study, Proceedings of the Seventh International Conference on Electro-Rheological Fluids and Magneto-Rheological Suspensions, Hawaii, USA, pp. 629-638.

45. Gordaninejad, F., Kelso, S.P. (2000). Magnetorheological Fluid Shock Absorbers for HMMWV, Smart Structures and Materials: Damping and Isolation, Proceedings of SPIE, Vol. 3989, pp.266-273.

46. Guo, D.L., Hu, H.Y., Yi, J.Q. (2004). Neural Network Control for Semi-Active Vehicle Suspension with Magnetorheological Dampers, Journal of Vibration and Control, Vol. 10(3), pp. 461-471.

47. Harrison, R F and Harmond, J. K. (1986). Approximate Time Domain, Non-stationary Analysis of Stochastically Excited, Nonlinear Systems with Particular Reference to the Motion of Vehicles on Rough Road", Journal Sound and Vibration, 105, (3), pp. 361-371.

48. Hao, T. (2002). Electrorheological Suspensions, Advances in Colloid and Interface Science, Vol. 97, pp. 1-53.

49. Heo, S.-J., Park, K., Son, S.-H. (2003). Modeling of Continuously Variable Damper for Design of Semi-Active Suspension Systems, International Journal of Vehicle Design, Vol. 31(1), pp. 41-57.

50. Hong, S.R., Choi, S.B., Choi, Y.T, Wereley, N.M. (2003). Comparison of Damping Force Models for An Electrorheological Fluid Damper, International Journal of Vehicle Design, Vol. 33 (1), pp.17-35.

51. Hrovat, D. (1997). Survey of Advanced Suspension Developments and Related Optimal Control Applications, Automatica, Vol. 33(10).

52. Joarder, M.N. (2003). Influence of Nonlinear Asymmetric Suspension Properties on the Ride Characteristics of Road Vehicle, M. A. Sc. Thesis, Concordia University, Montreal, Canada.

53. Jolly, M.R., Miller, L.R. (1989). The Control of Semi-active Dampers Using Relative Feedback Control Signals, SAE Technical Paper 892483, Society of Automotive Engineers, USA.

54. Jolly, M.R., Bender, J.W., Carlson, J.D. (1998). Properties and Applications of Commercial Magnetorheological Fluids, Proceedings of SPIE 5th Annual Symposium on Smart Structures and Materials, San Diego, CA, USA.

55. Joo, F. (1991). Dynamic Analysis of a Hydropneumatic Suspension System, M.A.Sc Thesis, Concordia University, Montreal, Canada.

56. Karnopp, D.C., Crosby M.J., Harwood, R.A. (1974). Vibration Controlling Semi-Active Generators, ASME Journal of Engineering for Industries, Vol. 96, B (2), pp. 619-626.

57. Kelso, S.P. Gordaninejad, F. (1999). Magneto-Rheological Fluid Shock Absorbers for Off-Highway, High-Payload Vehicles, SPIE Conference on Passive Damping and Isolation, CA, USA, SPIE Vol.3672, pp.44-54.

58. Kamath, G.M., Hurt, M.K., Wereley, N.M. (1996). Analysis and Testing of Bingham Plastic Behavior in Semi-active Electrorheological Fluid Dampers , Smart Materials and Structures, Vol. 5(5), pp.576- 590.

59. Kamath, G.M, Wereley, N.M. (1997). Nonlinear Viscoelastic-Plastic Mechanisms-Based Model of an Electrorheological Damper, Journal of Guidance, Control and Dynamics, Vol.20(6), pp.1125-1132.

60. Kelso, S.P. (2001). Experimental Characteristics of Commercially Practical Magnetorheological Fluid Damper Technology, Proceedings of SPIE Conference on Smart Structures and Materials, CA, USA, Paper No. 4332-34.

61. Khalil, H.K. (2002). Nonlinear System, 3rd Edition, Prentice Hall Inc., USA, ISBN: 0-13-067389-7.

62. Kim, K., Lee, J., Jeon, D. (1999). Vibration Suppression of an MR Fluid Damper System with Frequency Shaped LQ Control, Proceedings of the Seventh International Conference on Electro-Rheological Fluids and Magneto-Rheological Suspensions, Hawaii, USA, pp. 649-656.

63. Kim, J.W., Cho, Y.H., Choi H.J., Lee H.G., Choi S.B. (2001). Electrorheological Semi-Active Damper: Polyaniline Based ER System, Proceedings of the Eighth International Conference on Electrorheological Fluids and Magnetorheological Suspensions, Nice, France, pp. 229-235.

64. Kim, K.S., Choi, S.B., Cheong, C.C. (1999). ER Suspension System with Energy Generation, Journal of Intelligent Material Systems and Structures, Vol.10 (9), pp. 738-742.

65. Lam, H.F., Liao, W.H. (2001). Semi-Active Control of Automotive Suspension Systems with Magneto-Rheological Dampers, Proceedings of SPIE, the International Society of Optical Engineering, Vol. 4327, pp. 125-136.

66. Lee, H.S., Choi, S.B. (2000). Control Responses Characteristics of a Magneto-Rheological Fluid Damper for Passenger Vehicles, Journal of Intelligent Materials Systems and Structures, Vol. 11(1), pp. 80-87.

67. Lee, Y., Jeon D. (2001). A Study of the Vibration Attenuation of a Driver Seat Using a MR Fluid Damper, Proceedings of the Eighth International Conference on

Electrorheological Fluids and Magnetorheological Suspensions, Nice, France, pp. 70-76.

68. Lee, Y., Jeon, D. (2002). A Study of the Vibration Attenuation of a Driver Seat Using a MR Fluid Damper, Journal of Intelligent Materials Systems and Structures, Vol.13(4), pp. 437-441.
69. Liao, W.H., Wang, D.H. (2003). Semiactive Vibration Control of Train Suspension Systems via Magnetorheological Dampers, Journal of Intelligent Materials Systems and Structures, Vol. 14(3), pp. 161- 172.
70. Lindler, J.E., Wereley, N.M. (1999). Double Adjustable Shock Absorbers Using Electrorheological Fluid, Proceedings of the Seventh International Conference on Electro-Rheological Fluids and Magneto-Rheological Suspensions, Hawaii, USA, pp. 783-790.
71. Lord Corporation (2004). Publicity Material on 'Rheonetic' Magnetic Fluids & Systems, NC, USA.
72. Ma, X.Q., Wang, E.R., Rakheja, S., Su, C.-Y. (2002). Modeling Hysteretic Characteristics of MR-Fluid Damper and Model Validation, Proceedings of 41st Conference on Decision and Control, Las Vegas, Nevada, USA.
73. McManus, S. J. , Clair, K. A. ST., Boileau, P. É, Boutin, J., Rakheja, S. (2002). Evaluation of Vibration and Shock Attenuation Performance of a Suspension Seat with a Semi-Active Fluid Damper, Journal of Sound and Vibration, 253(1), pp. 313-327.
74. Milliken, W.F., Douglas, L.M. (1995). Race Car Vehicle Dynamics, Society of Automotive Engineers, PA, USA.
75. Monroe (2003). Monroe Ride Control Training Materials.

76. Muriuki, M.G., Clark, W.W. (2003). Modeling and Testing of the Force-Generating Characteristics of Magnetorheological Dampers, International Journal of Vehicle Design, Vol.33 (1-3), pp. 642-649.

77. Nam, M.H., Han, Y.M., Han, S.S., Lee, H.G., Choi, S.B., Cheong, C.C. (2001). Vibration Control Evaluation of a Commercial Vehicle Featuring MR Seat Damper, Proceedings of the Eighth International Conference on Electrorheological Fluids and Magnetorheological Suspensions, Nice, France, pp. 302-308.

78. Nakano, M. (1995). A Novel Semi-Active Control of Automotive Suspension Using An Electro-Rheological Shock Absorber, Proceedings of the Fifth International Conference on Electro-Rheological Fluids and Magneto-Rheological Suspensions, Sheffield, UK, pp. 645-653.

79. Oueslati, F. (1990). A Comparative Study of Advanced Suspensions Based On an In-Plane Vehicle Model, M. A. Sc. Thesis, Concordia University, and Montreal, Canada.

80. Parkin, M. J. (1999). Suspension System: Developments from 1900 to the Present Day, Mechanical Engineering Department, University of Bath, UK.

81. Patek, N.K. (1992). An Electronically Controlled Shock Absorber Using Electrorheological Fluid, SAE Technical Paper 920275, Society of Automotive Engineers, USA.

82. Phulé, P. P., Ginder, J. M. (1997). Synthesis and Properties of Novel Magnetorheological Fluids Having Improved Stability and Redispersibility, Sixth International Conference on ER Fluids and MR Suspensions and Their Applications, Yonezawa, Japan.

83. Phulé, P.P (2001). Magnetorheological (MR) Fluids: Principles and Applications, Smart Materials Bulletin, Vol. 2001(2), pp. 7-10.

84. Rabinow, J. (1948). The Magnetic Fluid Clutch, AIEE Transactions, Vol. 67, pp. 1308-1315.

85. Rengarajan S. (1991). An Analytical and Experimental Investigation on the Vibration Isolation Performance of Semi-Active Suspensions, M. A. Sc. Thesis, Concordia University, Montreal, Canada.

86. Rajalingham, C., Rakheja, S. (2003). Influence of Suspension Damper Nonlinearity on Vehicle Vibration Response of Ground Excitation, Journal of Sound and Vibration, Vol. 266 (5), pp. 1117–1129.

87. Rakheja, S., Ahmed, A. K. W. (1993). Frequency Response Analysis of Symmetric and Asymmetric Nonlinear Vehicle Suspensions, CSME, Special issue, Vol. 17(4B), Canada.

88. Rakheja, S., Ahmed, A. K. W. (1994). An Algorithm for Simulation of Nonlinear Mechanical Systems Using Energy and Force Similarity of its Elements, Finite Elements in Analysis and Design, Vol. 18, pp.141-154.

89. Rakheja, S., Woodrooffle, J. (1996). Role of Suspension Damping in Enhancement of Road Friendliness of Heavy Vehicle, Heavy Vehicle System, International Journal of Vehicle Design, Vol. 3(1-4), pp.363-381.

90. Rengarajan, S. (1991). An Analytical and Experimental Investigation on the Vibration Isolation Performance of Semi-Active Suspensions, M. A. Sc. Thesis, Concordia University, Montreal, Canada.

91. Sassi, S., Cherif, K., Thomas, M. (2003). On the Design and Testing of a Smart Car Damper Based on Electro-Rheological Technology, Smart Materials and Structure, Vol. 12, pp. 873-880.

92. Scibor-Rylski, A.J. (1984). Road Vehicle Aerodynamics, 2nd Edition, John Wiley & Sons, Inc., ISBN 0470200979.

93. Segel, L., Lang, H. H. (1981). The Mechanics of Automotive Hydraulic Dampers at High Stroking Frequencies, Proceedings of 7th IAVSD Symposium on the dynamics of vehicles on roads and on railways tracks, Cambridge, UK, pp. 194-214.

94. Shaohua, Z., Meiyan, L. (2001). Design of the Electrorheological Shock Absorber, Proceedings of the Eighth International Conference on Electrorheological Fluids and Magneto rheological Suspensions, Nice, France, pp. 91-96.

95. Sharp, R. S., Crolla, D. A. (1987). Road Vehicle Suspension System Design-A Review, Vehicle System Dynamics, Vol. 16, pp. 167-192.

96. Simon, T.M., Reitich, F., Jolly, M.R., Ito, K., Banks, H.T.(2001).The Effective Magnetic Properties of Magnetorheological Fluids, Journal of Mathematical and Computer Modeling, Vol. 33, pp. 273-384.

97. Sims, N. D., Peel, D. J., Stanway, R., Johnson, A. R., Bullough, W. A. (2000). The Electrorheological Long-Stroke Damper: A New Modeling Technique with Experimental Validation, Journal of Sound and Vibration, Vol. 229(2), pp. 207-227.

98. Sims, N. D., Peel, D. J., Stanway, R., Johnson, A. R. (1999). Vibration Control Using Smart Fluids: A State-of-art Review, The Shock and Vibration Digest, Vol.31 (3), pp. 195-203.

99. Sims, N.D., Stanway, R., Beck, B.M. (1997). Proportional Feedback Control of an Electro-Rheological Vibration Damper, Journal of Intelligent Material Systems and Structures, Vol.8, pp. 426-433.

100. Snowdon, J.C. (1968). Vibration and Shock in Damped Mechanical Systems, John Wiley and Sons, Inc. USA.

101. Snyder, R.A., Kamath, G.M., Wereley, N.M. (2000). Characterization and Analysis of Magnetorheological Damper Behavior Due to Sinusoidal Loading, Proceeding of SPIE- The International Society for Optical Engineering, Vol. 3989, pp. 213-229.

102. Snyder, R.A., Kamath, G.M., Wereley, N.M. (2001). Characterization and Analysis of Magnetorheological Damper Behavior under Sinusoidal Loading, AIAA Journal, Vol. 39(7), pp. 1240-1253.

103. Spencer, B.F., Dyke, D.J., Sain, K.M., Carlson, J.D. (1997). Phenomenological Model of a Magnetorheological Damper, Journal of Engineering Mechanics, Vol.123 (3), pp. 230-238.

104. Stanway, R., Sproston, J.L., El-Waled, A.K. (1996). Application of Electrorheological Fluids in Vibration Control: A Survey, Smart Materials and Structures, Vol. 5(4), pp. 464-482.

105. Stangroom, J.E. (1983). Electro-Rheological Fluids, Physics in Technology, Vol. 14, pp. 290- 296.

106. Su, H. (1990). An Investigation of Vibration Isolation Systems Using Active, Semi-Active and Tunable Passive Mechanisms with Applications to Vehicle, Ph.D. Thesis, Concordia University, Montreal, Canada.

107. Sun, T., Zhang, Y., Barak, P. (2002). 4-DOF Vehicle Ride Model, SAE Technical Paper 2002-01-1580, Society of Automotive Engineers, USA.

108. Suh, M.S., Yeo, M.S. (1999). Development of Semi-active Suspension Systems Using ER Fluids for the Wheeled Vehicle, Proceedings of the Seventh International Conference on Electro-Rheological Fluids and Magneto-Rheological Suspensions, Hawaii, USA, pp. 775-782.

109. Thompson, A. G. (1969-70). Optimization Damping in a Randomly Excited Non-linear Suspension, Proc. Inst. of Mech. Engrs, 184(2A), pp. 169-178.

110. Thomas, M. (1999). A Theoretical Model for Predicting Fatigue Limits of Lumbar Spine Incurred to Random Vibration Exposure During Driving, Proceedings of 26th International Conference on Computers and Industrial Engineering, Vol. 1(E), pp. 419–23.

111. Walker, D.G., Stein, J.L., Ulsoy, A.G. (1996). An Input-output Criterion for Linear Model Deduction. Proceedings of the 1996 ASME International Mechanical Engineering Congress and Exposition - Dynamic Systems and Control Division, Symposium on Automated Modeling, November, Atlanta, GA, USA.

112. Wang, E.R., Mz, X.Q., Rakheja, S., Su, C.Y. (2003). Semi-Active Control of Vehicle Vibration with MR-Damper, Proceedings of 42nd IEEE Conference on Decision and Control, Hawaii, USA, pp. 2270-2275.

113. Warner, B. (1996). An Analytical and Experimental Investigation of High Performance Suspension Dampers, PhD Thesis, Concordia University, Montreal, Canada.

114. Wen, Y.K. (1976). Method for Random Vibration Hysteresis Systems, Journal of Engineering Mechanics Division, pp. 249-263.

115. Wereley, N.M, Pang, L., Kamath, G.M. (1999). Idealized Hysteresis Modeling of Electrorheological Dampers, Journal of Intelligent Material Systems and Structures, Vol.9 (8), pp. 642-649.

116. Wereley, N.M., Linder, J., Rosenfled, N., Choi, Y.T. (2004). Biviscous Damping Behavior in Electrorheological Shock Absorbers, Smart Materials and Structures, Vol. 13 (4), pp. 743-752.

117. Williams, M. (2000). Shocked, Four Wheeler Magazine, Eastern Ontario Trailblazers, Canada.

118. Wong, J.Y. (2001).Theory of Ground Vehicles, 3rd Edition, John Wiley & Sons, Inc., USA, ISBN 0-471-35461-9.

119. Yao, G.Z., Yap, F.F., Chen, G., Li, W.H., Yeo, S.H. (2002). MR Damper and Its Application for Semi-Active Control of Vehicle Suspension System, Mechatronics, Vol.12 (7), pp. 963-973.

120. Yeo, M.S., Lee H.G., Kin M.C. (2001). A Study on the Performance Estimation of Semi-active Suspension System Considering the Response Time of Electro-rheological Fluid, Proceedings of the Eighth International Conference on Electrorheological Fluids and Magnetorheological Suspensions, Nice, France, pp. 180-186.

121. Yokoyama, M., Hedrick, J.K., Toyama, S. (2001). A Model Following Sliding Mode Controller for Semi-Active Suspension Systems with MR Dampers, Proceedings of American Control Conference, Vol. 4, pp. 2652-2657.

122. Yi, K., Song, B.S. (1999). A New Adaptive Sky-Hook Control of Vehicle Semi-Active Suspensions, Journal of Automobile Engineering, Vol. 213(3), pp. 293–303.

123. Youn, I., Hac, A. (1995). Semi-Active Suspensions with Adaptive Capability, Journal of Sound and Vibration, 180 (3), pp. 475-492.

124. ZF Sachs AG (2004). Publicity Material on Nivomat Suspension Systems, Germany.